Allylic Azides: Versatile Building Blocks to Heterocycles

A Dissertation

SUMMITTED TO THE FACULTY OF THE

UNIVERSITY OF MINNESOTA

BY

En-Chih Liu

IN PARTIAL FULFILLMENT OF THE REQUIREMENTS OF

DOCTOR OF PHILOSOPHY

Professor Joseph Topczewski, Advisor

May 2021

ACKNOWLEDGEMENTS

I would like to thank my supervisor, Prof. Joe Topczewski. Joe's enthusiasm in science profoundly drives me to my scientific work. As a young professor, Joe is extremely approachable. In the lab, he gives me advice based on his knowledge or past experience; Outside the lab, Joe also provides me, as an international student, a lot of support in a verity of areas. Joe is the best supervisor and I genuinely appreciate his support.

I also thank the Topczewski group as a whole. Language is usually a big challenge for international students, but all members of the Topczewski group are friendly and supportive. Thank you to Amy, Mary, Matt, Angela, Ryan, James, and Juliana for your support.

The support from my family and friends is crucial. I cannot finish my PhD career without their help. Thank you to my girlfriend, Winnie, for your emotional support. I also would like to thank Hsu-Chun, Ji-Pei, Jia-Hong, Jessica, Cheng-Yu, Ya-Lin, Yun-Kai, Jyun-Yin, and Ya-Chu for your care and support.

Thank you to Prof. Emeritus Wayland Noland and the University of Minnesota chemistry department for the Excellence in Graduate Studies Fellowship (2019) and the University of Minnesota graduate school for the Doctoral Dissertation Fellowship (2020).

I dedicate this thesis to my parents, Shu-Hua and Feng-Chang.

Abstract

Organic azides are versatile building blocks because they can be derivatized to a variety of functionalities. Allylic azides, as a subclass of organic azides, are viewed as a problematic precursor in organic synthesis because of the spontaneous rearrangement. The Topczewski lab has focused on the reactivity of allylic azides. This graduate work describes the unique reactivity of allylic azides to access enantioenriched heterocycles or densely functionalized heterocycles. Enantioselective copper-catalyzed alkyne-azide cycloaddition (E-CuAAC) by dynamic kinetic resolution (DKR) opens gates to α-*N*-chiral triazoles with high yields and enantioselectivity (Chapter 2). The spontaneous rearrangement of allylic azides was utilized as a racemization method. The newly developed chiral ligand in the E-CuAAC reaction can be further applied to non-allylic azides (Chapter 3). Enantioenriched benzylic triazoles can be accessed by kinetic resolution (KR). Enantioselective nickel-catalyzed alkyne-azide cycloaddition (E-NiAAC) was explored (Chapter 4). The E-NiAAC reaction gives the complementary 1,4,5-trisubstituted triazoles, which are not accessible via CuAAC reaction. Finally, densely functionalized tetrahydro-pyrrolo-pyrazoles can be prepared via a cascade reaction of cinnamyl azides (Chapter 5).

Table of Contents

List of Tables

List of Figures

List of Schemes

List of Abbreviations

$(CuOTf)_2 \cdot PhMe$	copper(I) trifluoromethanesulfonate toluene complex
Ac	acetate
$AgPF_6$	silver hexafluorophosphate
Ar	aryl
Bn	benzyl
BnBr	benzyl bromide
Boc	tert-butyloxycarbonyl
br	broad singlet (NMR)
Cbz	benzyloxycarbonyl
CCl_4	carbon tetrachloride
$CDCl_3$	deuterated chloroform
COD	1,5-cyclooctadiene
Cp_2Ni	bis(cyclopentadienyl)nickel(II)
$Cu_2Cr_2O_5$	copper(II) chromite
CuAAC	copper-catalyzed alkyne-azide cycloaddition
CuI	copper iodide
$CuSO_4$	copper(II) sulfate
d	doublet (NMR)
DBU	1,8-diazabicyclo[5.4.0]undec-7-ene
DCE	dichloroethane
DCM	dichloromethane
DFT	density function theory
DIAD	diisopropyl azodicarboxylate
DIPEA	*N*,*N*-diisopropylethylamine
DKR	dynamic kinetic resolution
DME	dimethoxyethane
DMF	dimethylformamide
DMSO	dimethyl sulfoxide
DPPA	diphenylphosphoryl azide

dr	diastereomeric ratio
ee	enantiomeric excess
EI	electron ionization
equiv	equivalents
er	enantiomeric ratio
ESI	electron spray ionization
Et	ethyl
EtOAc	ethyl acetate
FID	flame ionization detector
GC	gas chromatography
hfac	hexafluoroacetylacetone
HPLC	high-performance liquid chromatography
HRMS	high resolution mass spectrometry
Hz	hertz
IPA	isopropanol
^{i}Pr	isopropyl
IR	infrared
IrAAC	iridium-catalyzed alkyne-azide cycloaddition
J	coupling constant
KR	kinetic resolution
m	multiplet (NMR)
m-CPBA	meta-chloroperoxybenzoic acid
Me	methyl
MeCN	acetonitrile
MeOH	methanol
$MgSO_4$	magnesium sulfate
$NaBH_4$	sodium borohydride
NaCl	sodium chloride
NaOH	sodium hydroxide
NaOMe	sodium methoxide
^{n}Bu	n-butyl

$Ni(COD)_2$	bis(1,5-cyclooctadiene)nickel(0)
NiAAC	nickel-catalyzed alkyne-azide cycloaddition
NMO	*N*-Methylmorpholine *N*-oxide
NMR	nuclear magnetic resonance
Ph	phenyl
$PhCF_3$	trifluorotoluene
PhMe	toluene
Piv	pivaloyl
PMe_3	trimethylphosphine
PMP	para-methoxyphenyl
PPh_3	triphenylphosphine
PYBOX	bis(oxazolinyl)pyridine
q	quartet (NMR)
RuAAC	ruthenium-catalyzed alkyne-azide cycloaddition
s	singlet (NMR)
SFC	supercritical fluid chromatography
t	triplet (NMR)
TBS	tert-butyldimethylsilyl
tBu	tert-butyl
TEA	triethylamine
Tf	triflate
TFA	trifluoroacetic acid
THF	tetrahydrofuran
$TiCl_4$	titanium tetrachloride
TMS	trimethylsilyl
$TMSN_3$	trimethylsilyl azide
TOF	time-of-flight
TOX	trisoxazoline
Tr	trityl
Ts	tosyl
TsCl	4-toluenesulfonyl chloride

$Zn(OTf)_2$	zinc trifluoromethanesulfonate

Chapter 1 Introduction

1.1 Heterocycles

A heterocycle is a cyclic compound with at least two different elements contained in the ring.[1] Heterocycles are ubiquitous in material sciences, agricultural chemistry, medicinal chemistry, natural products, and pharmaceuticals.[2–5] Among the known heterocycles, a large percentage contain nitrogen. In 2014, 59% of US FDA-approved drugs contained nitrogen atoms.[6] Therefore, how to access these nitrogen-containing molecules, and more specifically heterocycles, has been a central challenge to the field of organic synthesis.

1.1.1 Heterocycles in Natural Products

Alkaloids, by definition, are naturally occurring organic molecules that contain at least one basic nitrogen.[1] One classic example is morphine (Figure 1.1). Morphine contains a piperidine core (Figure 1.1, shown in red). Morphine is frequently used in medical treatment, although it has well-known side effects and is notorious for its drug abuse. Morphine was first isolated from a poppy plant *Papaver somniferum* by Friedrich Sertürner between 1803 to 1805.[7] The isolation of morphine was generally believed to be the first active-component isolation from a plant. Morphine's biological activity, importance to human health, and historical significance as a synthetic target epitomizes the significance of nitrogen heterocycles to human health and society and the interplay with organic synthesis.[8]

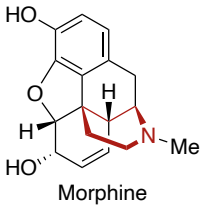

Figure 1.1 Morphine

In addition to the isolation of the desired product from the natural source, organic synthesis is another means to access this heterocyclic compound. However, the synthesis is usually challenging because of stereochemistry, especially when the stereogenic center locates the position adjacent to heteroatoms. Morphine has three possible key bond disconnections of the central nitrogen atom, numerous racemic or enantiopure morphine synthesis has been disclosed that have explored all these possibilities (Figure 1.2).[9–16]

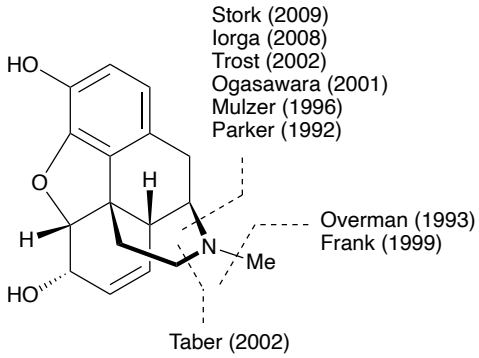

Figure 1.2 Key C-N Bond Disconnection

The first total synthesis of (±)-morphine was reported by Marshall in 1955 (Scheme 1.1a).[17] The key carbon-nitrogen bond formation was achieved via a reductive cyclization. Although the mechanism was ambiguous, the amide bond was formed in the presence of

copper(II) catalyst and hydrogen gas, affording amide **1.2**. In 2002, Trost and co-workers reported an enantioselective total synthesis of (-)-morphine (Scheme 1.2b).[18] The enantioselectivity was derived from a chiral building block (-)-**1.5**, which was accessed via a Tsuji-Trost reaction in the presence of palladium catalyst and a chiral ligand. The key carbon-nitrogen bond was generated via an intramolecular hydroamination (not shown).

Scheme 1.1 Total Synthesis of Morphine

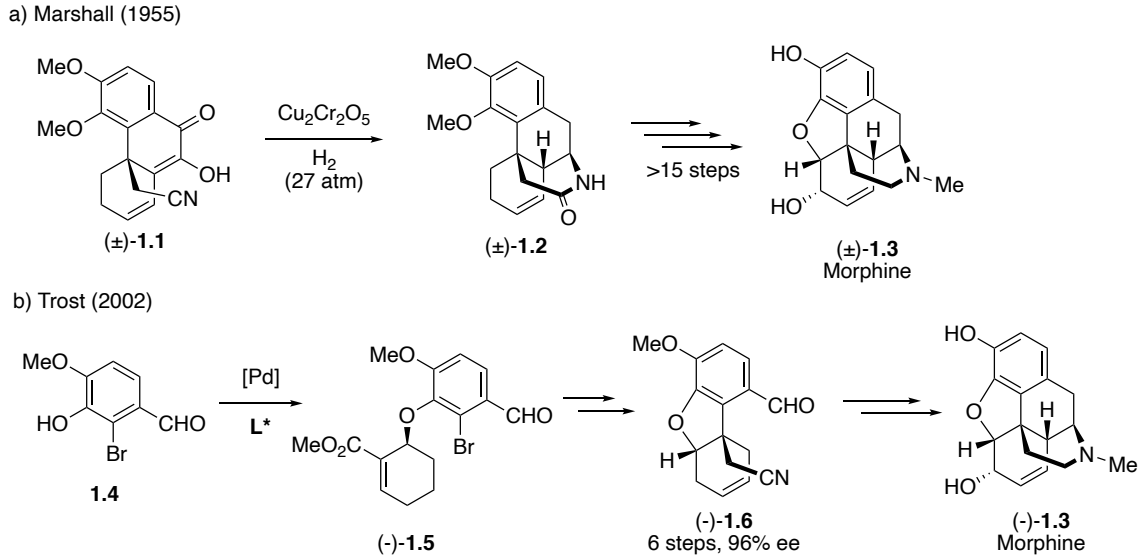

1.1.2 Heterocycles in Pharmaceuticals

Heterocycles can be easily found in a variety of pharmaceuticals, especially nitrogen-containing heterocycles (Figure 1.3). For example, apixaban can be used in the treatment of cardiovascular diseases.[19] This heterocyclic compound does not contain any stereogenic centers; therefore, the synthesis is less complex. Ibrutinib, on the other hand, has one stereocenter adjacent to the nitrogen. This pharmaceutical can be utilized in the treatment of B cell cancer.[20] Oseltamivir, also known as Tamiflu, has three contiguous

stereogenic centers all adjacent to a heteroatom. These molecules are synthetically challenging targets due to the additional complication of stereochemistry.[21]

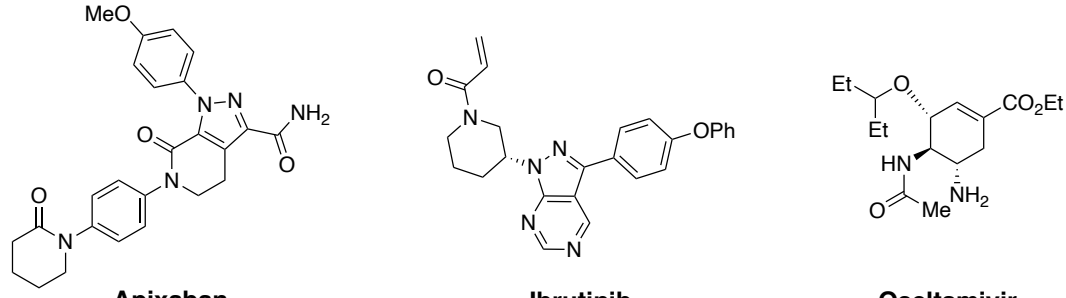

Apixaban
Cardiovascular Diseases Treatment

Ibrutinib
B Cell Cancer Treatment

Oseltamivir
Flu Treatment

Figure 1.3 Heterocycles in Pharmaceuticals

Liu and co-workers reported a synthesis of Ibrutinib in 2015 (Scheme 1.2).[20] The heterocycle **1.9** was accessed via the Suzuki coupling condition. The key step of carbon-nitrogen bond formation was achieved via Mitsunobu reaction condition with enantiopure building block **1.10**. Although the stereochemistry was well-controlled under the Mitsunobu reaction conditions, the synthesis of the enantiopure building block **1.10** was not very efficient and required a massive quantity of solvents and reagents. Enzymatic reduction or other traditional resolution via diastereoselective recrystallization were required.[22,23]

Scheme 1.2 Synthesis of Ibrutinib

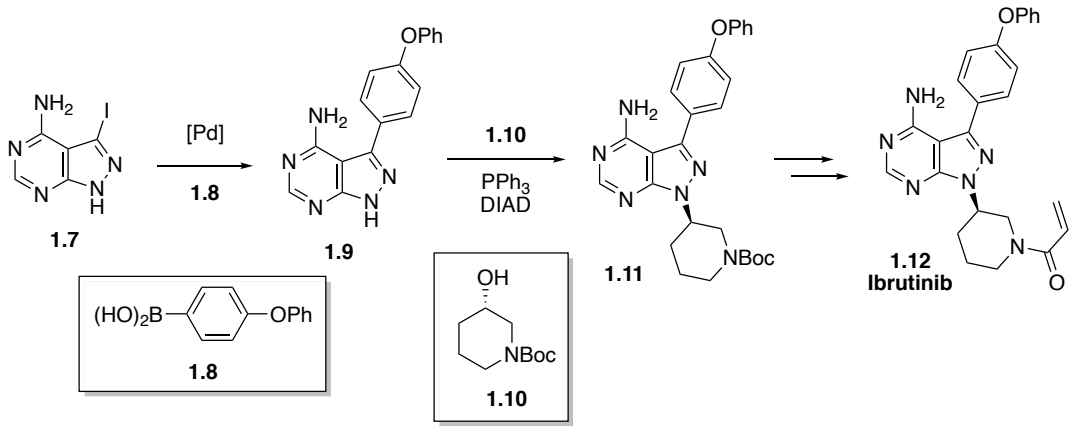

An efficient synthetic route to heterocycles bearing an α-*N*-chiral center plays a crucial role for the next generation of organic synthesis. However, the traditional synthesis of those compounds either relies on the utilization of enantiopure building blocks or the resolution with chiral auxiliary. Both methods require substantial amounts of resources. Therefore, this graduate work aims to develop more efficient methods to access heterocycles, especially those bearing an α-*N*-chiral center.

1.2 Organic Azides

Organic azides are regarded as versatile precursors because they can be derivatized into a variety of nitrogen containing products. The Topczewski group is particularly interested in allylic azides because of its spontaneous rearrangement, also known as the Winstein rearrangement (*vide infra*), which occurs near ambient temperature. The allylic azides can be viewed as surrogates of chiral amine and the enantioselectivity can be controlled in asymmetric environments.

1.2.1 Derivatization

The versatility of organic azides is summarized in Scheme 1.3.[24] As mentioned above, organic azides are viewed as surrogates for organic amines because azide reduction results in a primary amine (**1.14**). The cycloaddition of organic azides with alkynes and isocyanides affords triazoles (**1.15**) and tetrazoles (**1.16**), respectively.[25] A nitrene intermediate can be formed upon the release of nitrogen gas from an azide. The resulting nitrene species and gas evolution are a cause of safety concerns with working with organic azides. Safety must be taken into account because azides can be explosive. The nitrene intermediate can give various nitrogen-containing derivatives. The Schmidt reaction with carbonyl compound gives amide product (**1.17**).[26] Cyclization and addition reaction to the alkene gave pyrrole (**1.18**) and aziridine (**1.19**) derivatives, respectively.[25]

Scheme 1.3 Azide Derivatization

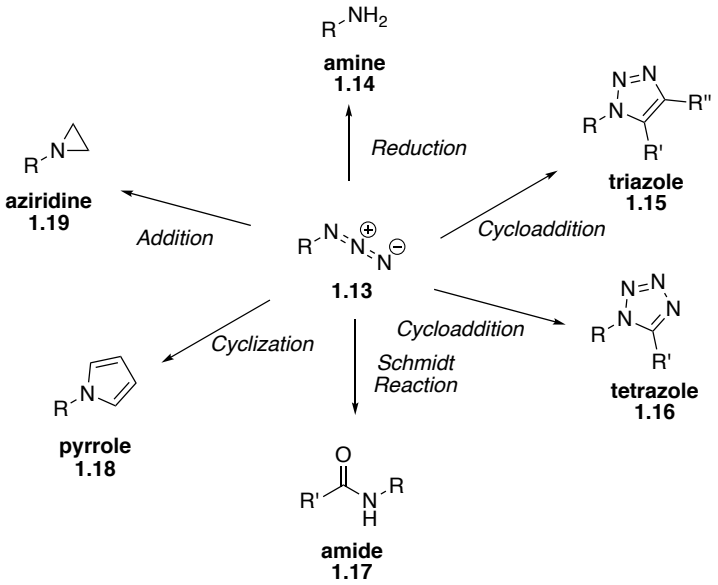

One classic example to demonstrate the versatility of organic azide is the synthesis of Oseltamivir by Zhang in 1998 (Scheme 1.4).[27] (-)-Quinic acid (**1.20**) can be extracted from plant sources, which can be derivatized to epoxide **1.21** in high stereoselectivity. Nucleophilic addition of the azide anion afforded the mixture of isomers **1.22** and **1.23**. Although the regioselectivity was not controlled, the relative configuration of the hydroxy and the azido group was *trans*. Upon the reductive cyclization, aziridine **1.24** was generated as a single product. Another azide anion opened the aziridine to give azide **1.25** with excellent diastereo- and regioselectivity. Overall, Oseltamivir could be synthesized in 12 steps in 4.4% yield from a readily available source. It is noteworthy that there are only two nitrogen atoms in this active pharmaceutical ingredient and both are derived from an azide.

Scheme 1.4 Total Synthesis of Oseltamivir (Zhang, 1998)

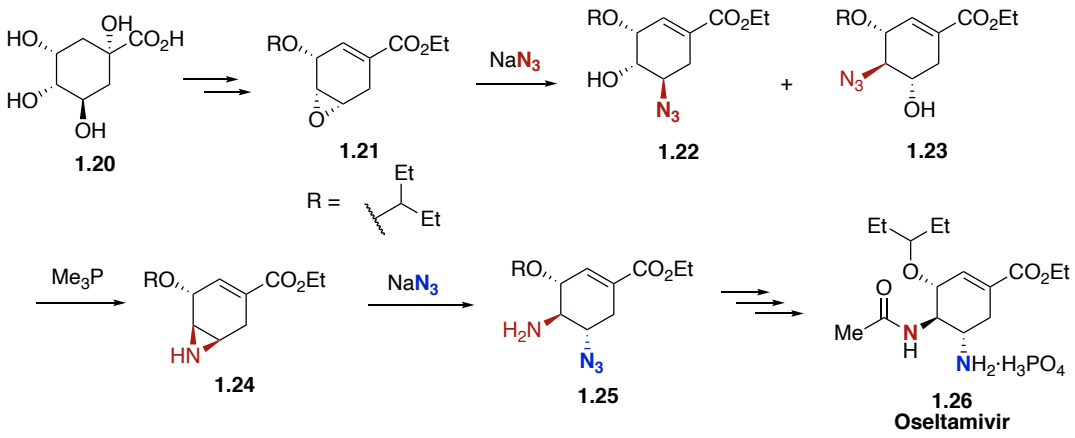

1.2.2 Allylic Azides

Allylic azides, as a subclass of organic azides, are counterintuitively problematic to utilize in organic synthesis. This is because of a spontaneous rearrangement, called the Winstein rearrangement, that occurs spontaneously near ambient temperature (Scheme 1.5).[28,29] Prenyl azide (**1.27**) was prepared from a straightforward substitution of prenyl chloride with sodium azide. The product was found to be a mixture of azide **1.27** and **1.28**. The two isomers can be separated and stored under low temperature (-80 °C) for a relatively long time with minimal isomerization. However, when the purified azide **1.27** was stored near ambient temperature, the isomerization occurred rapidly. This phenomenon was also observed in crotyl azide **1.29**. The ratio of prenyl azide **1.27** and the isomer **1.28** was ca. 75:25 near ambient temperature (Scheme 1.5a). This ratio was barely changed in a variety of solvents (Scheme 1.5b). The ratio of crotyl azide **1.29** and the isomer **1.30** was ca. 64:36. The isomerization rate was slightly dependent on the solvents (Scheme 1.5b).

Scheme 1.5 Winstein Rearrangement a) Prenyl Azides and Crotyl Azide Rearrangement b) Isomer Ratio and Rearrangement Rate

a)

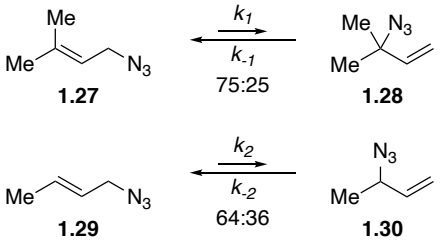

b)

	1.27:**1.28**	(k_1+k_{-1}) s^{-1}	**1.29**:**1.30**	(k_2+k_{-2}) s^{-1}
n-C_5H_{12}	70:30	4.9×10^{-5}	62:38	1.9×10^{-5}
Et_2O	73:27	11.1×10^{-5}	64:36	4.3×10^{-5}
Me_2CO	77:23	31.0×10^{-5}	65:35	11.0×10^{-5}
EtOH	74:26	24.1×10^{-5}	63:37	7.2×10^{-5}

A general allylic azide rearrangement is depicted in Scheme 1.6. Allylic azide (*E*)-**1.31** undergoes a sigmatropic rearrangement generating a tertiary azide **1.32**. Upon a rotation of the single bond and a second sigmatropic rearrangement, the allylic azide (*Z*)-**1.31** is formed. Therefore, an unsymmetrical allylic azide is in equilibrium with a mixture of four different isomers, including (*E*)/(*Z*) isomer of the alkene and both enantiomers of the tertiary azide.

Scheme 1.6 General Scheme of Winstein Rearrangement

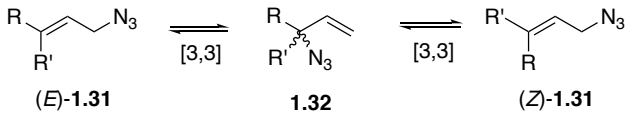

Allylic azides were seldom utilized in organic synthesis because this spontaneous rearrangement makes these intermediates difficult to control. In 2005, Sharpless and co-workers reported the selective derivatization of allylic azides (Scheme 1.7).[30] Crotyl azide **1.29** was present as a mixture of two isomers, which was consistent with Winstein's investigation. The azide mixture was subjected to an alkyne-azide cycloaddition reaction in the presence of a copper catalyst, a 72:28 ratio was observed in the triazole product mixture. This slight enrichment was attributed to the different reactivity of azide **1.29** and **1.30**. Crotyl azide **1.29** is a primary azide, which is more reactive than the secondary azide **1.30**. This reactivity difference was further enhanced in the epoxidation reaction. When the crotyl azide mixture was treated with *meta*-chloroperoxybenzoic acid (*m*-CPBA), only epoxide **1.36** was observed as a single product. The reactivity is highly dependent on the electron density of the alkene because *m*-CPBA is an electrophilic epoxidation reagent.

Azide **1.29** contains a disubstituted alkene, while azide **1.30** contains a terminal alkene. This substitution pattern impacts the alkene's reactivity. Overall, this study revealed that the reactivity of allylic azide isomers can be biased by the choice of reagents and reaction conditions.

Scheme 1.7 Selective Derivatization of Allylic Azides

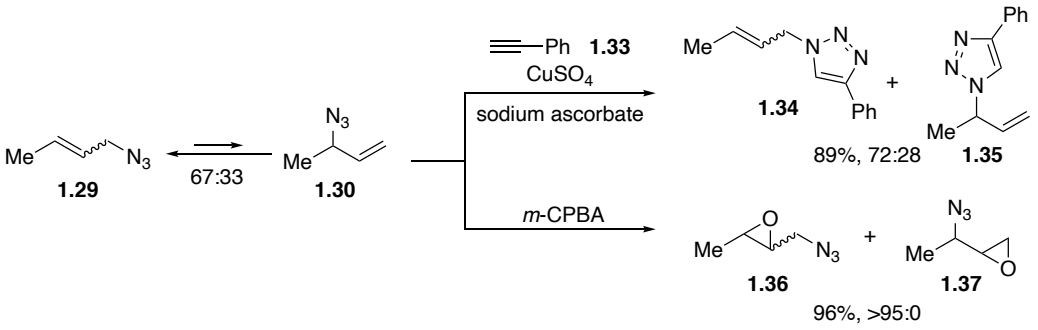

The chiral azide intermediate (**1.32**, Scheme 1.6) can be utilized in a stereocontrolled reaction. In 2012, Aubé and co-workers reported an intramolecular Schmidt reaction to access chiral lactam with phenomenal diastereoselectivity (Scheme 1.8a).[31] Due to the Winstein rearrangement, the allylic azide **1.39** is a mixture of four isomers in a 64:14:14:8 ratio (Scheme 1.8b). The major component of the azide mixture is the (*E*)-alkene species (*E*)-**1.39**. Upon being subjected to a Lewis acid catalyst, lactam **1.40** was isolated as a major product with a diastereomeric ratio >20:1. The excellent diastereoselectivity was illustrated in Scheme 1.8c. The active molecule is not the dominant species in the starting azide because of the ring size of the intermediate. The distal nitrogen in chiral azide **1.41** or **1.42** attacked the activated carbonyl through an *exo*- attack, generating intermediates **1.43** and **1.44**, respectively. The nitrogen attack was reversible

and intermediate **1.43** was favored over **1.44** because the 1,3-diaxial interaction resulted in **1.44** being less stable. Overall, the reaction was highly stereoselective, forming products from a minor component of the azide starting material.

Scheme 1.8 Stereocontrolled Intramolecular Schmidt Reaction a) Reaction Scheme b) Azide Isomer Equilibrium c) Intermediate Model of the Reaction

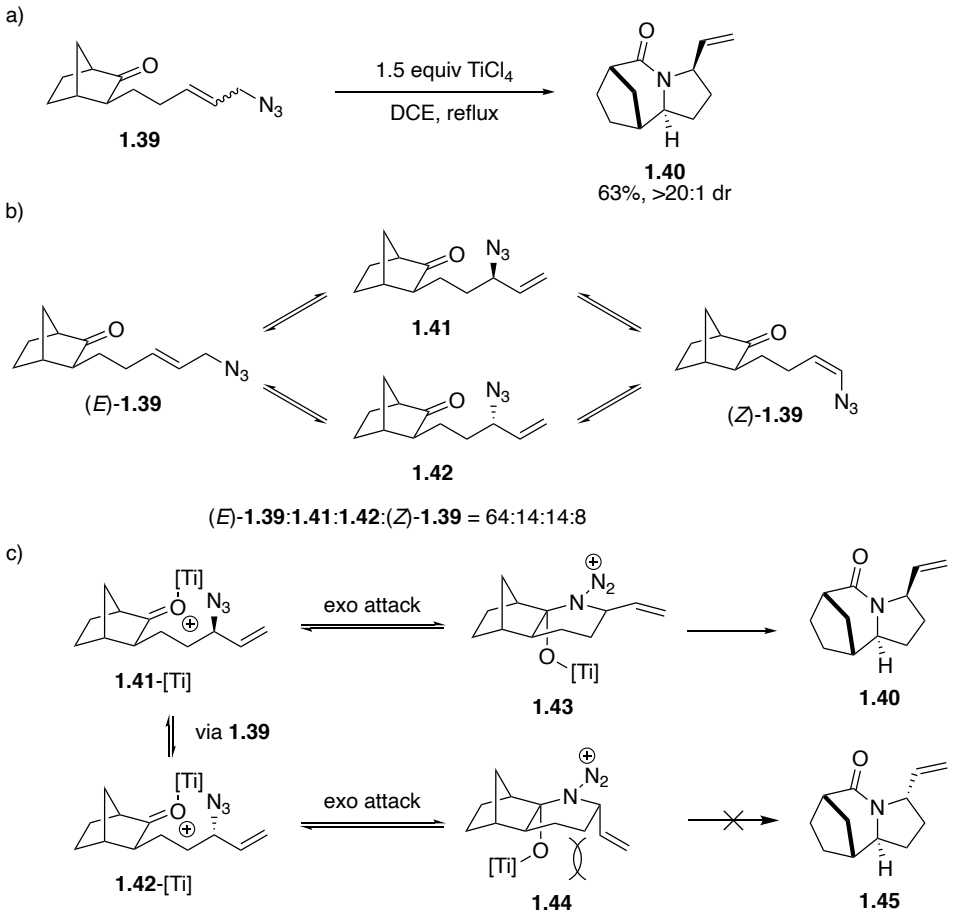

Inspired by Aubé's investigation and the versatility of allylic azides, this graduate work aims to explore the reactivity of allylic azides to access various heterocycles (Scheme 1.9). Starting from allylic azide **1.46**, the enantioenriched triazoles **1.48** and **1.50** can be

synthesized using terminal alkyne **1.47** and terminal alkyne **1.49**, respectively. This work takes advantage of the Winstein rearrangement to racemize the allylic azide **1.46** because the enantiomer *ent*-**1.46** is generated upon the rearrangement. The enantioselective synthesis was achieved via dynamic kinetic resolution. The reaction is exceptionally efficient because it converts the racemic starting material to enantioenriched products with excellent yields and selectivity. The second aim of this work is to synthesize highly functionalized tetrahydro-pyrrolo-pyrazole **1.54** using the cinnamyl azide **1.52**. The Winstein rearrangement still occurs in the mixture of allylic azide **1.51** and **1.52**. However, because of conjugation, cinnamyl azide **1.52** is strongly favored in the equilibrium. A highly functionalized heterocycle **1.54** can be accessed via a cascade reaction of azide **1.52** and acrylate **1.53**. The reaction is highly diastereoselective and product **1.54** can be utilized as a building block, which can be readily diversified. Both works show the versatility of allylic azides to access various heterocycles.

Scheme 1.9 a) Access to Enantioenriched Triazoles with Terminal Alkyne b) Access to Enantioenriched Triazoles with Internal Alkyne c) Access to Functionalized Heterocycles

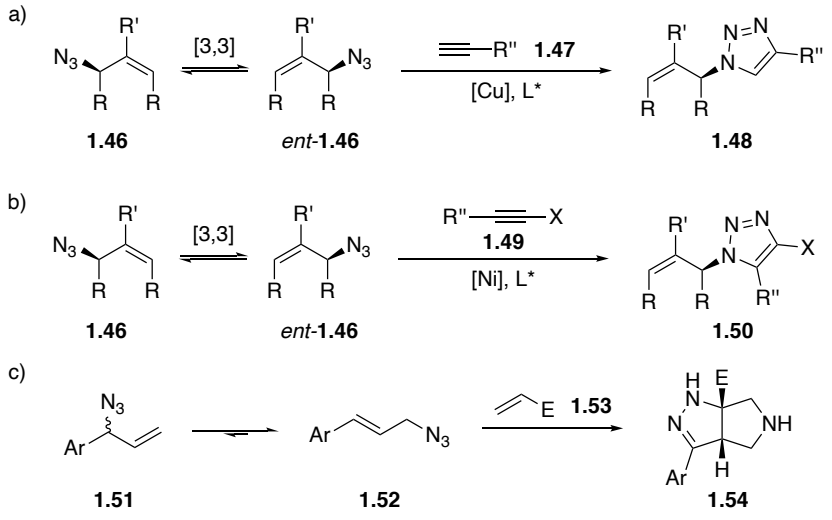

Chapter 2 DKR Azide-Alkyne Cycloaddition*

2.1 DKR Introduction

Asymmetric synthesis plays an important role in pharmaceutical and natural product syntheses.[32,33] Although a racemic mixture of synthesized products can be separated by a classic resolution with the help of a chiral auxiliary, this method requires a stoichiometric quantity of chiral reagent as well as solvents during the syntheses and purification.[34] In contrast to classical resolution, a conceptually more efficient way to prepare enantioenriched compounds is via asymmetric synthesis. Depending on the structures of starting materials, serval asymmetric syntheses are possible. One of the most powerful approaches to asymmetric synthesis is via a dynamic kinetic resolution (DKR). In an ideal DKR, the interconversion of starting materials, so-called racemization, is faster than other downstream reactions and any other possible side reactions (Scheme 2.1).

Scheme 2.1 Dynamic Kinetic Resolution

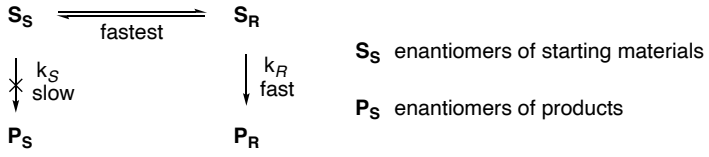

The utilization of an enzyme in a DKR reaction has been well-documented due to the exceptionally high stereoselectivity of most enzymes. However, an external reagent or catalyst is often required to promote the racemization of starting materials. Transition metal

* Reprinted (adapted) with permission from Liu, E.-C.; Topczewski, J. J. *J. Am. Chem. Soc.* **2019**, *141*, 5135 – 5138. Copyright (2019) American Chemical Society.

complexes, for instance, are a classic catalyst for racemization. In 1992, Bäckvall and coworkers reported a ruthenium(II)-catalyzed oxidation of secondary alcohols to the corresponding ketone (Scheme 2.2a).[35] Later, a DKR acetylation from a racemic secondary alcohol was reported by the same group (Scheme 2.2b and Scheme 2.2c).[36,37] The racemization was accomplished via hydrogen transfer with a ruthenium(II) catalyst. The enantioselective acetylation was conducted using the enzyme *Candida antarctica* component B lipase (Novozym 435 = N-435).

Scheme 2.2 DKR Enzyme Acetylation

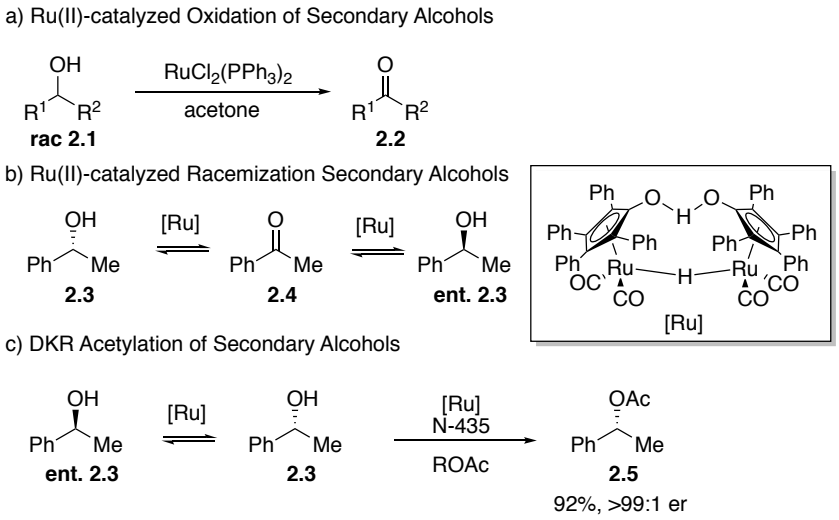

Although enzymatic reactions are usually conducted under mild conditions and proceed with excellent stereoselectivity, these reactions can be highly substrate dependent. This property hampers the substrate scope and many potential applications in syntheses. One way to address this issue is to derivatize the starting materials with a chiral auxiliary and then perform a DKR. One classic example is to install an oxoimidazolidine auxiliary

to α-bromo carboxylic acids. The bromo group can undergo nucleophilic substitution in a diastereoselective manner (Scheme 2.3).[38,39] In the presence of iodide, the α-bromo can epimerize or generate the α-iodo amide derivatives. The chiral auxiliary hampers the nucleophile attack to the bromide/iodide from a specific face resulting in the formation of enantioenriched products. This method provided an enantioenriched α-substituted amide which can undergo downstream functionalization to the corresponding esters or acids with an excellent enantiospecificity.

Scheme 2.3 Non-Enzymatic DKR

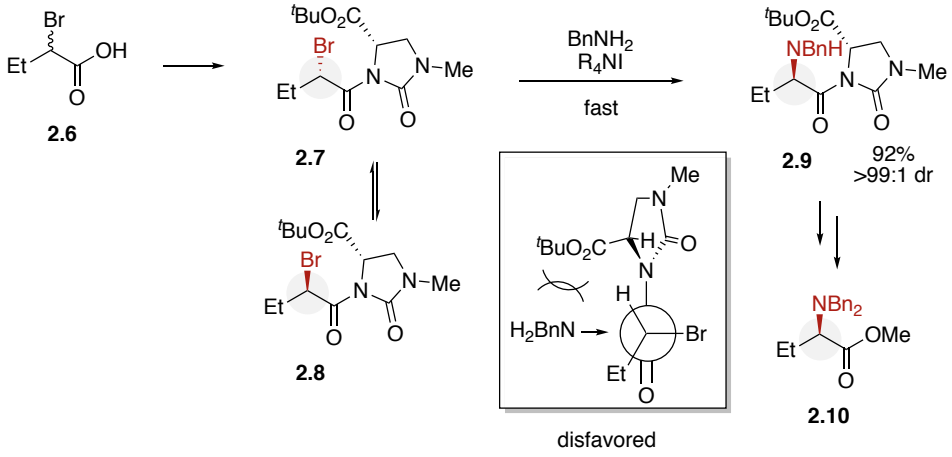

In order to achieve a DKR with small organic molecules, several aspects need to be considered. First, the catalysts for starting material racemization and for the downstream functionalization must be compatible with each other. Second, a fast racemization rate of the starting material, relative to the other chemical reactions, is required. Lastly, the conditions needed for racemization must be compatible with the catalyst used to derivative

the starting material. One promising candidate that meets all three criteria is the azide-alkyne cycloaddition.

2.2 Enantioselective Azide-Alkyne Cycloaddition

As mentioned in the previous chapter, the CuAAC reaction is a powerful method to generate 1,4-disubstituted triazoles. With the increasing synthetic demand for enantioenriched triazoles, research on the enantioselective CuAAC (E-CuAAC) reaction has been increasing.[40,41] However, facilitating an E-CuAAC reaction presents several fundamental challenges. First, the two coupling partners, azides and alkynes, are both linear-shaped molecules. The resulting triazole is an sp^2 hybridized and has a planar geometry. No new stereogenic center is formed in most CuAAC reactions. Therefore, E-CuAAC requires the transmission of stereochemical information beyond the forming triazole. Second, the traditional CuAAC proceeds in the absence of ligands, so the E-CuAAC reaction must outcompete the background CuAAC reactions.[42] Third, the newly formed triazoles are heterocycles and therefore able to coordinate to the copper(I) center. The asymmetric chemical environment is usually created by applying chiral ligands to a metal center. The newly formed triazoles might outcompete the external chiral ligand and disrupt the chiral environment.[43,44] These processes make developing an E-CuAAC reaction nontrivial.

Because of these fundamental challenges, only a few E-CuAAC reactions have been reported. The first attempted E-CuAAC was reported by Fokin and Finn.[45] The enantioenriched triazole **2.14** could be accessed via kinetic resolution (Scheme 2.4a). In their report, azide **2.11** was utilized as the limiting reagent and a series of

bis(oxazolinyl)pyridine (PYBOX) ligands and copper(I) precatalysts were explored. In the presence of PYBOX ligand **2.13**, the enantiomeric ratio (er) could reach up to 84:16. However, the substrate scope was extremely limited. Only two azides, which are both α-methylbenzyl azide derivatives, gave moderate er. Other azide substrates, including allylic azide derivatives, resulted in a low 57:43 er. In terms of the alkyne scope, only phenylacetylene was explored. Propargyl alcohol and amine derivatives gave nearly racemic triazole products.

In 2013, Zhou et al. reported an E-CuAAC reaction via desymmetrization of an oxindole-based *bis*-alkyne (Scheme 2.4b). In their studies, achiral *bis*-alkyne **2.15** was subject to a copper(I) catalyst and PYBOX ligand **2.17**. The *bis*-alkyne **2.15** approaches the chiral catalyst through a specific face and generates enantioenriched *mono*-triazole **2.18** with a 95:5 er. However, the major byproduct is the *bis*-triazole (not shown here). To achieve high enantioselectivity and decrease byproduct formation, a low reaction temperature (0 °C) was needed. This also necessitated a higher catalyst loading (15 mol %) to compensate for a decrease in the rate (96 h reaction time). Unfortunately, the achiral *bis*-triazole product was still formed (up to 2:1 *mono*-:*bis*- triazole). In their studies, a relatively broad scope of symmetric oxindoles was presented. Various substituents on the oxindoles are tolerated as well as on the amide nitrogen. Zhou and co-workers demonstrated a broad azide scope. However, the oxindole core is required in this E-CuAAC reaction. Although other desymmetrizations of *bis*-alkyne studies have been reported with higher yields and er, the elaboration on the quaternary carbon attaching to *bis*-alkyne is required.[46,47] This necessity and the inevitable byproduct formation restrict the synthetic applications of E-CuAAC via desymmetrization.

Recently, improvements have been made on both the reaction yield and the er of kinetic resolution and desymmetrization.[46,48–50] Nonetheless, one natural limitation of kinetic resolution can never be eliminated. The maximum yield of kinetic resolution is 50% because the starting materials with the opposite configuration do not form the desired product. One powerful approach to overcome this limitation is to utilize a dynamic kinetic resolution (DKR) to achieve E-CuAAC. However, no DKR E-CuAAC had been investigated. Therefore, the first aim of this work is to explore an E-CuAAC using allylic azides to perform DKR (Scheme 2.4c).

Scheme 2.4 Enantioselective CuAAC (E-CuAAC)

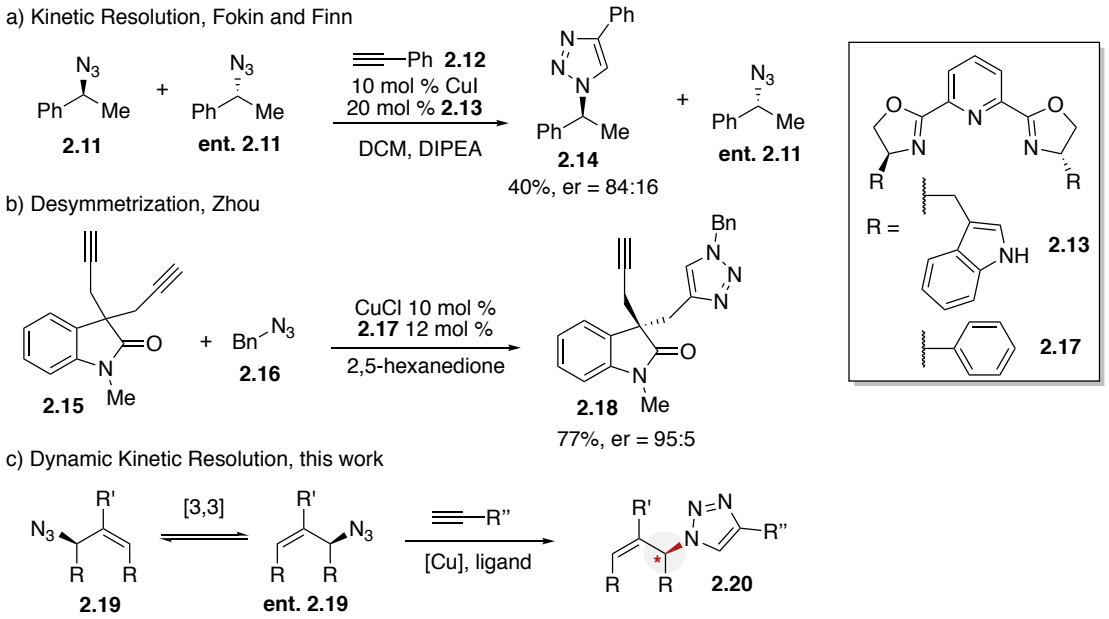

2.3 Experimental Results

2.3.1 Reaction Optimization

Allylic azides are a promising candidate for DKR because the Winstein rearrangement spontaneously occurs near ambient temperature. The model azide substrate **2.21** was designed to be "symmetric," at the transition state, generating its enantiomer by the Winstein rearrangement. One azide enantiomer can be trapped by alkyne **2.22** and generate enantioenriched triazole **2.23** in the presence of the chiral copper(I) complex (Table 2.1). Minimal enantioselectivity was observed when copper(I) iodide was utilized (entry 1). Changing to a cationic copper(I) precatalyst had a notable impact on both the rate and enantioselectivity of the reaction (entry 2). A collection of ligands was screened that included bidentate and tridentate phosphorus and nitrogen ligands (entries 2−9). On the basis of these initial results, aryl-PYBOX ligands appeared to be particularly effective (entry 4 and 5, *vide infra*).‡ We hypothesized that increasing the ligand loading would slow the background click reaction by saturating the copper center. An increase in ligand loading enhanced the observed er to 88:12 (entry 10). Increasing the temperature had a notable positive effect (entry 11), which resulted in a quantitative yield (>98%) and high enantioselectivity (>99:1 er). The increased temperature likely increased the relative rate of racemization via a sigmatropic pathway. Other copper(I) precatalysts were not as effective (entries 12 and 13), and the conditions outlined in entry 11 were selected as being optimal.

‡ For more ligand investigations, see Supporting Information of this manuscript: *J. Am. Chem. Soc.* **2019**, *141*, 5135−5138.

Table 2.1 Optimization of E-CuAAC by DKR[a]

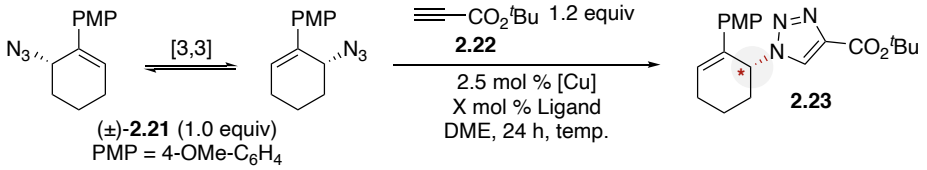

Entry	[Cu] precatalyst	Ligand	Temp (°C)	Yield (%)	er
1	CuI	**L1** (2.5 mol %)	rt	80	57:43
2	$(CuOTf)_2$·PhMe	**L1** (2.5 mol %)	rt	>98	60:40
3	$(CuOTf)_2$·PhMe	**L2** (2.5 mol %)	rt	95	53:47
4	$(CuOTf)_2$·PhMe	**L3** (2.5 mol %)	rt	93	86:14
5	$(CuOTf)_2$·PhMe	**L4** (2.5 mol %)	rt	80	76:24
6	$(CuOTf)_2$·PhMe	**L5** (2.5 mol %)	rt	58	51:49
7	$(CuOTf)_2$·PhMe	**L6** (2.5 mol %)	rt	87	52:48
8	$(CuOTf)_2$·PhMe	**L7** (2.5 mol %)	rt	65	52:48
9	$(CuOTf)_2$·PhMe	**L8** (2.5 mol %)	rt	>98	52:48
10	$(CuOTf)_2$·PhMe	**L4** (2.5 mol %)	rt	83	88:12
11	**$(CuOTf)_2$·PhMe**	**L4 (2.5 mol %)**	**40**	**>98**	**99:1**
12	$Cu(MeCN)_4PF_6$	**L4** (2.5 mol %)	40	73	90:10
13	$Cu(MeCN)_4BF_4$	**L4** (2.5 mol %)	40	82	91:9

[a]Reactions conducted with allylic azide **2.21** (0.1 mmol), alkyne **2.22** (0.12 mmol), in dimethoxyethane (0.2 M), with 2.5 mol % [Cu] and either 2.5 mol % or 5 mol % ligand. Yields based on ^{1}H NMR analysis using 1,3,5-trimethoxybenzene as an internal standard. Chiral HPLC was used to determine er. All yields and er values reflect the average of duplicate trials.

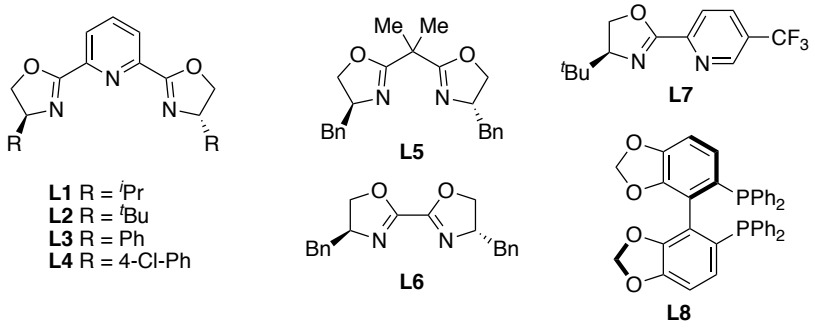

In the optimized process, PYBOX ligands provide measurable enantioselectivity (Table 2.1, **L1**-**L4**). Therefore, a series of PYBOX derivatives were prepared to finely tune the enantioselectivity. The PYBOX ligands could be prepared from commercially available 2,6-dicyanopyridine (**2.24**) and amino acids **2.26**. The preparation of PYBOX was adapted

from a known procedure with slight modification.[51] Bis(carbimidate) **2.25** was accessed via methanolysis under basic conditions. Amino alcohols **2.27** were prepared by reduction of commercial amino acids **2.26** using sodium borohydride. The condensation of **2.25** and **2.27** afforded PYBOX ligand **2.28**.‡

Scheme 2.5. Preparation of PYBOX Ligands

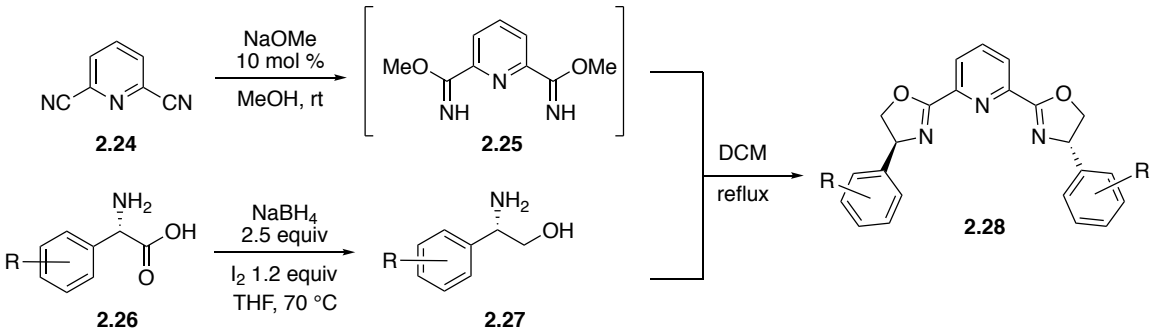

With more than fifteen PYBOX ligands in hand, a second ligand screen was conducted (Table 2.2). For substrate availability and accessibility, azide **2.29** and alkyne **2.30** were utilized in the PYBOX ligand optimization. Commercially available PYBOX ligand provides moderate ee (**L1**-**L3**), and the ee's are fairly consistent with those in Table 2.1. The *para*-chlorophenyl substituents (**L4**) still provided the highest enantioselectivity thus far. The enantioselectivity significantly decreased if the chloro substituent is on the *ortho*- position (**L5**). *Para*-fluorophenyl PYBOX (**L6**) gave comparable enantioselectivity with a slightly higher isolated yield. However, the precursor of the ligand enantiomer is prohibitively expensive for further mechanistic studies, so **L4** was chosen as the optimal

‡ For more ligand preparations, see Supporting Information of this manuscript: *J. Am. Chem. Soc.* **2019**, *141*, 5135−5138.

ligand. Other electron rich or deficient substituents did not improve the enantioselectivity (**L11**-**L13**). Increasing the steric bulk of the substituents did not translate to the higher enantiomeric ratio (**L14**-**L16**). Introducing a more congested environment to the oxazole core did not improve the selectivity either (**L17**-**L20**). Among the PYBOX investigated here, 4-Cl-Ph-PYBOX (**L4**) was chosen as the optimal ligand.

The ligand purity has a significant impact on the enantioselectivity of the E-CuAAC reaction. The PYBOX ligands were prepared from commercial amino acids, which have varying ee. After performing a double condensation of the amino alcohol to the pyridine core, a *meso*- impurity was observed by chiral HPLC. This *meso*- impurity decreases the enantiomeric ratio of triazole product because of the negative non-linear effect (*vide infra*). A ca. 92% pure **L4** (containing ca. 8% *meso*- impurity) resulted in 97:3 er of substrate **2.23**, while a >99% pure **L4** gave >99:1 er. Therefore, the synthesized PYBOX ligands were further purified by column chromatography and the purity was determined by chiral HPLC before use in an E-CuAAC reaction.

Table 2.2 Reaction Optimization – Ligand Screen[a]

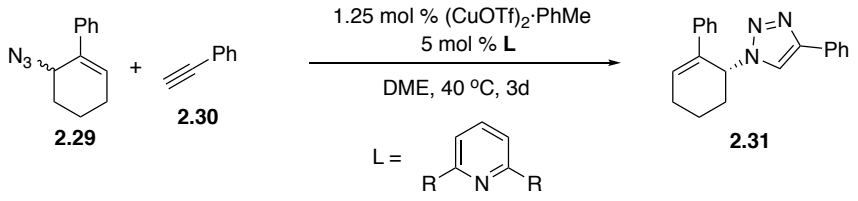

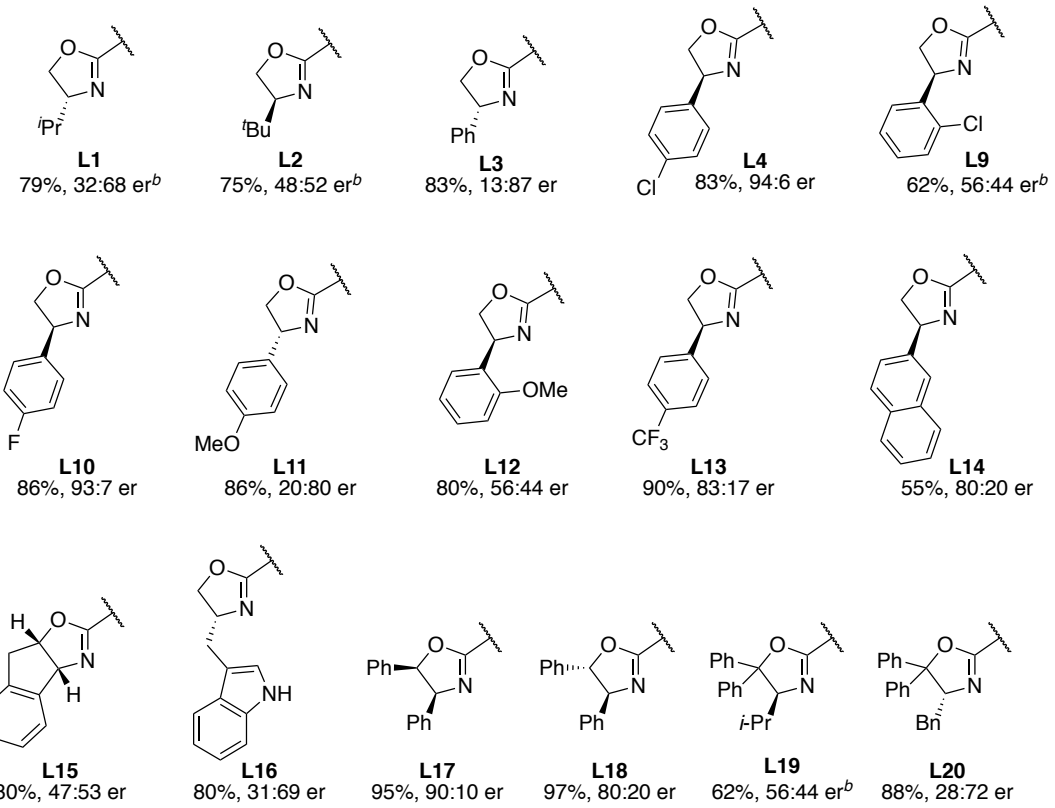

[a]Reactions conducted with allylic azide **2.29** (0.1 mmol), alkyne **2.30** (0.12 mmol), in dimethoxyethane (0.2 M), with 1.25 mol % $(CuOTf)_2$·PhMe and 5 mol % PYBOX ligand. Isolated yields are reported. Chiral HPLC was used to determine er. All er values reflect the average of duplicate trials.

2.3.2 Substrate Scope

With the optimal reaction conditions in hand, the scope of the E-CuAAC reaction was investigated (Table 2.3). Using the azide as the limiting reagent, the model substrate **2.23** was isolated in 95% yield and >99:1 er. The scope of the alkyne was quite broad.

Electron rich and electron deficient aryl alkynes could participate in the E-CuAAC (**2.32**−**2.40**). A crystal of product **2.38** was suitable for diffraction analysis, which unambiguously assigned the absolute configuration of the product generated from the (*S*,*S*)-4-Cl-Ph-PYBOX/Cu catalyst as having the (*R*)-configuration.[‡] The configuration of the other products was assigned based on analogy to product **2.38**. An *ortho*-substituted arene provided an acceptable yield in high er (**2.40**). An alkyne containing a *tert*-butyl (**2.41**), heterocycle (**2.42**), protected alcohol (**2.43**), ketone (**2.44**), and cyclopropyl (**2.45**) group could all be used in E-CuAAC.

A variety of azide components were conducted. The alkyls on the propiolate could be varied (**2.46** and **2.47**). The arene component on the cyclohexene ring could be modified, covering from electron neutral to electron deficient (**2.31, 2.48**, and **2.49**) The cyclohexyl-ring could be modified (**2.50**), contracted (**2.51**), or expanded (**2.52**). Dihydropyran derivative (**2.53**) resulted in high yield and moderate er, but alkyne component as limiting reagent was required. We hypothesized that the oxygen somehow restrains the configuration of the 6-membered ring and thus affects the Winstein rearrangement. The substituents on the 2-position of the cyclohexene core could be varied (**2.54** and **2.55**). Acyclic allylic azide could proceed with high yield and er (**2.56**).

[‡]For a full list of ligands investigated, see the Supporting Information of this manuscript: *J. Am. Chem. Soc.* **2019**, *141*, 5135−5138.

Table 2.3 Substrate Scope of DKR E-CuAAC[a]

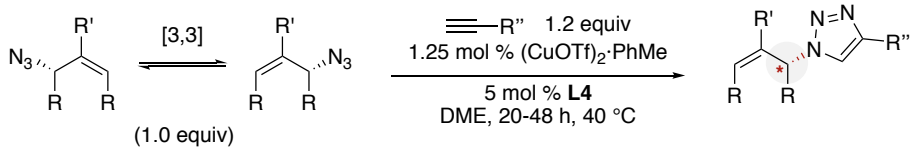

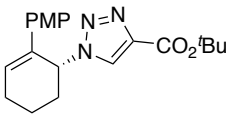

2.23, 95%, >99:1 er

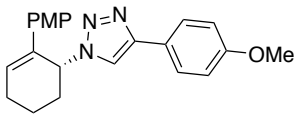

2.32, 89%, 93:7 er

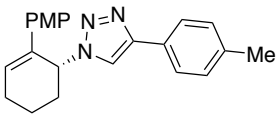

2.33, 91%, 93:7 er

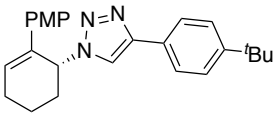

2.34, 96%, 92:8 er

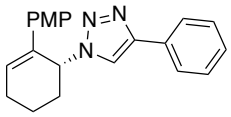

2.35, 85%, 96:4 er

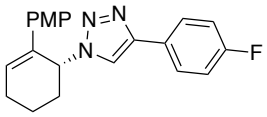

2.36, 90%, 93:7 er

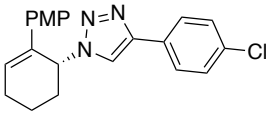

2.37, 91%, 92:8 er

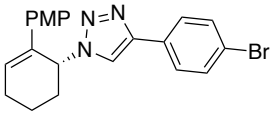

2.38, 86%, 95:5 er

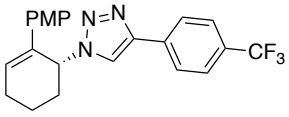

2.39, 92%, 90:10 er

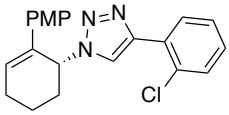

2.40, 80%, 95:5 er

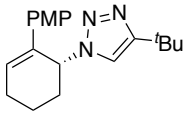

2.41, 71%, 92:8 er

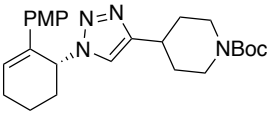

2.42, 96%, 93:7 er

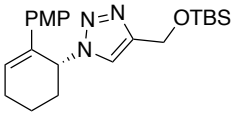

2.43, 95%, 94:6 er

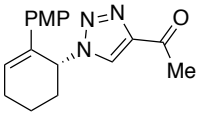

2.44, 96%, 92:8 er

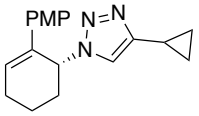

2.45, 80%, 97:3 er

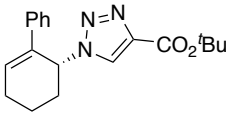

2.46, 96%, 95:5 er

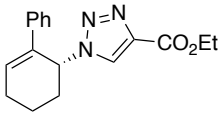

2.47, 85%, 96:4 er

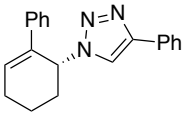

2.31, 85%, 96:4 er

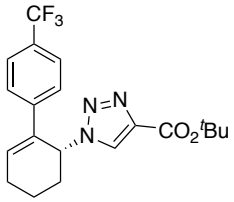

2.48, 96%, 94:6 er

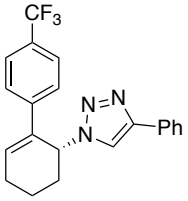

2.49, 82%, 93:7 er

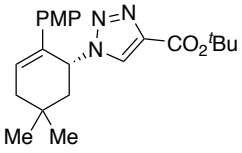

2.50, 85%, 96:4 er

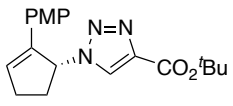

2.51, 79%, 94:6 er

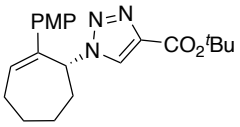

2.52, 99%, 90:10 er

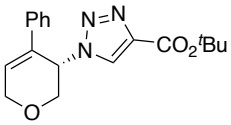

2.53,[b] 90%, 85:15 er

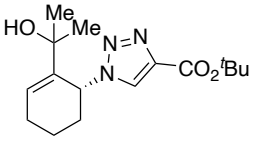

2.54, 96%, 90:10 er

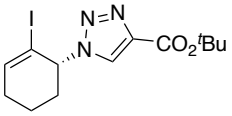

2.55,[b] 89%, 87:13 er

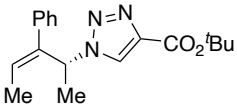

2.56, 92%, 86:14 er
93:7 *E*:*Z*

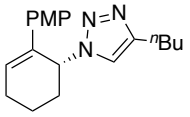

2.57, 63%, 86:14 er

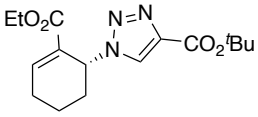

2.58, 94%, 78:22 er

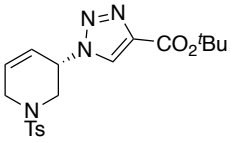

2.59, 85%, 50:50 er
96%, 76:24 er[b]

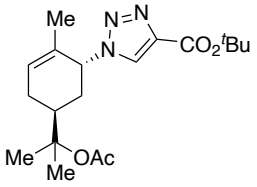

2.60, 97%, 50:50 dr
73%, 60:40 dr[b]

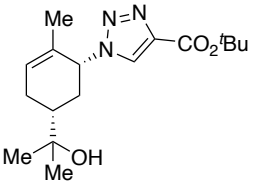

2.61, 93%, 51:49 dr

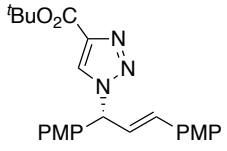

2.62, 91%, 70:30 er

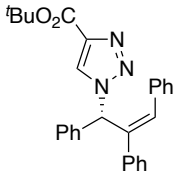

2.63, 79%, 73:27 er
>99:1 E/Z

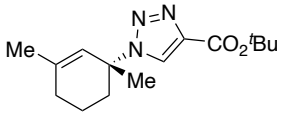

2.64, 67%, 66:34 er

[a]Yields are reported for isolated and purified products. Enantiomeric ratio was determined by chiral HPLC. Yields and er values reflect the average of duplicate trials. [b]Reactions used alkyne as limiting reagent.

However, few azide substrates reflect the limitation of this E-CuAAC condition (**2.57**-**2.64**). The alkyne component with a linear carbon chain gave a moderate reaction

yield with mediocre er (**2.57**). An ester group on the 2-position of cyclohexene motif decreases the enantioselectivity (**2.58**). Tetrahydropyridine derivative resulted in racemic triazole under DKR condition (**2.59**). The heteroatom in the 6-membered ring likely slows the Winstein rearrangement. The reaction forming product **2.43** has the same complication. The er was increased to 76:24 under kinetic resolution conditions (excess azide and limiting alkyne). The terpene derivative gave nearly racemic triazole in both DKR and KR conditions (**2.60** and **2.61**). Chalcone derivatives could be applied to the E-CuAAC condition, but a 70:30 er was observed (**2.62** and **2.63**). Tertiary allylic azide lowered both the yield and enantioselectivity (**2.64**). Not only did the steric bulk hamper the azide binding to the copper center, but the lack of substituents on the 2-position of the cyclohexene ring also decreased the enantioselectivity. Overall, although few substrates gave low enantioselectivity, the broadness of the substrate scope demonstrates the robustness of the E-CuAAC by DKR using allylic azides.

Several additional examples demonstrate that the E-CuAAC is viable in a complex molecular setting (Table 2.4). Derivatives of vitamin E (**2.65**), estrone (**2.66**), glucose (**2.67**), gibberellic acid (**2.68**), mycophenolate mofetil (**2.69**), and moexipril (**2.70**) could all be successfully "clicked" by E-CuAAC in near perfect yield and excellent selectivity. This illustrates that E-CuAAC is capable of generating α-*N*-chiral triazoles in the presence of densely functionalized molecules with robust stereochemical fidelity.

Table 2.4 DKR E-CuAAC in Complex Molecular Setting[a]

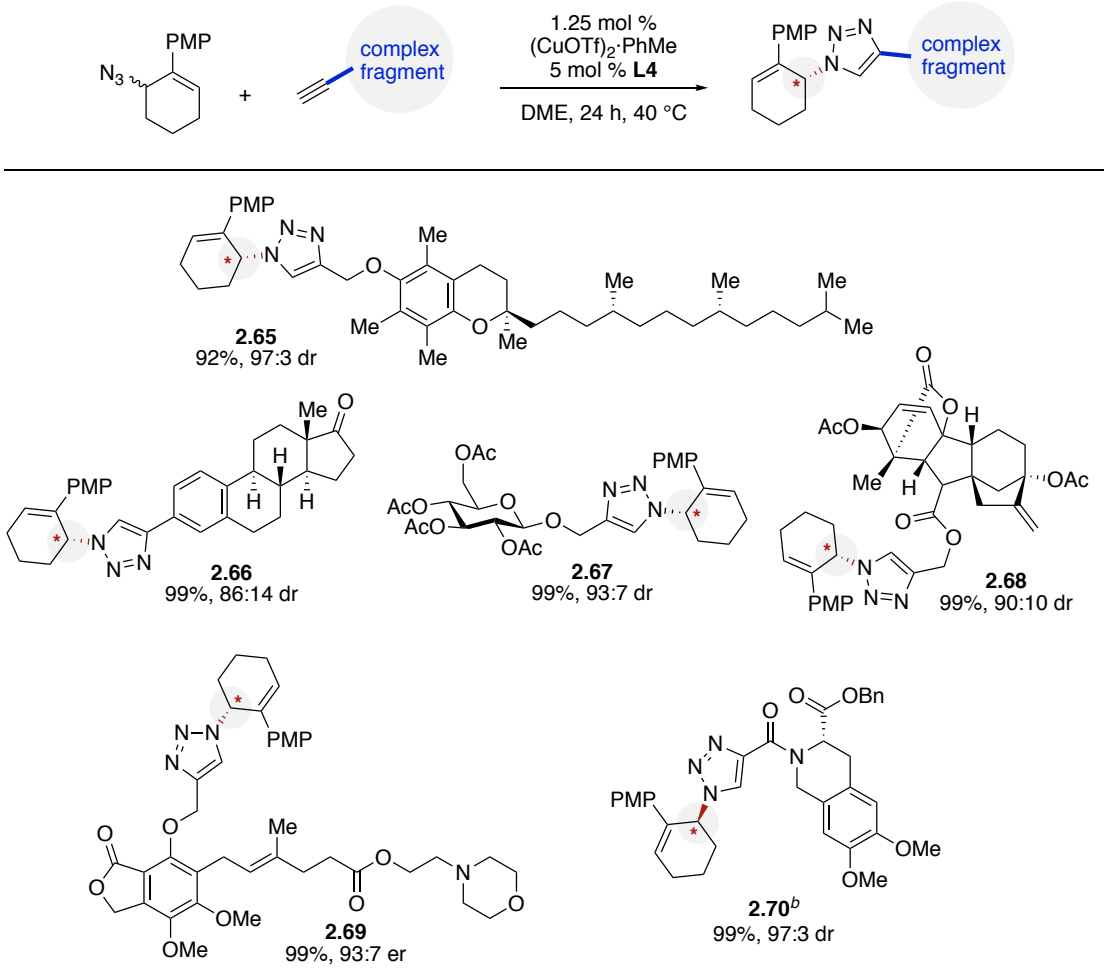

[a]Yields are reported for isolated and purified products. Enantiomeric ratio was determined by chiral HPLC. Yields and er values reflect the average of duplicate trials. [b]Substrate **2.63** was prepared using (*R*,*R*)-4-Cl-Ph-PYBOX ligand (***ent*-L4**).

2.3.3 Mechanistic Investigations

With a broad substrate scope in hand, attention was turned to mechanistic studies of the DKR E-CuAAC reaction. A non-linear effect study was conducted (Figure 2.1a). The enantiomeric excess (ee) of the product was determined with varying ligand's enantiopurity. It has been reported that E-CuAAC by desymmetrization can proceed with

a positive[52,53] or negative[54] non-linear effect. A negative non-linear effect was observed for this E-CuAAC reaction. This observation reflects the hypothesis that the active catalyst is a dicopper complex. The pyridine nitrogen, the nitrogen from the adjacent oxazole, and one nitrogen from the other PYBOX oxazole bind to one copper(I) center. The same binding repeats to another copper(I) ion and affords a dimerization structure of the Cu(I)-PYBOX complex (Figure 2.1b). The PYBOX scaffold may promote dimerization, which is consistent with crystallographic data on Cu(I)-PYBOX complexes[55,56] and reflects the proposed dicopper complex in the CuAAC catalytic cycle.[57] This unique binding mode of the PYBOX ligand to Cu(I) results in enantioselectivity of the triazole products (Table 2.1, **L1**-**L4**). Other chiral phosphine and nitrogen ligands provide limited enantioselectivity (Table 2.1, **L5**-**L8**).

In addition to the unique PYBOX binding, the cationic copper(I) precatalyst also plays an important role. Díez and coworkers reported that PYBOX ligands form complexes with the various equivalence of CuX, forming $[Cu_4I_4(^{i}Pr\text{-}PYBOX)_2]$ and $[Cu_2Cl(^{i}Pr\text{-}PYBOX)_2][CuCl_2]$, respectively.[56] In either complexes, the halide binds to the copper(I) center. The strong copper-halide interaction results in one of the nitrogen ligands dangling from the copper(I) center before binding to azide or alkyne substrate. This explains why copper(I) iodide gave poor enantioselectivity in the presence of the PYBOX ligand (Table 2.1, entry 1).

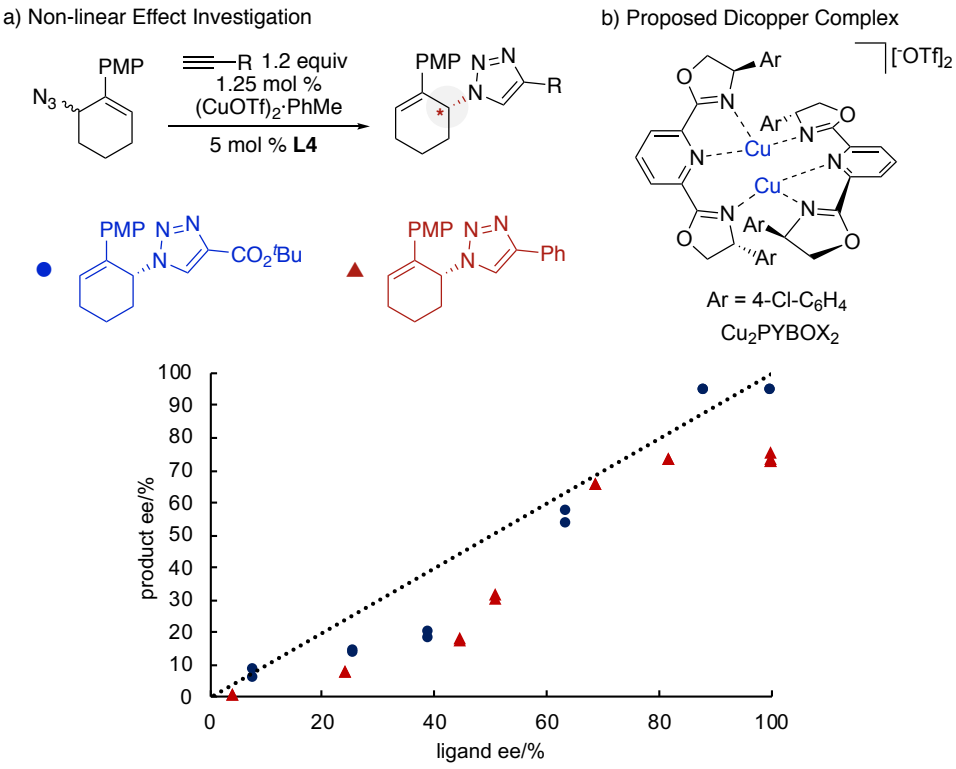

Figure 2.1 Non-linear Effect. a) Non-linear Effect Investigation b) Proposed Dicopper Complex

To further demonstrate the features of this E-CuAAC reaction, the model substrate was subjected to (*R*)-1-phenyl-2-propyn-1-ol (**2.71**, Scheme 2.6). Both enantiomers of the ligand were used to test for matched/mismatched behavior related to double diastereoselectivity. The alkyne substrate **2.71** is a chiral molecule. When it interacts with the chiral dimeric Cu(I)-PYBOX complex, two diastereomeric intermediates are generated. The resulting intermediate with relatively lower free energy, the so-called "matched" pair, gives higher product diastereoselectivity. On the other hand, the other diastereomeric intermediate, the so-called "mismatched" pair, generates the corresponding diastereomeric product with lower diastereoselectivity. In this E-CuAAC reaction, the (*S*,*S*)-4-Cl-Ph-

PYBOX (**L4**) and the alkyne **2.71** are the matched pair, resulting in higher yield and diastereoselectivity of triazole **2.72**. When the ligand enantiomer (***ent*-L4**) was applied, the triazole product **2.73** was obtained with a lower yield and diastereoselectivity. The opposite configuration of the α-*N* carbon center illustrates that this E-CuAAC reaction is ligand-controlled, instead of substrate-controlled. The high yields and diastereoselectivity also indicate the robustness of the copper(I) catalyst.

Scheme 2.6 Test for Matched/Mismatched Behavior

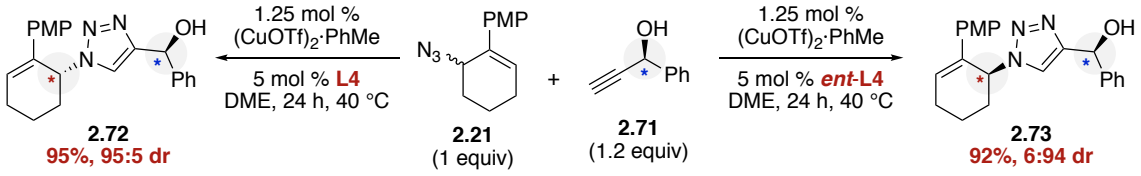

2.4 Conclusion

Dynamic kinetic resolution is a powerful means to achieve asymmetric synthesis. The enantioselective CuAAC (E-CuAAC) by DKR had not been investigated. Herein, an effective system for the E-CuAAC "click" reaction is reported that is enabled by the dynamic kinetic resolution of allylic azides. The reaction proceeds in high yield and high selectivity. The scope of this process is broad and the reaction can proceed in a complex molecular environment. The mechanistic investigation reveals that this E-CuAAC reaction is ligand-controlled. The active catalyst is a dimeric [Cu(I)-PYBOX]$_2$ complex and a negative non-linear effect was observed.

2.5 Experimental

2.5.1 Substrate Synthesis

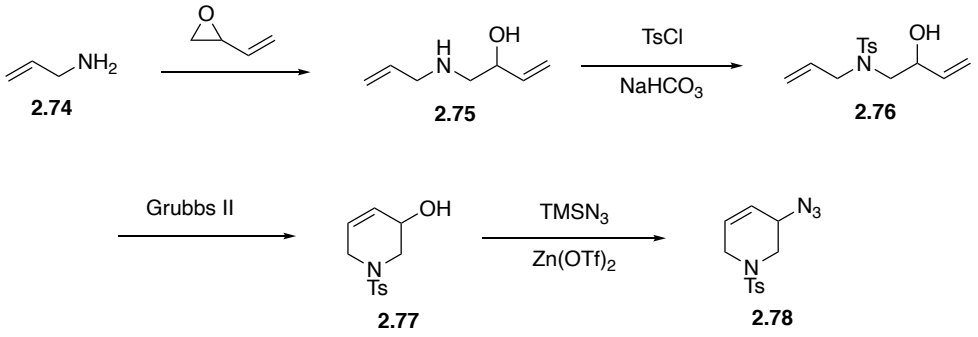

The preparation of hydroxyamine **2.75** and *N*-tosyl protected hydroxyamine **2.76** was adapted from a known procedure.[58] A round bottom flask was equipped with a condenser and charged with stir bar, butadiene monoxide (0.81 mL, 9.9 mmol), allylamine (2.3 mL, 31 mmol), and water (45 mL). The reaction was heat to 100 °C. After 6 h, the reaction was cooled to ambient temperature. A solution of sodium hydroxide (2 mL, 5 M aqueous solution) was added, and the resulting solution was extracted with DCM (50 mL x 3). The combined organic solution was washed with brine, dried ($MgSO_4$), filtered, and concentrated under reduced pressure. The resulting crude **2.75** (1.04 g, 82%) was used without further purification.

A 2-necked round bottom flask was charged with crude hydroxyamine **2.75** (prepared above, ca. 8.2 mmol), sodium bicarbonate (1.74 g, 9.1 mmol), and ethanol (20 mL) under argon atmosphere using Schlenk technique. The reaction was cooled into an acetone/dry ice bath. Dropwise addition of tosyl chloride (10 mL, 0.9 M in ethanol) was conducted over 10 minutes. The reaction was gradually warmed up. After 16 h, the reaction was filtered through Celite and rinsed with ethyl acetate. The resulting solution was washed

with water (3 x 50 mL), brine, dried ($MgSO_4$), filtered, and concentrated under reduced pressure. Purification by column chromatography (gradient EtOAc/hexane from 0-60%) afforded *N*-tosyl protected hydroxyamine **2.76** in 39% yield (910 mg) as a colorless liquid. The characterization of this material has been reported.[58] The obtained material provided an identical ^1H NMR.

A 2-necked round bottom was charged with Grubbs Catalyst® 2nd Generation (82 mg, 0.10 mmol) and a stir bar in a nitrogen-filled glovebox. The flask was removed from the glovebox and filled with argon atmosphere using Schlenk technique. Dichloromethane (10 mL) was added to the flask. The addition of *N*-tosyl protected hydroxyamine **2.76** (50 mL, 0.07 M in DCM) was conducted over 30 minutes. After 16 h, the solvent was removed under reduced pressure and the crude was loaded to the cartridge. Purification by column chromatography (gradient EtOAc/hexane from 0-60%) afforded *N*-protected piperidine **2.77** in 90% yield (734 mg) as a white solid. The characterization of this material has been reported.[58] The obtained material provided an identical ^1H NMR.

A 20 mL vial was charged with *N*-protected piperidine **2.77** (112 mg, 0.44 mmol), and toluene (1 mL). The reaction was cooled into an ice bath. Diphenyl phosphoryl azide (0.11 mL, 0.53 mmol) was added to the vial followed by DBU (80 µL, 0.53 mmol). After 16 h, the reaction was quenched by the addition of water (10 mL). The resulting solution was extracted with EtOAc (10 mL x 3). The combined organic solution was washed with brine, dried ($MgSO_4$), filtered, and concentrated under reduced pressure. Purification by column chromatography (gradient EtOAc/hexane from 0-50%) afforded allylic azide **2.78** in 94% yield (116 mg) as a white solid.

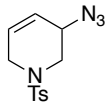

2.78

^{1}H NMR (400 MHz, $CDCl_3$): δ 7.68 (d, *J* = 8.3 Hz, 2H), 7.34 (d, *J* = 8.0 Hz, 2H), 6.06 – 5.96 (m, 1H), 5.88 – 5.78 (m, 1H), 3.81 (br, 1H), 3.73. (d, *J* = 17.1 Hz, 1H), 3.52 – 3.42 (m, 1H), 3.37 (dd, *J* = 12.0, 4.8 Hz, 1H), 3.19 (dd, *J* = 12.1, 4.1 Hz, 1H), 2.43 (s, 3H). **^{13}C{^{1}H} NMR (101 MHz, $CDCl_3$)**: δ 144.1, 133.0, 129.9, 128.3, 127.6, 122.8, 53.7, 47.6, 44.6, 21.5. **IR (NaCl, thin film, cm^{-1})**: 3041, 2918, 2845, 2101, 1591, 1446, 1351, 1166. **HRMS (ESI-TOF)**: $[M+Na]^+$ Calculated for $C_{12}H_{14}N_4O_2SNa^+$, 301.0730; found, 301.0739.

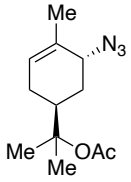

2.79

The preparation of allylic azide **2.79** was adapted from a known procedure.[59] The obtained material provided an identical ^{1}H NMR.

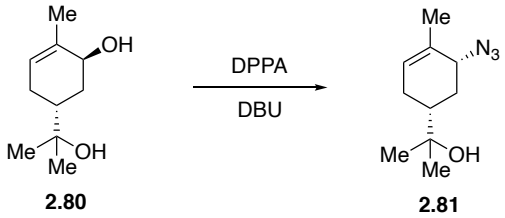

2.80 **2.81**

A 20 mL vial was charged with *trans*-sobrerol (**2.80**, 170 mg, 1.00 mmol), and toluene (2 mL). The reaction was cooled into an ice bath. Diphenyl phosphoryl azide (0.26 mL, 1.2 mmol) was added to the vial followed by DBU (0.18 μL, 1.2 mmol). After 16 h, the reaction was quenched by the addition of water (10 mL). The resulting solution was

extracted with EtOAc (10 mL x 3). The combined organic solution was washed with brine, dried ($MgSO_4$), filtered, and concentrated under reduced pressure. Purification by column chromatography (gradient EtOAc/hexane from 0-50%) afforded allylic azide **2.81** in 83% yield (161 mg) as a colorless oil.

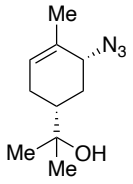

2.81

^{1}H NMR (400 MHz, $CDCl_3$): δ 5.61 – 5.51 (m, 1H), 3.89 – 3.74 (m, 1H), 2.33 – 2.22 (m, 1H), 2.12 – 1.97 (m, 1H), 1.92 – 1.75 (m, 2H), 1.75 – 1.68 (m, 3H), 1.67 – 1.56 (m, 1H), 1.43 – 1.30 (m, 1H), 1.17 (s, 3H), 1.16 (s, 3H). **^{13}C{^{1}H} NMR (101 MHz, $CDCl_3$)**: δ 132.6, 126.0, 72.0, 62.7, 44.2, 30.3, 27.5, 26.8, 26.1, 19.6. **IR (NaCl, thin film, cm^{-1})**: 3046, 2972, 2095, 1451, 1378. **HRMS (EI-TOF)**: $[M-N_2]^+$ Calculated for $C_{10}H_{17}NO^+$, 167.1305; found, 167.1299.

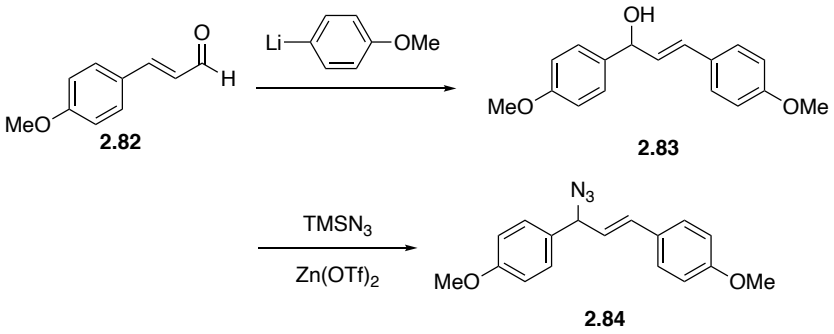

2.82 **2.83** **2.84**

A 2-necked round bottom flask was charged with ^{n}BuLi (2.2 mL, 2.5 M in hexanes, 5.5 mmol), and THF (5 mL) under argon atmosphere using Schlenk technique. The reaction was cooled in an acetone/dry ice bath. Dropwise addition of 4-bromoanisole (0.69 mL, 5.5 mmol) was conducted over 5 mins. The reaction was stirred at the same temperature for 1

h. A solution of 4'-methoxycinnamaldehyde (3 mL, 1.7 M in THF, 5.1 mmol) was added slowly. The reaction was gradually warmed up to ambient temperature. After 16 h, the reaction was quenched by the addition of water (10 mL). The resulting solution was extracted with DCM (30 mL x 3). The combined organic solution was washed with brine, dried ($MgSO_4$), filtered, and concentrated under reduced pressure. Purification by column chromatography (gradient EtOAc/hexane from 0-50%) afforded allylic alcohol **2.83** in quantitative yield (1.23 g) as an orange oil. The characterization of this material has been reported.[60] The obtained material provided an identical ^{1}H NMR.

A 20 mL vial was charged with zinc trifluoroacetate hydrate (32 mg, 0.11 mmol) and DCM (3 mL). The reaction was cooled in an ice bath. Trimethylsilyl azide (0.33 mL, 2.5 mmol) was added followed by the stock solution of allylic alcohol **2.83** (2.0 mL, 0.56 M in DCM, 1.1 mmol). After 30 mins, the reaction was quenched by the addition of triethylamine (1 mL). The resulting solution was pass through a short plug of basic alumina. The resulting solution was concentrated under reduced pressure. The afforded crude material was directly loaded to the cartridge. Purification by column chromatography (gradient EtOAc/hexane from 0-50%) afforded allylic alcohol **2.84** in 75% yield (249 mg) as a white solid.

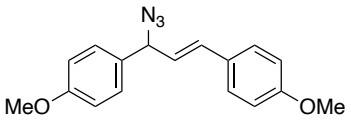

2.84

^{1}H NMR (400 MHz, $CDCl_3$): δ 7.40 (d, *J* = 8.7 Hz, 2H), 7.35 (d, *J* = 8.7 Hz, 2H), 6.97 (d, *J* = 8.7 Hz, 2H), 6.92 (d, *J* = 8.7 Hz, 2H), 6.69 (d, *J* = 15.7 Hz, 1H), 6.22 (dd, *J* = 15.7, 7.2 Hz, 1H), 5.19 (d, *J* = 7.2 Hz, 1H), 3.852 (s, 3H), 3.847 (s, 3H). **^{13}C{^{1}H} NMR (101 MHz,**

$CDCl_3$): δ 159.7, 159.5, 132.2, 131.0, 128.8, 128.4, 128.0, 125.0, 114.2, 114.1, 67.0, 55.3 (tentatively assigned as 2C). **IR (NaCl, thin film, cm^{-1})**: 2997, 2953, 2836, 2095, 1607, 1512, 1301, 1252, 1174, 1034. **HRMS (EI-TOF)**: $[M-N_2]^+$ Calculated for $C_{17}H_{17}NO_2^+$, 267.1254; found, 267.1243.

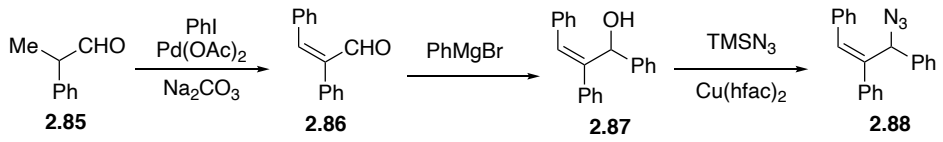

The synthesis of aldehyde **2.86** was adapted from a known procedure.[61] A 2-necked round bottom flask was equipped with a condenser and charged with palladium acetate (25 mg, 0.11 mmol) and sodium carbonate (1.08 g, 10.2 mmol) under argon atmosphere using Schlenk technique. A separate 20 mL vial was charged with 2-phenylpropanal (673 mg, 5.02 mmol), iodobenzene (2.60 g, 12.7 mmol), and DMSO (18 mL) to prepare a stock solution. The stock solution of substrates was added to the flask using syringe. The reaction was heated to 120 °C. After 16 h, the reaction was cooled to ambient temperature and filtered through a plug of Celite. The resulting solution was diluted with water (50 mL) and extracted with hexanes (50 mL x3). The combined organic solution was washed with brine, dried ($MgSO_4$), filtered, and concentrated under reduced pressure. Purification by column chromatography (gradient EtOAc/hexane from 0-30%) afforded aldehyde **2.86** in 34% yield (354 mg) as a white solid. The characterization of this material has been reported.[62] The obtained material provided an identical ^1H NMR.

A 2-necked round bottom was charged with aldehyde **2.86** (278 mg, 1.33 mmol) and THF (5 mL) under argon atmosphere using Schlenk technique. The reaction was cooled into an ice bath. Phenylmagnesium bromide (0.53 mL, 1.6 M in diethyl ether, 1.60 mmol) was added slowly. After 30 mins, the reaction was quenched by the addition of

water (10 mL). The resulting solution was diluted with water (50 mL) and extracted with ethyl acetate (20 mL x3). The combined organic solution was washed with brine, dried ($MgSO_4$), filtered, and concentrated under reduced pressure. Purification by column chromatography (gradient EtOAc/hexane from 0-30%) afforded allylic alcohol **2.87** in 95% yield (364 mg) as a white solid. The characterization of this material has been reported.[63] The obtained material provided an identical ^{1}H NMR.

A 20 mL vial was charged with copper(II) hexafluoroacetylacetonate (125 mg, 0.262 mmol) and DCM (3 mL). The reaction was cooled in an ice bath. Trimethylsilyl azide (0.37 mL, 2.79 mmol) was added followed by the stock solution of allylic alcohol **2.87** (5.0 mL, 0.25 M in DCM, 1.3 mmol). After 16 h, the reaction was quenched by the addition of triethylamine (1 mL). The resulting solution was pass through a short plug of basic alumina. The resulting solution was concentrated under reduced pressure. The afforded crude material was directly loaded to the cartridge. Purification by column chromatography (gradient EtOAc/hexane from 0-50%) afforded allylic azide **2.88** in 90% yield (357 mg) as a pale yellow solid.

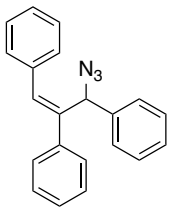

***Z*-2.88**

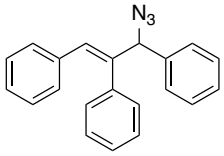

***E*-2.88**

Allylic azide **2.88** was isolated as a mixture of *Z*/*E* isomer in an 8.3:1 ratio. **^{1}H NMR (400 MHz, $CDCl_3$)** of *Z*-**2.88**: δ 7.47 – 7.00 (m, 15H), 6.94 (s, 1H), 5.56 (s, 1H). **^{1}H NMR (400 MHz, $CDCl_3$)** of *E*-**2.88**: δ 7.52 – 7.00 (m, 15H), 6.94 (s, 1H), 6.31 (s, 1H). **^{13}C{^{1}H} NMR (101 MHz, $CDCl_3$)** of *Z*-**2.88**: δ 140.1, 137.9, 137.5, 135.9, 129.8, 129.5, 129.4, 128.60,

128.57, 128.55, 128.2, 128.1, 127.7, 127.4, 72.3. **IR (NaCl, thin film, cm^{-1})**: 3057, 2026, 2099, 1600, 1492, 1447, 1254. **HRMS (EI-TOF)**: $[M\text{-}N_2]^+$ Calculated for $C_{21}H_{17}N^+$, 283.1356; found, 283.1339.

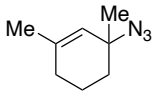

2.89

The preparation of allylic azide **2.89** was adapted from a known procedure.[59] The obtained material provided an identical ^{1}H NMR.

2.5.2 E-CuAAC by DKR

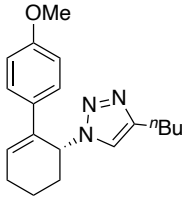

2.57

^{1}H NMR (400 MHz, $CDCl_3$): δ 7.17 (d, *J* = 8.9 Hz, 2H), 7.14 (s, 1H), 6.77 (d, *J* = 8.9 Hz, 2H), 6.46 (t, *J* = 4.0 Hz, 1H), 5.77 (br, 1H), 3.75 (s, 3H), 2.65 – 2.55 (m, 2H), 2.49 – 2.38 (m, 1H), 2.38 – 2.21 (m, 2H), 2.21 – 2.09 (m, 1H), 1.82 – 1.70 (m, 1H), 1.67 – 1.41 (m, 3H), 1.25 (h, *J* = 7.3 Hz, 2H), 0.87 (t, *J* = 7.3 Hz, 3H). **^{13}C{^{1}H} NMR (101 MHz, $CDCl_3$)**: δ 159.0, 147.4, 132.8, 131.2, 130.1, 126.4, 120.3, 113.9, 56.2, 55.2, 31.4, 31.0, 25.6, 25.4, 22.2, 17.3, 13.8. **IR (NaCl, thin film, cm^{-1})**: 2934, 2870, 1607, 1514, 1250, 1037. **HRMS (ESI-TOF)**: $[M+Na]^+$ Calculated for $C_{19}H_{25}N_3ONa^+$, 334.1890; found, 334.1891.

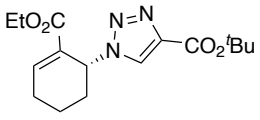

2.58

^{1}H NMR (400 MHz, $CDCl_3$): δ 7.91 (s, 1H), 7.55 – 7.45 (m, 1H), 5.65 (br, 1H), 4.11 (q, *J* = 7.1 Hz, 2H), 2.59 – 2.42 (m, 1H), 2.38 – 2.19 (m, 2H), 2.06 – 1.95 (m, 1H), 1.79 – 1.67 (m, 1H), 1.59 (s, 9H), 1.58 – 1.69 (m, 1H), 1.17 (q, *J* = 7.1 Hz, 3H). **^{13}C{^{1}H} NMR (101 MHz, $CDCl_3$)**: δ 164.9, 160.2, 147.2, 140.6, 126.64, 126.55, 82.2, 61.0, 53.8, 29.6, 28.2, 25.5, 16.0, 14.0. **IR (NaCl, thin film, cm^{-1})**: 3127, 2980, 2938, 1715, 1533, 1367, 1247, 1153. **HRMS (ESI-TOF)**: $[M+Na]^+$ Calculated for $C_{16}H_{23}N_3O_4Na^+$, 344.1581; found, 344.1586.

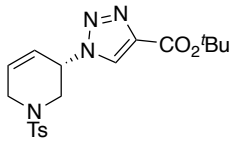

2.59

^{1}H NMR (400 MHz, $CDCl_3$): δ 8.08 (s, 1H), 7.61 (d, *J* = 8.4 Hz, 2H), 7.33 (d, *J* = 8.0 Hz, 2H), 6.24 – 6.15 (m, 1H), 6.00 – 5.90 (m, 1H), 5.42 (br, 1H), 4.00 (apparent d, *J* = 17.2 Hz, 1H), 3.69 (dd, *J* = 12.5, 3.7 Hz, 1H), 3.55 – 3.44 (m, 1H), 3.28 (dd, *J* = 12.5, 4.1 Hz, 1H), 2.43 (s, 3H), 1.62 (s, 9H). **^{13}C{^{1}H} NMR (101 MHz, $CDCl_3$)**: δ 159.8, 144.5, 141.4, 132.4, 130.01, 129.98, 127.7, 126.4, 121.9, 82.3, 54.4, 48.1, 44.6, 28.3, 21.6. **IR (NaCl, thin film, cm^{-1})**: 3148, 3057, 2980, 2931, 1718, 1537, 1367, 1351, 1224, 1168, 1040. **HRMS (ESI-TOF)**: $[M+Na]^+$ Calculated for $C_{19}H_{24}N_4O_4SNa^+$, 427.1410; found, 427.1425.

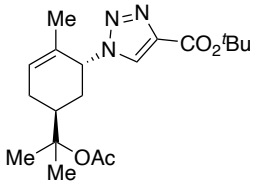

2.60

^{1}H NMR (400 MHz, $CDCl_3$): δ 7.94 (s, 1H), 6.01 – 5.92 (m, 1H), 5.22 – 5.13 (m, 1H), 2.35 – 2.12 (m, 2H), 2.10 – 1.96 (m, 1H), 1.90 (s, 3H), 1.91 – 1.81 (m, 2H), 1.69 – 1.65

(m, 3H), 1.62 (s, 9H), 1.38 (s, 6H). **$^{13}C\{^{1}H\}$ NMR (101 MHz, $CDCl_3$)**: δ 170.2, 160.3, 141.0, 130.2, 128.0, 126.3, 83.0, 82.4, 59.9, 37.4, 30.9, 28.2, 26.1, 23.3, 23.0, 22.3, 20.7. **IR (NaCl, thin film, cm^{-1})**: 3127, 2979, 2935, 1728, 1536, 1448, 1367, 1258, 1152, 1038. **HRMS (ESI-TOF)**: $[M+Na]^+$ Calculated for $C_{19}H_{29}N_3O_4Na^+$, 386.2050; found, 386.2061.

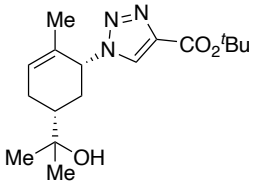

2.61

^{1}H NMR (400 MHz, $CDCl_3$): δ 7.95 (s, 1H), 5.83 – 5.73 (m, 1H), 5.38 – 5.25 (m, 1H), 2.50 – 2.41 (m, 1H), 2.31 – 2.15 (m, 1H), 2.11 – 1.99 (m, 1H), 1.89 – 1.78 (m, 1H), 1.78 – 1.70 (m, 1H), 1.61 (s, 9H), 1.38 (s, 3H), 1.52 (br, 1H), 1.23 (s, 3H), 1.21 (s, 3H). **$^{13}C\{^{1}H\}$ NMR (101 MHz, $CDCl_3$)**: δ 160.1, 141.7, 130.5, 128.0, 125.5, 82.3, 71.8, 62.8, 44.3, 33.1, 28.2, 27.7, 26.8, 26.4, 18.8. **IR (NaCl, thin film, cm^{-1})**: 3435, 2975, 2934, 1272, 1539, 1455, 1368, 1250, 1222, 1158, 1038. **HRMS (ESI-TOF)**: $[M+Na]^+$ Calculated for $C_{17}H_{27}N_3O_3Na^+$, 344.1945; found, 344.1955.

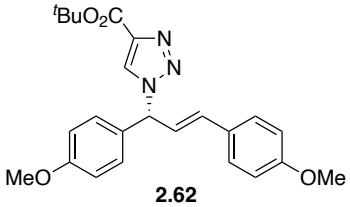

2.62

^{1}H NMR (400 MHz, $CDCl_3$): δ 7.96 (s, 1H), 7.34 (d, J = 8.7 Hz, 2H), 7.25 (d, J = 8.7 Hz, 2H), 6.94 (d, J = 8.7 Hz, 2H), 6.88 (d, J = 8.6 Hz, 2H), 6.57 – 6.47 (m, 2H), 6.44 – 6.34 (m, 1H), 3.84 (s, 3H), 3.83 (s, 3H), 1.62 (s, 9H).**$^{13}C\{^{1}H\}$ NMR (101 MHz, $CDCl_3$)**: δ 160.1, 160.00, 159.96, 141.5, 134.1, 129.4, 128.9, 128.13, 128.11, 126.2, 123.1, 114.5, 114.1, 82.4, 66.2, 55.4, 55.3, 28.2. **IR (NaCl, thin film, cm^{-1})**: 2978, 2934, 2836, 1726, 1608,

1513, 1367, 1254, 1176, 1153. **HRMS (ESI-TOF)**: $[M+Na]^+$ Calculated for $C_{24}H_{27}N_3O_4Na^+$, 444.1894; found, 444.1894.

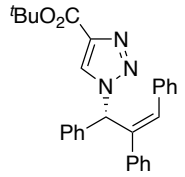

2.63

^{1}H NMR (400 MHz, $CDCl_3$): δ 7.96 (s, 1H), 7.49 – 7.32 (m, 5H), 7.30 – 7.21 (m, 3H), 7.21 – 7.06 (m, 5H), 6.98 – 6.83 (m, 3H), 6.27 (s, 1H), 1.62 (s, 9H). **^{13}C{^{1}H} NMR (101 MHz, $CDCl_3$)**: δ 160.1, 141.1, 138.6, 137.9, 135.8, 135.3, 132.1, 129.4, 129.2, 129.1, 129.02, 128.97, 128.3, 128.1, 128.0, 127.64, 127.57, 82.4, 71.3, 28.2. **IR (NaCl, thin film, cm^{-1})**: 3113, 3060, 2979, 2935, 1720, 1495, 1447, 1367, 1222, 1153, 1038, 698. **HRMS (ESI-TOF)**: $[M+Na]^+$ Calculated for $C_{21}H_{27}N_3O_2Na^+$, 460.1996; found, 400.2004.

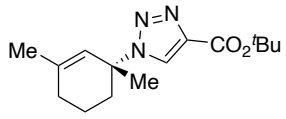

2.64

^{1}H NMR (400 MHz, $CDCl_3$): δ 8.01 (s, 1H), 5.53 (br, 1H), 2.48 – 2.37 (m, 1H), 2.06 – 1.96 (m, 2H), 1.82 (s, 3H), 1.81 – 1.76 (m, 1H), 1.74 (s, 3H), 1.72 – 1.63 (m, 1H), 1.61 (s, 9H), 1.32 – 1.18 (m, 1H). **^{13}C{^{1}H} NMR (101 MHz, $CDCl_3$)**: δ 160.6, 141.9, 140.0, 126.7, 122.9, 82.0, 61.5, 36.3, 29.7, 29.2, 28.2, 23.8, 18.4. **IR (NaCl, thin film, cm^{-1})**: 2977, 2935, 1732, 1711, 1535, 1366, 1232, 1217, 1152, 1031. **HRMS (ESI-TOF)**: $[M+Na]^+$ Calculated for $C_{15}H_{23}N_3O_2Na^+$, 300.1683; found, 300.1696.

Chapter 3 Enantioselective CuAAC by Kinetic Resolution*

3.1 Kinetic Resolution Introduction

Inspired by the DKR E-CuAAC work (Chapter 2), the next aim of this work was to expand the substrate scope to other azides. Our group member, Amy Ott, reported that benzylic azides and other activated azides undergo fast racemization in the presence of gold(I) and other precatalysts (Scheme 3.1a).[64] This investigation made benzylic azides promising candidates for E-CuAAC. Amy Ott conducted a series of preliminary experiments under CuAAC reaction conditions using benzylic azide **3.2** as a model substrate (Scheme 3.1b). The racemization studies disclosed that benzylic azide substrates need a stronger Lewis acid to promote racemization. Silver hexafluorophosphate was used to test the viability of E-CuAAC by DKR of benzylic azides **3.2**. Unfortunately, a silver mirror was observed when a stock solution of silver(I) catalyst and copper(I) catalyst were mixed. This observation suggested that silver(I) was not compatible with copper(I) precatalyst because they undergo spontaneously redox reaction to generate silver(0) and copper(II), respectively. Other precatalysts either did not facilitate the racemization or prohibited the downstream CuAAC reaction. Therefore, another strategy, kinetic resolution, was adapted to achieve E-CuAAC using benzylic azide substrates.

---

* Reprinted (adapted) with permission from Alexander, J. R.; Ott, A. A.; Liu, E.-C.; Topczewski, J. J. *Org. Lett.* **2019***, 21*, 4355 – 4358. Copyright (2019) American Chemical Society.

Scheme 3.1 Attempted E-CuAAC by DKR

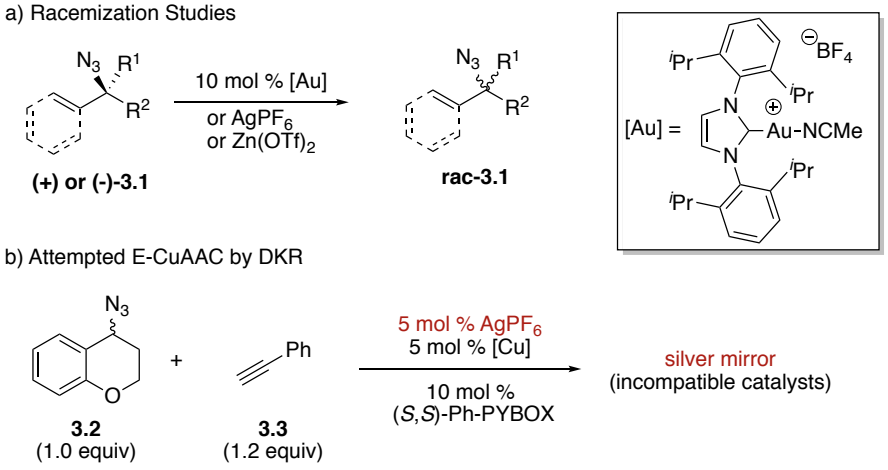

Since the first E-CuAAC by kinetic resolution was reported by Finn and Fokin,[45] only a few attempts to this strategy were reported.[48,50,65,66] In 2015, Brittain and co-workers disclosed an E-CuAAC by KR using quaternary oxindoles **3.4** (Scheme 3.2a). The copper(I) chloride and the chiral ligand (*R*,*R*)-Ph-PYBOX provided the enantioenriched triazole product **3.5** in 46% conversion with respect to excess reagent alkyne **3.4** and an 83:17 er of **3.5** was observed. Unlike Fokin and Finn's investigation, Brittain *et al*. utilized organic azides as the limiting reagent. However, there have been several drawbacks of this asymmetric synthesis. Firstly, although the triazole product showed a comparable enantiomeric ratio to that in Fokin and Finn's work, the substrate scope was quite limited. Only four benzyl azide derivatives were explored in their studies. Secondly, the reaction needs to be stopped at the very early stage to get higher er. A 90:10 er of triazole **3.5** was obtained when the reaction was terminated at 8% conversion. This limitation significantly decreases the synthetic efficiency if an enantioenriched triazole is the target molecule. The

last but not least, the catalyst loading was relatively high (12.5 mol %) to compensate for the slow reaction rate at a lower temperature (0 °C).

In 2020, Zhou *et al.* reported an enantioselective synthesis of *P*-chiral tertiary phosphine oxide (Scheme 3.2b).[50] Racemic alkynophosphine oxide **3.6** could be resolved by E-CuAAC in the presence of PYBOX ligand **3.8**. The substrate **(*R*)-3.6** preferentially "clicked" with azide **3.7** and generated enantioenriched triazole **3.9**. The er's were up to >99:1. A variety of functional groups could be tolerated, including thienyl, triazolyl, and other aryl substituents. This methodology is synthetic valuable because both unreacted starting azides and triazole products are enantioenriched, which can be utilized as chiral building blocks for downstream functionalization. In the same investigation, the authors also reported an E-CuAAC reaction by desymmetrization using *bis*-alkynophosphine oxide (not shown here). Both strategies provide an efficient way to prepare trisubstituted chiral phosphines, which can be applied in a variety of asymmetric syntheses.[67]

Inspired by Ott's conceptual approach to a DKR E-CuAAC using benzylic azides and the precedent KR E-CuAAC investigations, the second aim of this work is to utilize a KR strategy to prepare α-*N*-chiral triazoles (Scheme 3.2c). Enantioenriched triazole **3.11** can be accessed from the resolution of racemic azide **3.10** using alkynes as the limiting reagent. The remaining scalemic azide can be racemized under the catalytic condition and recycled as a racemic mixture, which can be utilized in the next batch of E-CuAAC reactions. Overall, this strategy can be regarded as a two-staged DKR E-CuAAC because the reaction products after two steps are enantiopure triazole and racemic azides. This approach broadens the scope of the E-CuAAC reaction that is developed by our group.

Scheme 3.2 E-CuAAC by Kinetic Resolution

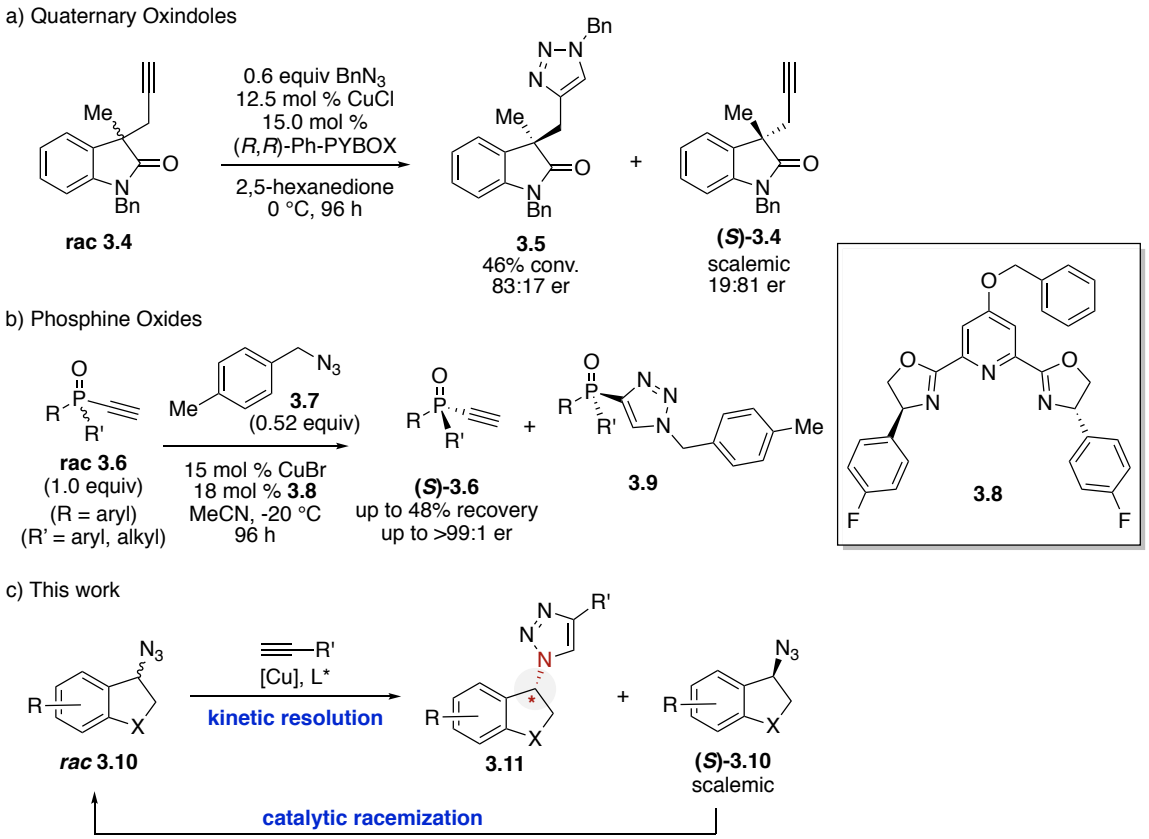

3.2 Experimental Results

3.2.1 Reaction Optimization

The PYBOX ligands have been widely used in numerous studies towards E-CuAAC reaction. The PYBOX ligands bind to the copper(I) center with three nitrogen atoms and thus can be viewed as an L_3 type ligand. In previous DKR E-CuAAC studies, a series of PYBOX ligands were synthesized and investigated. Similar to the L_3 type PYBOX ligand, trisoxazoline (TOX) is another promising chiral ligand for E-CuAAC. Firstly, TOX derivatives have been utilized in tremendous amounts of enantioselective synthesis, including conjugated addition,[68–73] cycloaddition,[74–77], cyclopropanation,[78] and other

reactions.[79–82] The three nitrogen atoms are L-type binding sites. Secondly, although no crystal structures of the TOX-metal complex have been reported, the three nitrogens potentially create a caged structure for dimeric copper(I) complex that is similar to Cu(I)-PYBOX dimeric structures. Third, chiral phosphine ligands are inappropriate for E-CuAAC reactions because phosphines can reduce azides to the corresponding amines via the Staudinger reduction.[83,84] Utilization of nitrogen-based ligand can avoid the possible side Staudinger reaction. Therefore, the study was commenced with the synthesis of the TOX ligand (Scheme 3.3). Trimethyl ester **3.12** was methylated to afford compound **3.13** without further purification. Triamide **3.14** was obtained upon the coupling reaction with (*S*)-phenylglycinol. Appel reaction of **3.14** with slight modification resulted in (*S*)-Ph-TOX **3.15** in 50% isolated yield.

Scheme 3.3 Synthesis of Ph-TOX Ligand

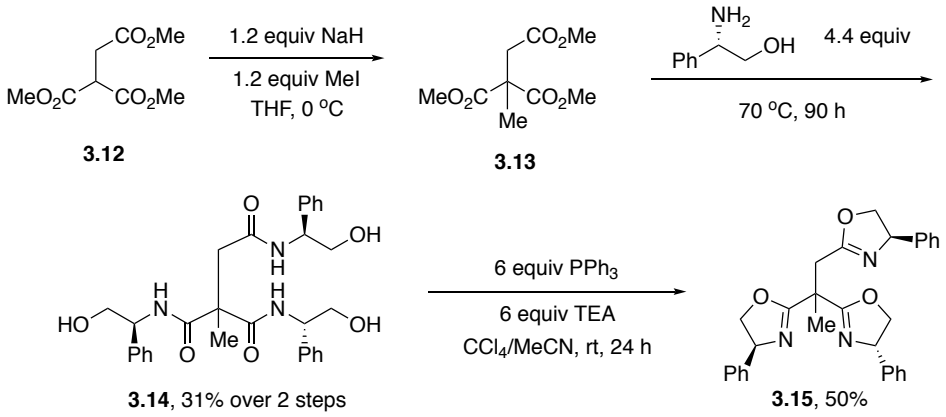

The reaction screen started with the investigation of a series of PYBOX ligands (Table 3.1), performed by our group member, Juliana Alexander.‡ Excess azide **3.16** was utilized in the presence of cationic copper(I) precatalyst. Most PYBOX ligands provided conversions and moderate to good er's, except **L12** and **L15**. *Tert*-butyl PYBOX **L2** resulted in a racemic product mixture. The complex Cu(I)-^{t}Bu-PYBOX is probably inactive because of the congested environment. The reaction was catalyzed by the trace amount of free copper(I) cation conducting background CuAAC. Among ligands investigated, 4-Cl-Ph-PYBOX **L4** and 4-F-Ph-PYBOX **L6** gave comparably high er of triazole products. PYBOX **L6** was chosen as the optimal ligand thus far since it provided a slightly higher er.

Reaction temperature plays a crucial role in kinetic resolution for the enantiomeric ratio. Therefore, the temperature investigation was conducted using **L6** as a ligand (Table 3.1).‡ The reaction was close to completion at ambient temperature after 72 h (entry 1). The enantioselectivity was slightly improved with decreasing reaction temperature, albeit the yield was lower (entries 2-4). The optimal reaction temperature was 0 °C because the yield was moderate with acceptably high er.

‡ For more ligand and temperature investigations, see Supporting Information of this manuscript: *Org. Lett.* **2019**, *21*, 4355–4358.

Table 3.1 Ligand Screen 1[a]

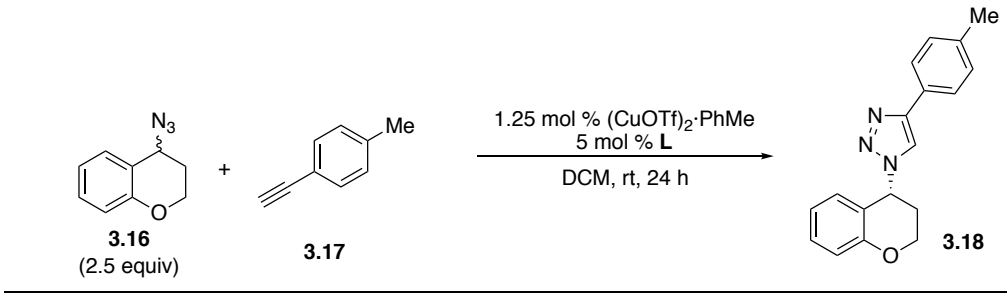

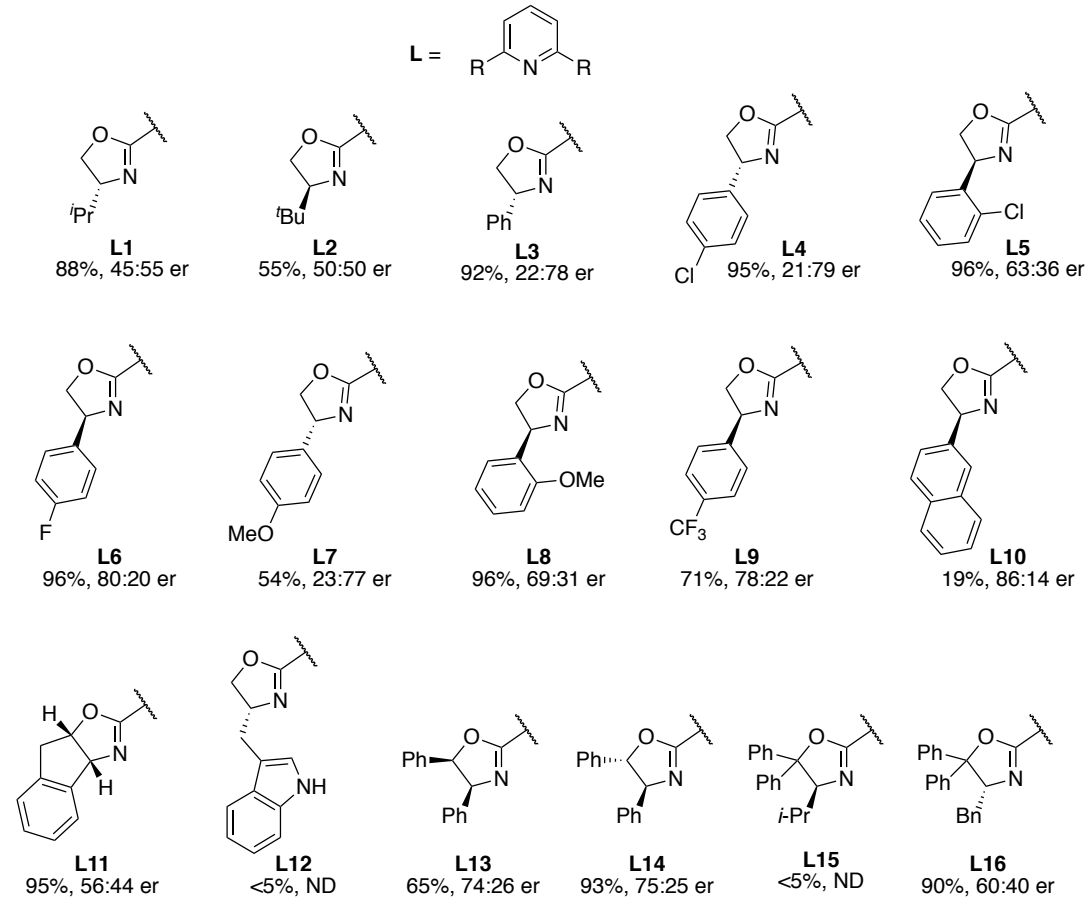

[a]Reactions conducted with azide **3.16** (0.125 mmol) and alkyne **3.17** (0.05 mmol) at 0.1 M in DCM (0.2 M), with $(CuOTf)_2$·PhMe (0.62 µmol) and ligand (2.5 µmol). All yield and er value reflect the average of duplicate trials. Yields determined using calibrated GC with triphenylmethane as an internal standard. Chiral HPLC was used to determine er.

ND = not determined

Table 3.2 Temperature Screen[a]

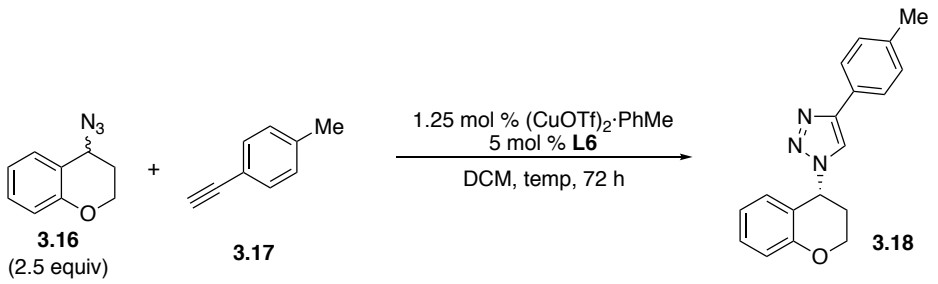

3.16 (2.5 equiv) + **3.17** → **3.18**

Entry	Temp (°C)	Yield (%)	er
1	rt	96	80:20
2	0	84	84:16
3	-10	80	86:14
4	-20	34	89:11

[a]Reactions conducted with azide **3.16** (0.125 mmol) and alkyne **3.17** (0.05 mmol) at 0.1 M in DCM (0.2 M), with $(CuOTf)_2$·PhMe (0.62 μmol) and **L6** (2.5 μmol). All yield and er value reflect the average of duplicate trials. Yields determined using calibrated GC with triphenylmethane as an internal standard. Chiral HPLC was used to determine er.

Solvents with various polarities were also screened by Alexander, showing that $PhCF_3$ was the optimal reaction solvent.‡ With optimal reaction temperature and solvent in hand, a second ligand screen was performed under this reaction condition. Amy Ott, our group member, synthesized a variety of imine-based L_3 type ligands. After the synthesis, a series of L_3 type ligands, including (*S*)-Ph-TOX and other imine ligands, were investigated (Table 3.3). Unfortunately, only **L17** gave comparable enantioselectivity to that from previously optimal ligand **L6**. However, the conversion was much lower when **L17** is utilized. Other L_3-type ligands resulted in either low conversion or poor enantioselectivity (**L18**-**L25**).

‡ For the complete solvent screens, see Supporting Information of this manuscript: *Org*. *Lett*. **2019**, *21*, 4355–4358.

Table 3.3 Ligand Screen 2[a]

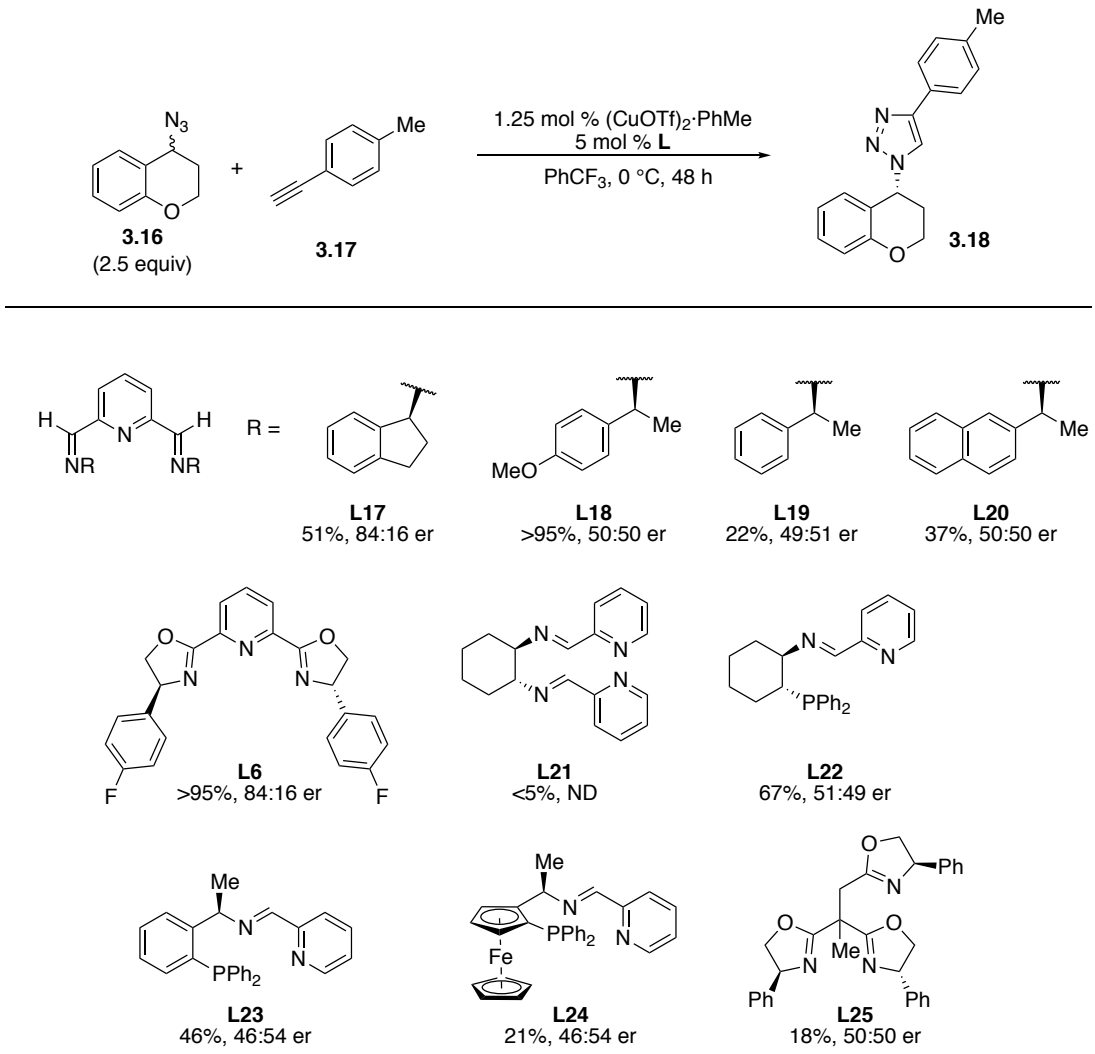

[a]Reactions conducted with azide **3.16** (0.125 mmol) and alkyne **3.17** (0.05 mmol) at 0.125 M in $PhCF_3$ (0.2 M), with $(CuOTf)_2$·PhMe (0.62 μmol) and ligand (2.5 μmol). Isolated yield was reported. Chiral HPLC was used to determine er.

ND = Not Determined

The optimal ligand is PYBOX ligand **L6** upon the investigation of a wide range of ligands (Table 3.1 and 3.3). Other minor variables were investigated.[‡] The optimal reaction condition is shown in Scheme 3.4. In the presence of cationic copper(I) catalyst and chiral ligand **L6**, the α-*N*-chiral triazole **3.18** could be isolated in 90% yield with a 90:10 er.

Scheme 3.4 Optimized KR E-CuAAC Reaction Condition

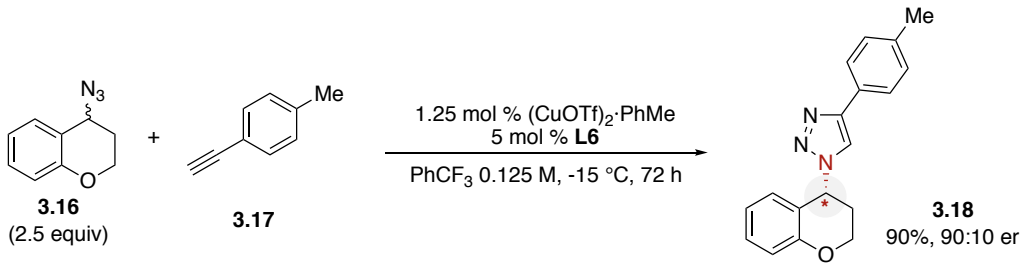

3.2.2 Substrate Scope

With the optimized condition being identified, the scope with respect to the alkyne was investigated (Table 3.4). In addition to the model substrate **3.18**, other aryl alkynes were tolerated with electron-rich (**3.20** and **3.21**), electron-neutral (**3.22** and **3.23**), and electron-deficient substituents (**3.24**–**3.26**) on the arene. Substituents positioned *meta*- and *ortho*- on the aryl alkyne provided good enantioselectivity (**3.27**–**3.30**). Ethyl propiolate (**3.31**), cycloalkyl alkynes (**3.32** and **3.33**), and a heterocyclic alkyne (**3.34**) were tolerated, although several substrates required higher catalyst loadings or longer reaction times to reach the higher conversion. Note that long reaction times are not uncommon for other E-CuAAC reactions.[47,48,54] Two isolated yields were reported herein, based on the alkyne

[‡] For the complete reaction screens, see this manuscript: *Org*. *Lett*. **2019**, *21*, 4355–4358

(limiting reagent, shown in maroon) and the azide (kinetic resolution component, shown in blue), respectively. Conventionally, the selectivity factor *s* was based on the conversion and the enantiomeric excess of the excess reagent.[85] Yields based on the excess azide allow to calculate traditional selectivity factor *s*, in terms of "resolving" the racemic azides. Herein, the aim of this work is to access α-*N*-chiral triazoles. The enantiomeric ratio is more synthetic meaningful. Therefore, the yields based on the limiting reagent and the enantiomeric ratio were reported.

The scope of the azide component that could be resolved was explored (Table 3.5). Substituents on the chromane arene core were tolerated, including methyl (**3.36**) and halogens (**3.37**−**3.39**). Groups could also be added α to the oxygen atom (**3.40**). Azido-tetrahydroquinolines with various *N*-protecting groups (**3.41**−**3.43**) provided triazoles in high yield and acceptable enantioselectivity. Interestingly, the free N-H azido-tetrahydroquinolines substrate (**3.44**) was obtained in high yield with a moderate enantiomeric ratio. Azidothiochromanes (**3.45** and **3.46**), azido-dihydrobenzofuran (**3.47**), and azido-indane (**3.48** and **3.49**) could also be resolved. Substrates **3.48** and **3.49** are noteworthy because the original E-CuAAC by KR reported by Fokin and Finn described this as a problematic substrate ($s < 1.3$).[45] Acyclic substrate **3.50** provided lower conversion and slightly reduced selectivity. The substrate scopes presented in Table 3.4 and 3.5 have shown the broadness and the high yielding of the E-CuAAC by KR of non-allylic substrates.

Table 3.4 KR E-CuAAC Substrate Scope of Alkyne Coupling Partner[a]

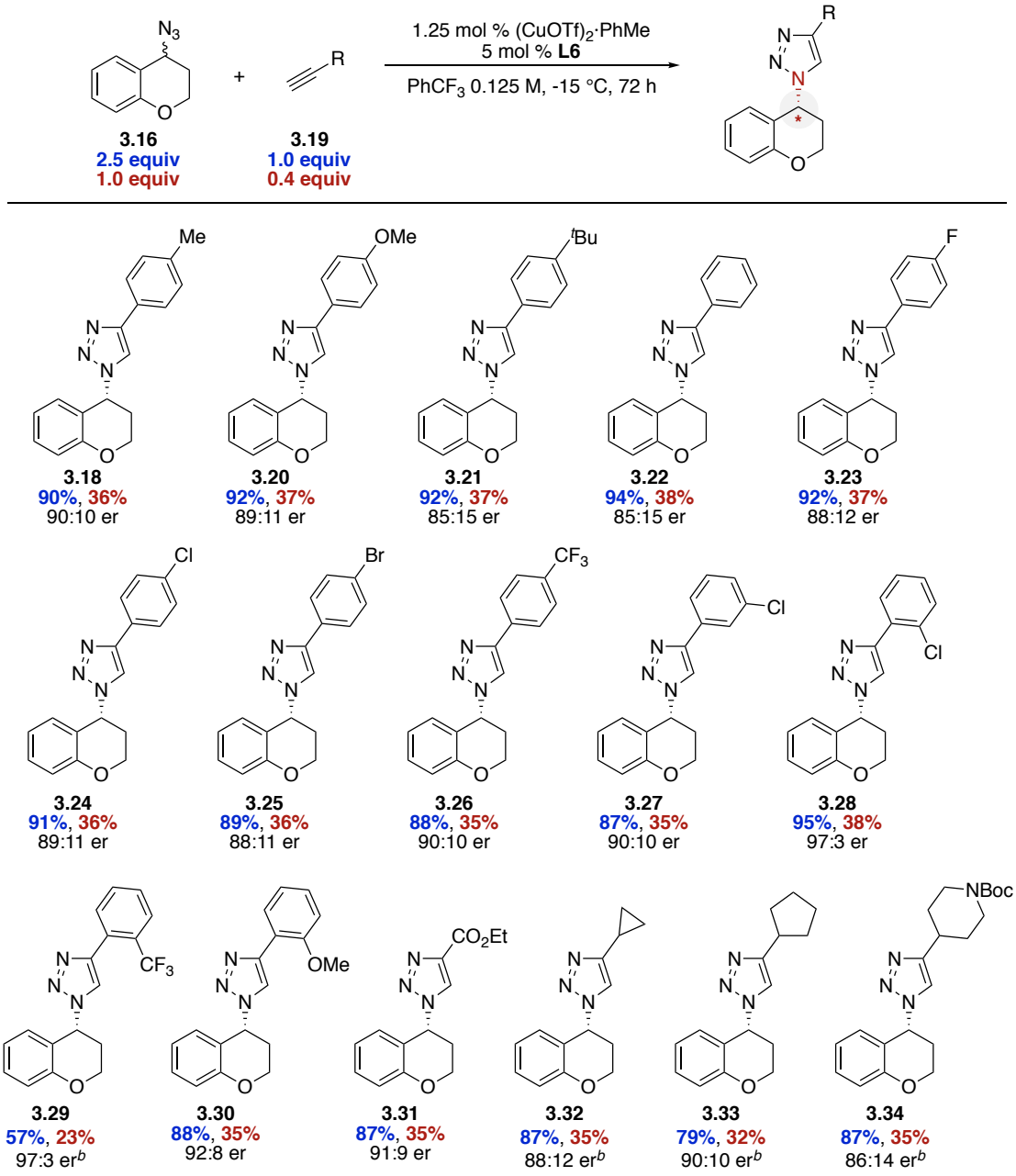

[a]Isolated yields are reported. The yield is calculated based on either the *alkyne* (limiting reagent) or *azide* (kinetic resolution component). Enantiomeric ratio was determined by chiral HPLC. Yields and er values are the average of duplicate trials. [b]2.5 mol % $(CuOTf)_2$·PhMe, 10 mol % **L6**, and 0.1 M in $PhCF_3$.

Table 3.5 KR E-CuAAC Substrate Scope of Azide Coupling Partner[a]

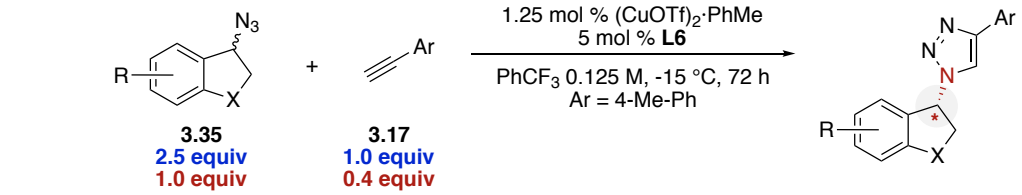

3.35 2.5 equiv 1.0 equiv

3.17 1.0 equiv 0.4 equiv

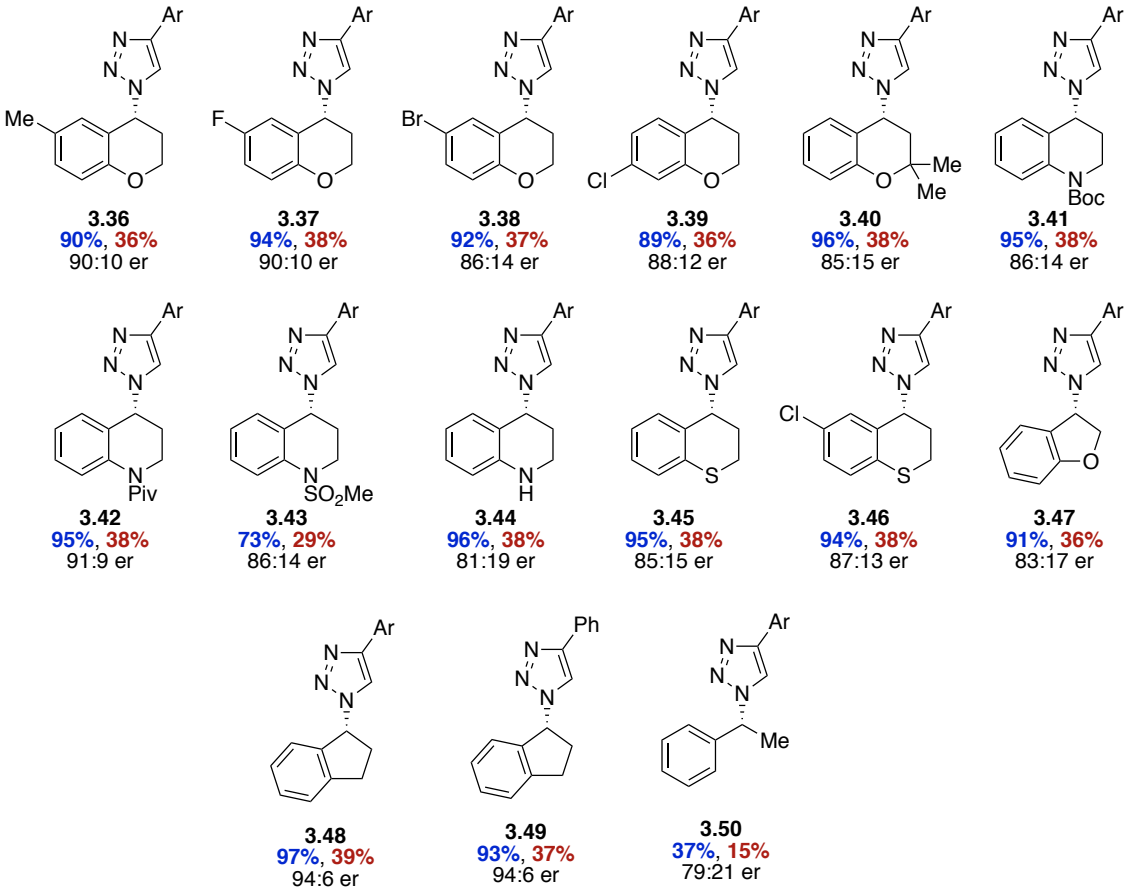

3.36 90%, 36% 90:10 er

3.37 94%, 38% 90:10 er

3.38 92%, 37% 86:14 er

3.39 89%, 36% 88:12 er

3.40 96%, 38% 85:15 er

3.41 95%, 38% 86:14 er

3.42 95%, 38% 91:9 er

3.43 73%, 29% 86:14 er

3.44 96%, 38% 81:19 er

3.45 95%, 38% 85:15 er

3.46 94%, 38% 87:13 er

3.47 91%, 36% 83:17 er

3.48 97%, 39% 94:6 er

3.49 93%, 37% 94:6 er

3.50 37%, 15% 79:21 er

[a]Isolated yields are reported. The yield is calculated based on either the *alkyne* (limiting reagent) or *azide* (kinetic resolution component). Enantiomeric ratio was determined by chiral HPLC. Yields and er values are the average of duplicate trials.

Chiral alkyne **3.51** was utilized to test for matched/mismatched behavior (Scheme 3.5). Treating azide **3.16** with chiral alkyne **3.51** and either enantiomer of ligand **L6** resulted in a moderate yield of α-*N*-chiral triazoles with opposite diastereoselectivity

(**3.52**,14:1 dr and **3.53**, 1:13 dr, respectively). Similar to the dynamic kinetic resolution E-CuAAC study, this reversal of diastereoselectivity indicates this reaction is under catalyst control.

Scheme 3.5 Match/Mismatched Experiment

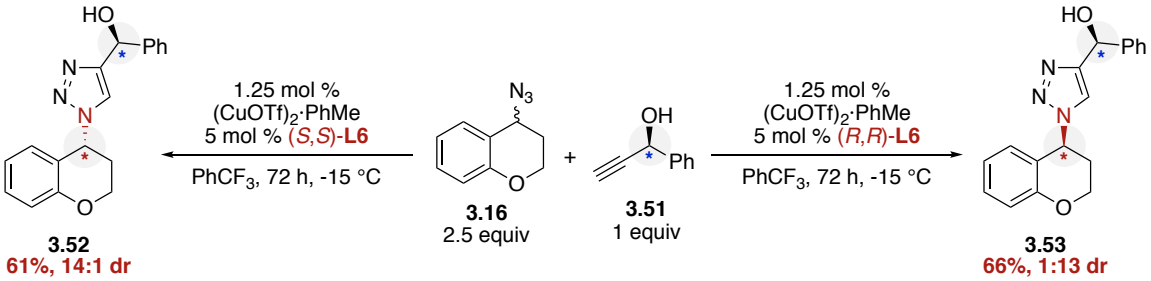

3.2.3 Scalemic Azide Racemization

This kinetic resolution could be successfully scaled to provide more than one gram of triazole **3.18** (Scheme 3.6). The initial enantioselectivity was 89:11 er, which corresponds to a selectivity factor s = 13.5. The enantiopurity could be enhanced upon recrystallization (99:1 er).‡ The excess azide **3.16** was recovered (scalemic, 76:24 er). Upon treatment with $AgPF_6$, a catalyst for racemization disclosed by Ott,[64] the excess azide could be recovered as a racemic mixture and used in a subsequent reaction. The racemic azides can produce α-*N*-chiral triazoles and the unreacted azides can be recycled as a racemic mixture. This two-operation synthesis enables an outcome to be the same as dynamic

‡ For more details of recrystallization and determination of the enantiomeric ratio of azides, see Supporting Information of this manuscript: *Org. Lett.* **2019**, *21*, 4355–4358.

kinetic resolution. The substrate scope, compared to allylic azides in chapter 2, can be further expanded to benzylic azides in the virtue of the racemization catalyst.

Scheme 3.6 Racemization of Recovered Azide

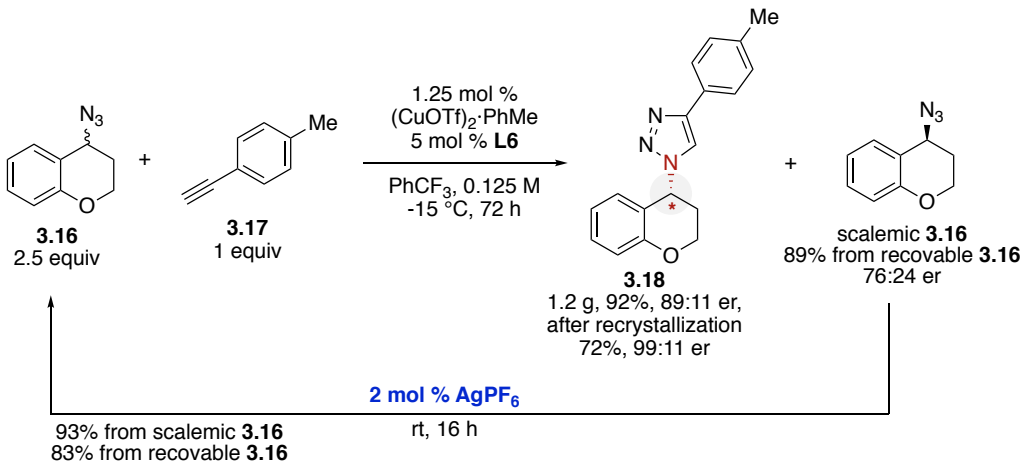

3.3 Conclusion

This work describes an expanded scope for organic azides in an E-CuAAC. More L_3 type ligands were prepared and investigated for the KR E-CuAAC, although the best enantioselectivity was still driven by the PYBOX derived ligands. The resulting α-*N*-chiral triazole products were obtained in up to 97% yield and up to 97:3 er. The reaction can be conducted to isolate more than one gram of product and the excess azide can be recovered, racemized, and recycled. The er of the product triazoles can be readily improved to 99:1 with single recrystallization.

Chapter 4 Enantioselective NiAAC by Dynamic Kinetic Resolution*

4.1 Other MAAC

Prior work described α-*N*-chiral 1,4-disubstituted triazole synthesis. The next aim of this work is to expand the scope to complementary triazole regioisomers. In 2002, Sharpless and Meldal made contemporaneous disclosures that copper(I) could catalyze the alkyne-azide cycloaddition reaction (CuAAC).[86,87] CuAAC provides exquisite regioselectivity for the 1,4-disubstituted triazole and CuAAC is the quintessential click reaction.[88,89] With a few noted exceptions,[90–92] CuAAC is traditionally limited to terminal alkynes.[40,93] Other metals can catalyze the alkyne-azide cycloaddition reaction (MAAC), including zinc,[94] rhodium,[95,96] silver,[97] iridium,[98–100] nickel,[101,102] and gold.[103] These reactions often provide complementary selectivity or reactivity relative to CuAAC. For instance, the ruthenium-catalyzed alkyne-azide cycloaddition (RuAAC) typically affords 1,5-disubstituted 1,2,3-triazole products **4.4**.[104,105] Selective examples are depicted in Scheme 4.1.

---

* Reprinted (adapted) with permission from Liu, E.-C.; Topczewski, J. J. *J. Am. Chem. Soc.* **2021**, *X*, X – X. Copyright (2021) American Chemical Society.

Scheme 4.1 MAAC

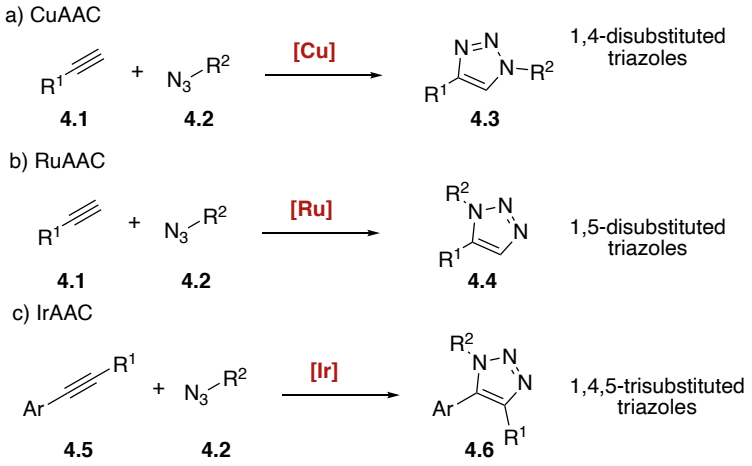

In 2017, Hong and co-workers disclosed the first homogeneous NiAAC reaction.[101] In the presence of a nickel catalyst, the 1,5-disubstituted triazoles can be synthesized (Scheme 4.2a). The same group described the chemo- and regio-selective NiAAC using internal alkynes to access 1,4,5-trisubstituted triazoles (Scheme 4.2b). These reactions provided complementary access to CuAAC products. A series of DFT calculations suggested that the NiAAC reaction may occur through a monometallic Ni complex with turn-over limiting azide attack (*vide infra*).[102] These attributes appeared to be well suited for the development of an enantioselective NiAAC (E-NiAAC) reaction. Therefore, the next aim of this work is to investigate E-NiAAC by DKR, providing complementary access to trisubstituted α-*N*-chiral triazoles not accessible by E-CuAAC (Scheme 4.2c).

Scheme 4.2 NiAAC Reactions

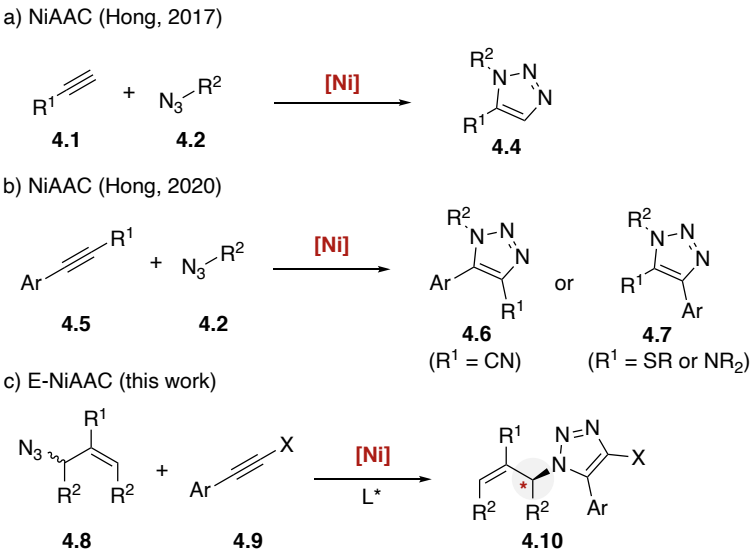

In Hong's studies, the regioselectivity of the triazole depends on the electron density of the substituents on the triple bond.[101,102] The relatively electron-deficient substituents locate the position adjacent to the distal nitrogen of the azide (Scheme 4.3a). The competitive experiments revealed that cyanoalkynes (alkynonitriles) are much more reactive than thioalkynes, and terminal alkynes are the least reactive species among these three (not shown here). The proposed mechanism by Hong is shown in Scheme 4.3b.[102] The resting state of nickel(0) catalyst **4.14** is generated from the precatalyst Ni_2Cp via reductive elimination and association with the Xantphos ligand. Upon coordination to the alkynonitrile, forming complex **4.15**, the distal nitrogen of the azide approaches the cyano substituent. A series of DFT calculations revealed that the azide attack is the turn-over limiting step. The resulting complex **4.16** generates the aza-nickelacycle complex **4.17**. Reductive elimination gives the triazole product **4.18** and regenerates the active catalyst. Based on Hong and co-worker's studies, the E-NiAAC via DKR is promising because 1)

the active catalyst is a monomeric nickel species, which is suitable for creating a chiral environment by applying a chiral ligand to the nickel precatalyst, and 2) the turn-over limiting step is azide attack. Thus, alkynonitriles, the most reactive species in Hong's work, were chosen as the coupling partner to investigate E-NiAAC.

Scheme 4.3 Alkyne Scope and Proposed Mechanism

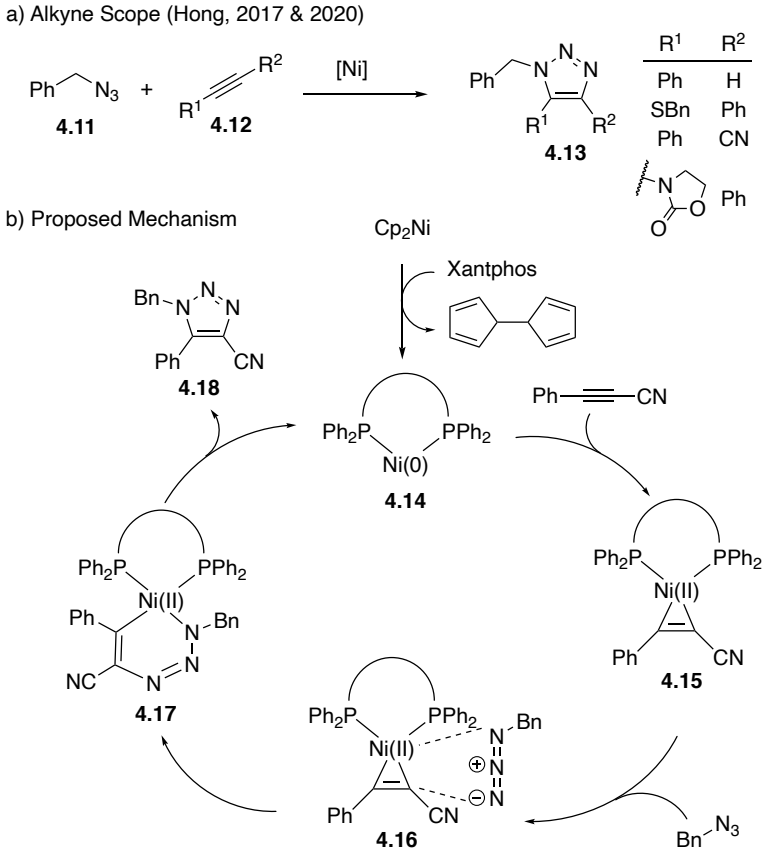

4.2 Experimental Results

4.2.1 Reaction Optimization

This study began with a preliminary ligand screen using allylic azide **4.19**, alkynonitrile **4.20**, and $Ni(COD)_2$ (Table 4.1). Common bidentate phosphine ligands gave poor conversion (**L1**-**L10**). The PYBOX scaffold (**L11**) is privileged in E-CuAAC reactions (Chapter 2 and 3); however, this reactivity did not translate to the NiAAC system. Nitrogen-containing bidentate ligand (**L12**) provided an observable er. Alternate ligand scaffolds were investigated and amino-phosphine ligands (**L13**-**L16**) provided promising enantiomeric ratios. The amino-phosphine ligand **L16** provided the product in moderate yield and the highest er thus far. It is worth noting that the **L16** derivative, **L17**, was inactive in the E-NiAAC. This result suggested that the primary amine is non-innocent.

Table 4.1 Ligand Screen of E-NiAAC by DKR[a]

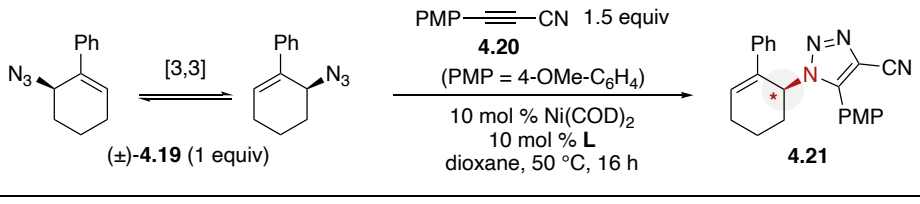

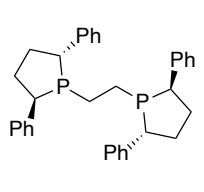

L1: <2%, er = N.D.

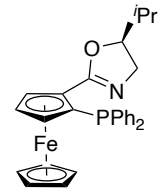

L2: 4%, er = N.D.

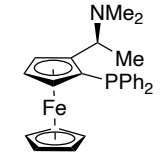

L3: <2%, er = N.D.

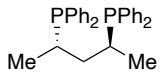

L4: <2%, er = N.D.

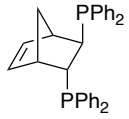

L5: <2%, er = N.D.

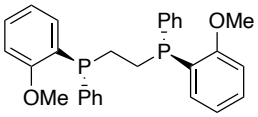

L6: <2%, er = N.D.

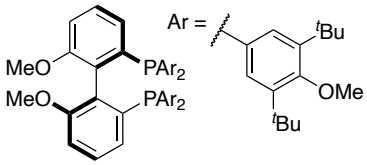

L7: <2%, er = N.D.

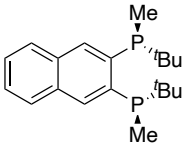

L8: <2%, er = N.D.

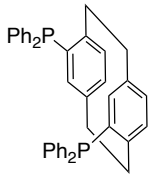

L9: <2%, er = N.D.

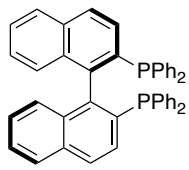

L10: <2%, er = N.D.

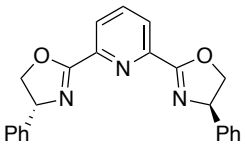

L11: 10%, er = 47:53

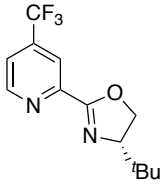

L12: 20%, er = 40:60

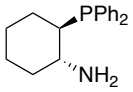

L13: 68%, er = 28:72

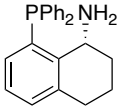

L14: 66%, er = 20:80

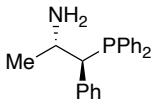

L15: 53%, er = 83:17

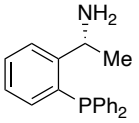

L16: 58%, er = 13:87

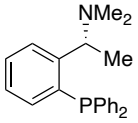

L17: 0%, er = N.D.

[a]Reactions conducted with allylic azide **4.19** (0.05 mmol), alkynonitrile **4.20** (0.15 mmol), in dioxane (0.10 M), with 10 mol % $Ni(COD)_2$ and 10 mol % ligand. Yields were determined by SFC analysis using 2',4',6'-trimethylacetophenone as an internal standard. Enantiomeric ratio was determined by chiral SFC. N.D. = Not determined.

The full optimization was shown in Table 4.2. Several competing reactions were identified including i) the Staudinger reduction with a phosphine ligand,[106] and ii) alkyne [2+2+2] cyclotrimerization, resulting in arene **4.22** and **4.23**.[107] Representative ligands were chosen and gave comparative yields and er's (entries 1-6). Only traces of triazole **4.21** were observed using chiral monodentate or bidentate phosphine ligands. In these initial results, **L16** gave a moderate yield and promising enantioselectivity (entry 5). A series of solvents were investigated (entries 7-9). While hexanes resulted in a higher yield, the enantioselectivity decreased. Toluene was superior to dioxanes and the system maintained homogeneity. The reaction temperature was critical given the rate of the Winstein rearrangement[28,29,108,109] and the number of competing reaction pathways (entries 9-11). Increasing the reaction temperature decreased selectivity relative to trimerization. Lowering the temperature slightly improved the enantioselectivity but diminished

conversion. Increasing the concentration (entry 12) significantly increased the yield. The reaction conditions outlined in entry 12 were selected as being optimal.

Table 4.2 Optimization of E-NiAAC by DKR[a]

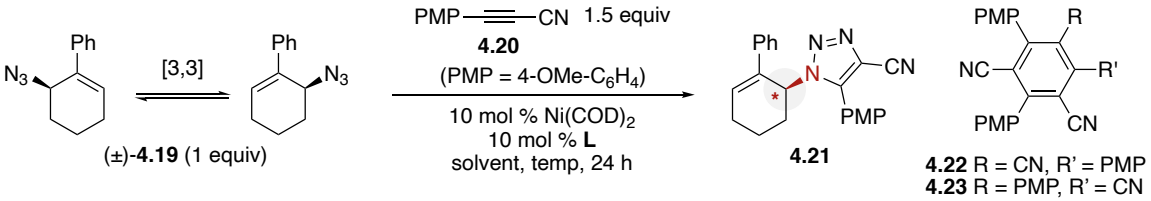

Entry	Ligand	Solvent	Temp (°C)	Yield of **4.21** (%)[b]	% **4.20** consumed[b]	er[c]
1	**L10**	dioxane	50	0	0	N/A
2	**L11**	dioxane	50	11	98	51:49
3	**L12**	dioxane	50	27	59	61:39
4	**L15**	dioxane	50	56	58	17:83
5	**L16**	dioxane	50	52	72	87:13
6	**L17**	dioxane	50	0	24	N/A
7	**L16**	hexanes	50	82	78	83:17
8	**L16**	1,2-DCE	50	0	0	N/A
9	**L16**	PhMe	50	62	77	89:11
10	**L16**	PhMe	60	56	84	88:12
11	**L16**	PhMe	40	56	64	91:9
12	**L16**	PhMe[d]	40	86	65	90:10

[a]Reactions conducted with allylic azide **4.19** (0.05 mmol), alkynonitrile **4.20** (0.15 mmol), in various solvent (0.10 M), with 10 mol % $Ni(COD)_2$ and 10 mol % ligand. [b]Yields were determined by SFC analysis using 2',4',6'-trimethylacetophenone as an internal standard. [c]Enantiomeric ratio was determined by chiral SFC. [d]The reaction concentration was 0.25 M. All yields and er values reflect the average of duplicate trials.

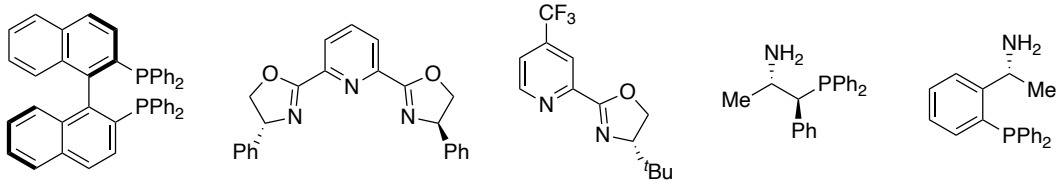

4.2.2 Substrate Scope

With the optimized condition identified, the scope with respect to the alkyne was investigated (Table 4.3). Using the azide as the limiting reagent, the model substrate **4.21** was isolated in 88% yield and 90:10 er. Electron rich (**4.21** and **4.24**), neutral (**4.25** and **4.26**), and deficient (**4.27** and **4.28**) substituents on the aryl group had a minimal effect on the enantioselectivity. Arenes with strong withdrawing groups (**4.27** and **4.28**) did suffer a decrease in regioselectivity and a lower yield because the [2+2+2] cyclotrimerization is faster than the NiAAC. The lower regioselectivity is expected given the similar electronic nature of the two groups (e.g. -CN vs -4-C_6H_4-CF_3, **4.27**). Both *ortho*- (**4.29**) and *meta*- (**4.30**) substituents were tolerated, albeit the regioselectivity was slightly lower. Both electron rich (**4.31**) and electron deficient (**4.32**) heterocycles could be incorporated. Beyond alkynonitriles, alkynoesters (**4.33** – **4.35**), and a trifluoromethyl alkyne (**4.36**) also provide the E-NiAAC product with good selectivity. Alkynosulfides (**4.37** – **4.39**) also provide good to moderate enantioselectivity, albeit the yield was lower. Ynamides (**4.40** – **4.42**) were problematic substrates with limiting enantioselectivity. The scope of allylic azides was explored. The pendent aryl tolerated both electron rich and electron deficient groups (**4.42**-**4.44**). The absolute configuration of triazole product was determined by the single crystal X-ray diffraction of product **4.44** and the configuration of other product was assigned based on the configuration of **4.44**. The cyclohexyl- core was modified (**4.45**-**4.48**). In the acyclic allylic azide **4.44**, both the (*E*)- and (*Z*)- alkene isomers were observed (7:1 *Z*/*E*). Interestingly, triazole **4.44** was isolated as a single isomer. It is likely that the nickel catalyst preferentially reacts with (*E*)-alkene isomer.

Table 4.3 Substrate Scope of E-NiAAC by DKR

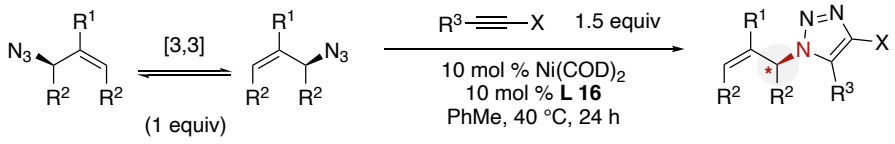

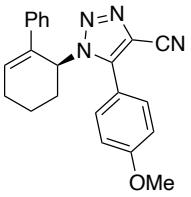

4.21 88%, **90:10 er**
>20:1 rr

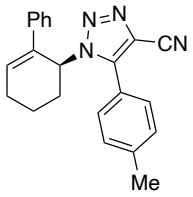

4.24 76%, **93:7 er**
>20:1 rr

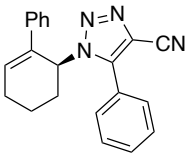

4.25 74%, **90:10 er**
8.3:1 rr

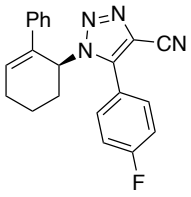

4.26 88%, **90:10 er**
13:1 rr

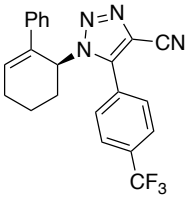

4.27 71%, **88:12 er**
6.1:1 rr

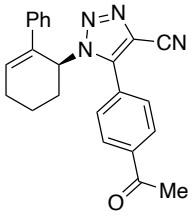

4.28 49%, **90:10 er**
12:1 rr

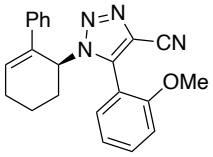

4.29 76%, **87:13 er**
4.2:1 rr

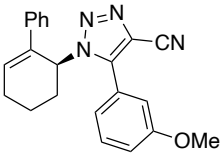

4.30 85%, **90:10 er**
19:1 rr

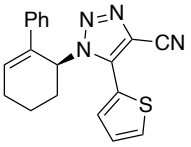

4.31 65%, **89:11 er**
>20:1 rr

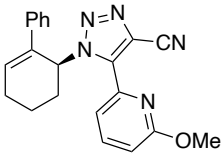

4.32 80%, **89:11 er**
>20:1 rr

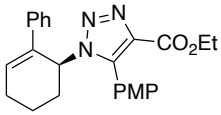

4.33 86%, **84:16 er**
8.1:1 rr

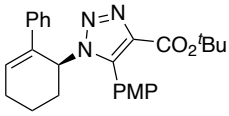

4.34 77%, **76:24 er**
>20:1 rr

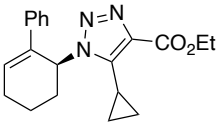

4.35 94%, **85:15 er**
>20:1 rr

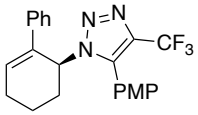

4.36 33%, **85:15 er**
>20:1 rr

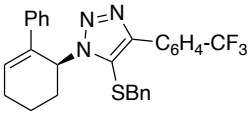

4.37 23%, **85:15 er**
>20:1 rr

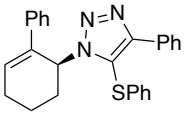

4.38 9%, **85:15 er**
>20:1 rr

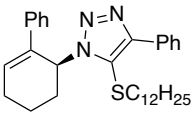

4.39 19%, **75:25 er**
>20:1 rr

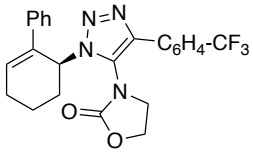

4.40 94%, **58:42 er**
>20:1 rr

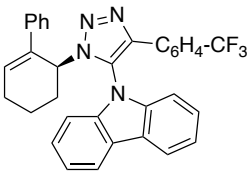

4.41 35%, **58:42 er**
>20:1 rr

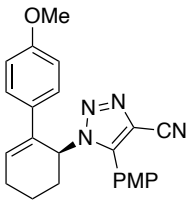

4.42 88%, **89:11 er**
>20:1 rr

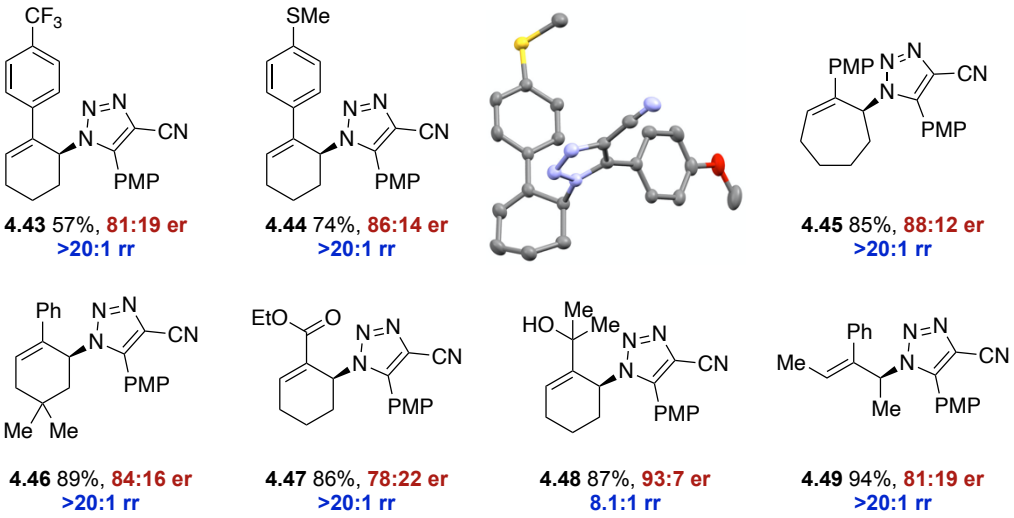

Yields are reported for isolated and purified products. Regiomeric ratio (rr) was determined by SFC analysis. Enantiomeric ratio was determined by chiral SFC. Yield, rr values, and er values reflect the average of duplicate trials.

4.2.3 Mechanistic Studies

A series of preliminary mechanistic experiments were conducted to contrast E-CuAAC and E-NiAAC (Figure 4.1). First, the er of azide **4.19** and triazole **4.21** were determined as a function of the reaction time course (Figure 4.1a). At very early time points, a slight enrichment of the azide er was measurable (up to 55:45), indicating that this DKR[110–113] likely occurs in a non-ideal kinetic regime.[113] The er of triazole **4.21** was constant as a function of reaction progression and the smooth time course data indicated well-behaved kinetics. Next, a non-linear experiment was conducted.[114] E-CuAAC reactions are known to proceed with positive[52,53] or negative[54,115] non-linear effects. In contrast, the E-NiAAC reaction did not demonstrate a non-linear effect (Figure 4.1b), indicating that only one equivalent of ligand **L16** is involved in the enantio-determining step. Lastly, the reaction was found to be first order in catalyst by initial rates (Figure 4.1c).

This result is consistent with the DFT calculations on NiAAC[102] and contrasts with the higher order catalyst for the CuAAC reaction.[116] Together, the data in Figure 4.1b and 4.1c indicate that NiAAC likely proceeds through a mono-nuclear **L16**-Ni complex, which is distinct from CuAAC, which is thought to proceed through $[L_2Cu_2X_2]$ dimers or higher order oligomers.

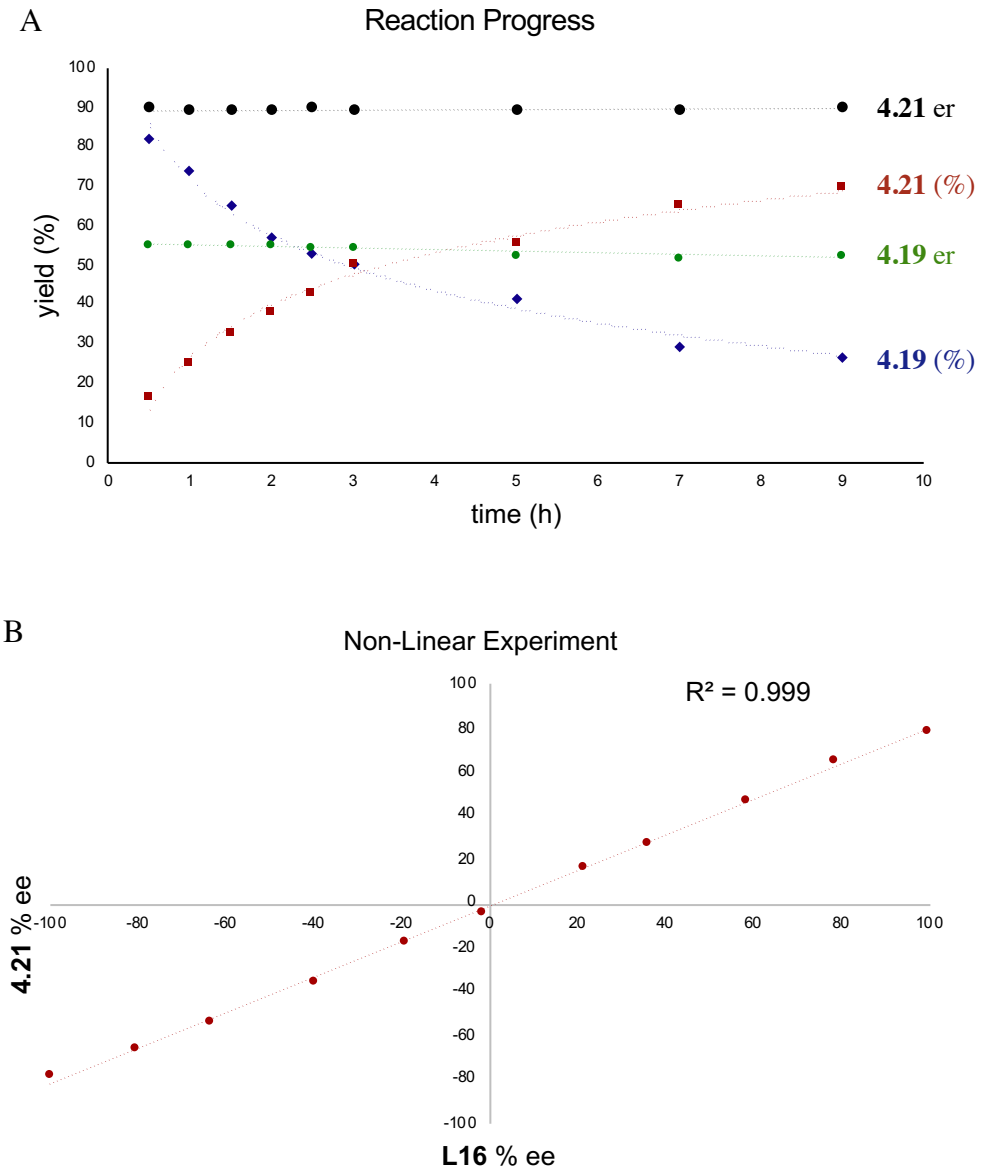

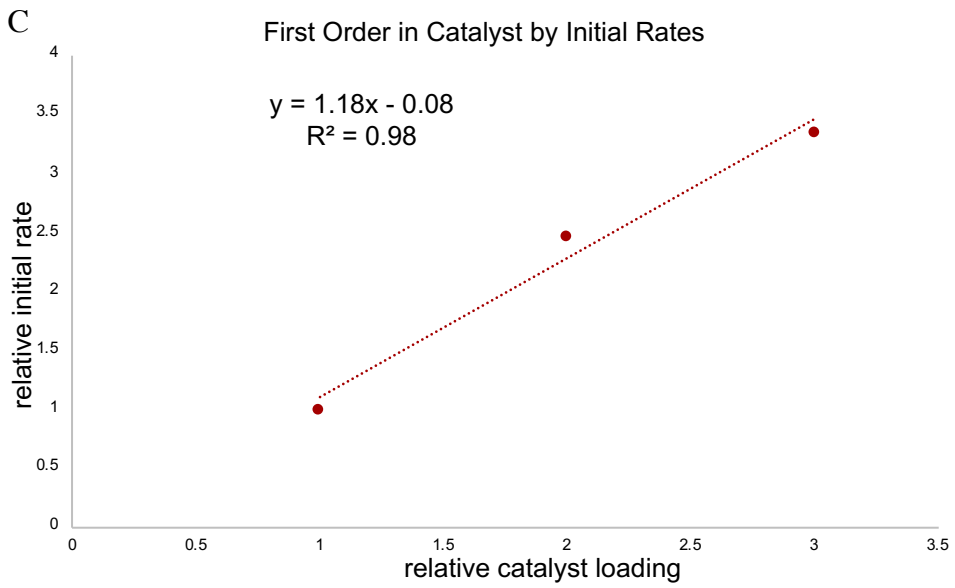

Figure 4.1 Mechanistic Studies A) Reaction Progress B) Non-linear Effect C) Initial Rates Studies

4.2.4 Derivatization

The triazole **4.21** can be derivatized to a variety of functionalities (Scheme 4.4). Upon treatment of Grignard reagents followed by acidic hydrolysis, triazolyl ketone **4.50** can be synthesized in 44% yield. Hydrolysis under basic conditions afforded triazolyl carboxylic acid **4.51** in 67%. The nitrile can be converted to a tetrazole **4.52** via a cycloaddition to an azide anion in a 95% yield. In addition to the nitrile manipulation, the alkene functional groups can be derivatized. Dihydroxylation of triazole **4.21** gave dihydroxytriazole **4.53** in 68% yield. It is noteworthy that this reaction is highly diastereoselective. The dihydroxy groups approach the alkene from the opposite face to the triazole. These reactions show that the triazole **4.21** can be utilized as a building block to access other functionalities.

Scheme 4.4 Derivatization of Triazole **4.21**

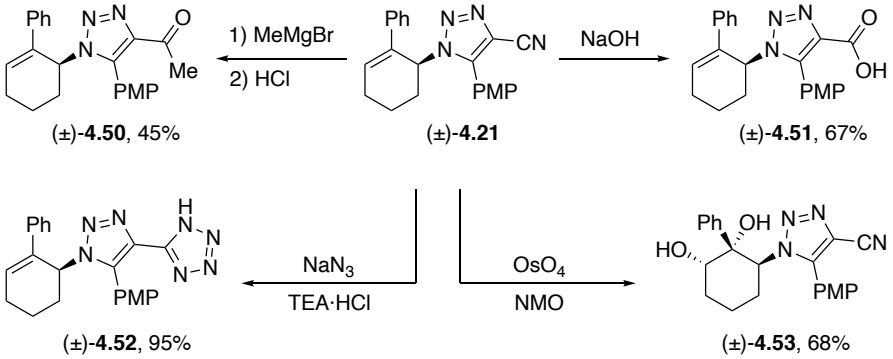

4.3 Conclusion

In conclusion, ligand **L16** can promote an E-NiAAC reaction by DKR. This is the first enantioselective alkyne-azide cycloaddition that is reported to be catalyzed by a metal other than copper. The E-NiAAC reaction provides synthetic access to 1,4,5-trisubstituted α-*N*-chiral triazoles that are not directly accessible by E-CuAAC. Furthermore, preliminary mechanistic experiments indicate that the nature of the NiAAC catalyst is a mono-metallic L_1 species, which is distinct from CuAAC.

4.4 Experimental

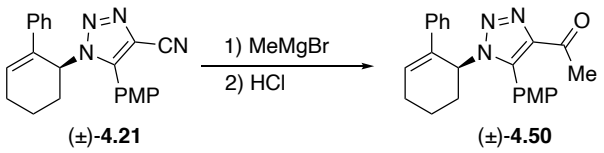

A 2-necked round bottom flask was charged with triazole **4.21** (29.7 mg, 0.083 mmol) and THF (2 mL) under argon using Schlenk technique. The reaction was cooled into an ice bath. Dropwise addition of methylmagnesium bromide (0.12 mL, 3.0 M in diethyl ether, 0.36 mmol) was conducted over 10 min. The reaction was gradually warmed up to room temperature. After 16 h, the reaction was cooled into an ice bath and quenched by the addition of 1 M HCl (2 mL). After 2 h, the resulting solution was diluted with water (10 mL) and extracted with ethyl acetate (10 mL x3). The combined organic solution was washed with brine, dried ($MgSO_4$), filtered, and concentrated under reduced pressure. Purification by column chromatography (gradient acetone/hexane from 0-50%) afforded compound **4.50** in 45% yield (14.1 mg) as a colorless oil.

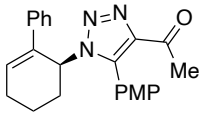

(±)-**4.50**

^{1}H NMR (400 MHz, $CDCl_3$): δ 7.22 – 7.12 (m, 5H), 7.05 (d, *J* = 8.8 Hz, 2H), 7.00 – 6.92 (m, 2H), 6.32 – 6.23 (m, 1H), 5.32 (br, 1H), 3.91 (s, 3H), 2.59 (s, 3H), 2.55 – 2.42 (m, 1H), 2.35 – 2.10 (m, 4H), 1.84 – 1.71 (m, 1H). **^{13}C{^{1}H} NMR (101 MHz, $CDCl_3$)**: δ 193.0, 160.9, 143.0, 139.5, 139.3, 134.9, 131.8, 131.2, 128.2, 127.3, 126.4, 118.4, 114.3, 55.4, 54.6, 31.2, 27.9, 25.4, 18.3. **IR (NaCl, thin film, cm^{-1})**: 2942, 2836, 1687, 1613, 1498, 1456, 1252, 1179, 835, 736, 700. **HRMS (ESI-TOF)**: $[M+Na]^+$ Calculated for $C_{23}H_{23}N_3O_2Na^+$, 396.1683; found, 396.1680.

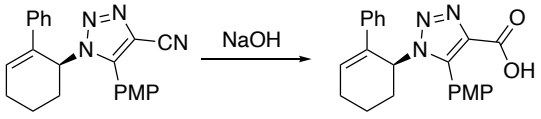

(±)-**4.21** (±)-**4.51**

A 20 mL vial was charged with triazole **4.21** (62.8 mg, 0.176 mmol), solid sodium hydroxide (33.4 mg, 0.835 mmol), and methanol (1 mL). The vial was sealed with a Teflon lined cap and heated to 80 °C. After 16 h, the reaction was cooled to room temperature. The reaction was diluted with water (20 mL) and extracted with ethyl acetate (10 mL). The aqueous layer was acidified using 1 M HCl until the pH was below 1. The resulting suspension was extracted with DCM (10 mL x 3). The combined organic solution was washed with brine, dried ($MgSO_4$), filtered, and concentrated under reduced pressure. This afforded compound **4.51** in 67% yield (44.2 mg) as a pale yellow solid.

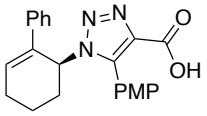

(±)-**4.51**

^{1}H NMR (400 MHz, DMSO-*d*$_6$): δ 12.72 (br, 1H), 7.27 (d, *J* = 8.3 Hz, 2H), 7.24 – 7.09 (m, 5H), 6.96 (d, *J* = 7.3 Hz, 2H), 6.31 (br, 1H), 5.27 (br, 1H), 3.86 (s, 3H), 2.44 – 2.30 (m, 1H), 2.30 – 2.17 (m, 1H), 2.17 – 2.05 (m, 2H), 1.98 – 1.83 (m, 1H), 1.76 – 1.62 (m, 1H). **^{13}C{^{1}H} NMR (101 MHz, DMSO-*d*$_6$)**: δ 162.3, 160.8, 141.0, 139.5, 136.7, 134.7, 131.9, 131.7, 128.6, 127.6, 126.2, 118.6, 114.6, 55.8, 54.3, 30.8, 25.5, 18.1. **IR (NaCl, thin film, cm^{-1})**: 3056, 2938, 2837, 1698, 1614, 1505, 1445, 1296, 1254, 1179, 836, 734. **HRMS (ESI-TOF)**: $[M+Na]^+$ Calculated for $C_{22}H_{21}N_3O_3Na^+$, 398.1476; found, 398.1477.

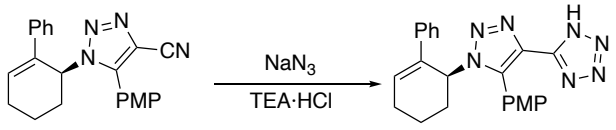

(±)-**4.21** (±)-**4.52**

The synthesis of tetrazole **4.52** was adapted from a known procedure.[117] A 20 mL vial was charged with triazole **4.21** (52.6 mg, 0.149 mmol), sodium azide (29.6 mg, 0.455 mmol), triethylamine hydrochloride (66.6 mg, 0.422 mmol), methanol (0.5 mL), and

toluene (1.5 mL). The reaction was sealed with a Teflon lined cap and heated to 110 °C. After 16 h, the reaction was cooled to room temperature. The reaction was diluted with water (10 mL) and extracted with DCM (10 mL x3). The resulting suspension was extracted with DCM (10 mL x 3). The combined organic solution was washed with brine, dried ($MgSO_4$), filtered, and concentrated under reduced pressure. Purification by column chromatography (gradient acetone/1% acetic acid in hexane from 0-70%) afforded compound **4.52** in 95% yield (55.9 mg) as a white solid.

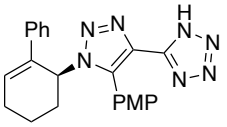

(±)-**4.52**

^{1}H NMR (400 MHz, acetic acid-*d*$_4$): δ 7.39 (d, *J* = 8.2 Hz, 2H), 7.24 – 7.10 (m, 5H), 7.04 (d, *J* = 7.2 Hz, 2H), 6.39 (br, 1H), 5.57 (br, 1H), 3.94 (br, 3H), 2.57 – 2.42 (m, 1H), 2.41 – 2.24 (m, 3H), 2.20 – 2.09 (m, 1H), 1.89 – 1.76 (m, 1H). **^{13}C{^{1}H} NMR (101 MHz, acetic acid-*d*$_4$)**: δ 161.6, 139.1, 138.7, 134.5, 132.0, 131.8, 130.0, 128.2, 127.4, 126.0, 116.5, 114.5, 55.2, 54.8, 30.7, 25.1, 17.8 (note: The tetrazole carbon was not observed in deuterated acetic acid). **IR (NaCl, thin film, cm^{-1})**: 3054, 2942, 2837, 1634, 1610, 1546, 1502, 1294, 1255, 1178, 1039, 836, 761, 735, 700. **HRMS (ESI-TOF)**: $[M+Na]^+$ Calculated for $C_{22}H_{21}N_7ONa^+$, 422.1700; found, 422.1696.

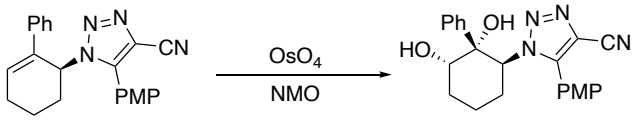

(±)-**4.21** (±)-**4.53**

A 4 mL vial was charged with triazole **4.21** (53.8 mg, 0.151 mmol), *N*-methylmorpholine *N*-oxide (21.6 mg, 0.184 mmol), and solvent (1.4 mL, THF:^{t}BuOH:H_2O

= 1:0.2:0.2). A solution of osmium tetroxide (30 μL, 0.202 M aqueous solution, 6.1 μmol) was added to the reaction. After 40 h, the reaction was diluted with water (10 mL) and extracted with ethyl acetate (10 mL x3). The combined organic solution was washed with brine, dried ($MgSO_4$), filtered, and concentrated under reduced pressure. Purification by column chromatography (gradient ethyl acetate/hexane from 0-70%) afforded compound **4.53** in 68% yield (39.9 mg) as a white solid.

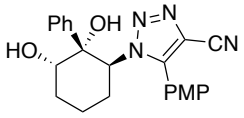

(±)-**4.53**

^{1}H NMR (400 MHz, DMSO-*d*$_6$): δ 7.17 (t, *J* = 7.2 Hz, 1H), 7.10 (t, *J* = 7.4 Hz, 2H), 7.03 (d, *J* = 8.8 Hz, 2H), 6.87 (d, *J* = 7.3 Hz, 2H), 6.65 (d, *J* = 8.8 Hz, 2H), 5.24 (s, 1H), 4.86 (q, *J* = 7.3 Hz, 1H), 4.52 (d, *J* = 6.6 Hz, 1H), 4.40 (apparent d, *J* = 3.5 Hz, 1H), 3.83 (s, 3H), 2.36 – 2.20 (m, 2H), 2.01 – 1.83 (m, 3H), 1.77 – 1.65 (m, 1H).**^{13}C{^{1}H} NMR (101 MHz, DMSO-*d*$_6$)**: δ 161.5, 145.6, 143.1, 130.9, 128.0, 127.3, 126.2, 118.5, 115.1, 115.0, 112.8, 76.6, 67.4, 64.8, 55.9, 30.1, 26.5, 20.4. **IR (NaCl, thin film, cm^{-1})**: 3426, 3376, 2925, 2245, 1614, 1496, 1299, 1249, 1010. **HRMS (ESI-TOF)**: $[M+Na]^+$ Calculated for $C_{22}H_{22}N_4O_3Na^+$, 413.1585; found, 413.1580.

Chapter 5 Beyond Click Reaction – A Cascade Reaction of Cinnamyl Azides*

5.1 Introduction

After shedding light upon the enantioselective synthesis of α-*N*-chiral triazoles, this work refocused on the synthesis of highly functionalized heterocycle building blocks. Heterocycle synthesis is often complex. Densely functionalized heterocycles are synthetically valuable but usually consume a large quantity of chemical reagents and solvents to synthesize. Thus, the third aim of this graduate work is to prepare complex and modular nitrogen-containing building blocks in a concise and direct fashion.

5.1.1 Pyrrolo-Pyrazole Fused Structure Synthesis

Nitrogen-containing heterocycles are ubiquitous in pharmaceuticals, agrochemicals, and natural products.[6] Often, saturated heterocycles provide particularly advantageous properties. Specifically, substituted tetrahydro-pyrrolo-pyrazole heterocycles are known to be biologically active with a variety of potential applications (Figure 5.1).[118–122]

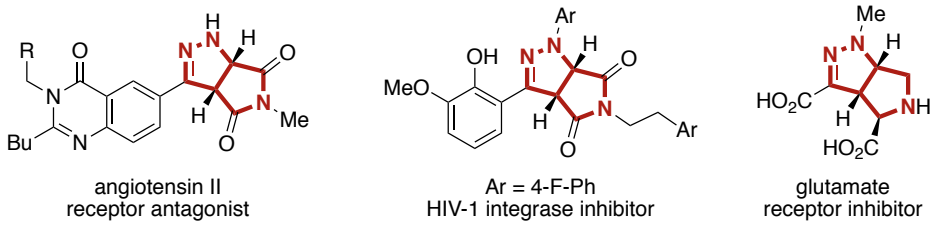

Figure 5.1 Biologically Active Fused Heterocycles

*Reprinted (adapted) with permission from Carlson, A. S.; Liu, E.-C.; Topczewski, J. J. *J. Org. Chem.* **2020**, *85*, 6044 – 6059. Copyright (2020) American Chemical Society.

5.1.2 Precedent Work

Classically, tetrahydro-pyrrolo-pyrazole heterocycles are generated through 1,3-dipolar cycloaddition of a hydrazone species or tetrazole derivatives with activated maleimide derivatives (Scheme 5.1a).[118,119] In 2006, Zard and co-workers demonstrated that hydrazones with pendant alkenes can be oxidized to the corresponding diazo species in the presence of iodine and DBU, which subsequently undergoes an intramolecular cycloaddition (Scheme 5.1b).[123] Jahn demonstrated that a domino *aza*-Michael reaction can afford similar heterocycles using ^{n}BuLi and NfN_3 (not shown here).[124,125]

Scheme 5.1 Synthesis of Tetrahydro-Pyrrolo-Pyrazoles

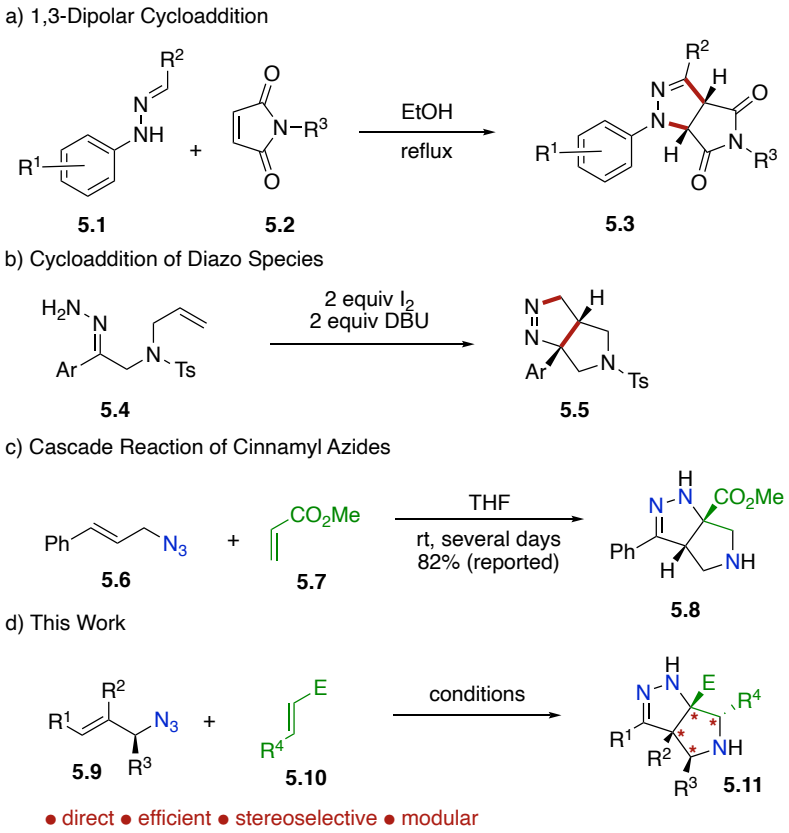

Our lab is developing synthetic methods that leverage the unique properties of allylic azides. Both alkene and azide functional groups can be selectively derivatized.[59,115,126,127] These results led us to ask if a reaction could synergistically utilize both functional groups. Inspired by our previous investigation, cinnamyl azides are a promising candidate. Although cinnamyl azides undergo the Winstein rearrangement via a [3,3] sigmatropic pathway, only one isomer is observed by NMR due to conjugation of the π system.[109,128] This phenomenon reduces the number of observed isomers. Yang reported a cycloaddition cascade with cinnamyl azide (**5.6**) and methyl acrylate (**5.7**) to form tetrahydro-pyrrolo-pyrazole heterocycles **5.8** (Scheme 5.1c).[129,130] The reported yield was 82%. Unfortunately, both of Yang's reports lacked full experiment details and our attempts to replicate the procedure using cinnamyl azide (**5.6**) afforded a low yield (< 15% obtained). We speculated that this cascade could be a powerful tool if a more reproducible procedure could be developed and if the scope of this reaction was expanded. Therefore, the next aim of this work is to reinvestigate this cascade reaction (Scheme 5.1d). A highly functionalized building block tetrahydro-pyrrolo-pyrazole **5.11** can be accessed from simple cinnamyl azide derivatives **5.9** and electrophiles **5.10** in high yields and broad scope. Enantioenriched starting materials will be employed to explore the enantiospecificity. To demonstrate the synthetic value of heterocycle **5.11**, a series of derivatization of **5.11** was conducted.

5.1.3 Reaction Mechanism

Byproduct formation accounted for the low yields and thus minimized the synthetic utility of this cascade reaction. A plausible reaction mechanism is summarized in Scheme

5.2. This proposal was based on Yang[129,130] and L'abbé's[131] reports. The cascade initiates with a Huisgen cycloaddition to afford triazoline **5.14** and **5.15**.[132–136] This cycloaddition generally proceeds with good selectivity, but the regioisomeric triazoline **5.14** was frequently observed (~5%).[137] When diethyl vinyl phosphonate was used as the Michael acceptor, the regioisomeric triazoline **5.14** was a significant byproduct (ca. 1:1, *vide infra*). In some cases, the triazoline **5.15** was stable and could be isolated. A crystal structure of one triazoline, derived from *N*-phenylmaleimide, was obtained to verify the structure.[‡] Triazoline **5.15** can equilibrate to achiral diazo species **5.16**.[137,138] Amine bases were reported to facilitate this equilibrium.[131,137] The role of the amine is most likely to deprotonate at the α position of the electron withdrawing group. The resulting ammonium salt then can facilitate proton transfer to the distal nitrogen, leading to fragmentation and forming diazo species **5.16**. Intermediate **5.16** can undergo an intramolecular cycloaddition between the diazo and alkene to afford compound **5.18**.[129,130] When compound **5.18** contains a hydrogen atom at the benzylic position, it can tautomerize to generate tetrahydro-pyrrolo-pyrazole **5.20**.[129,130] This tautomerization was readily accomplished with TFA or DBU during workup (*vide infra*).

[‡]For the crystal structure of triazoline, see the Supporting Information of this manuscript: *J. Org. Chem.* **2020**, *85*, 6044−6059.

Scheme 5.2 Plausible Reaction Mechanism of Cascade Reaction

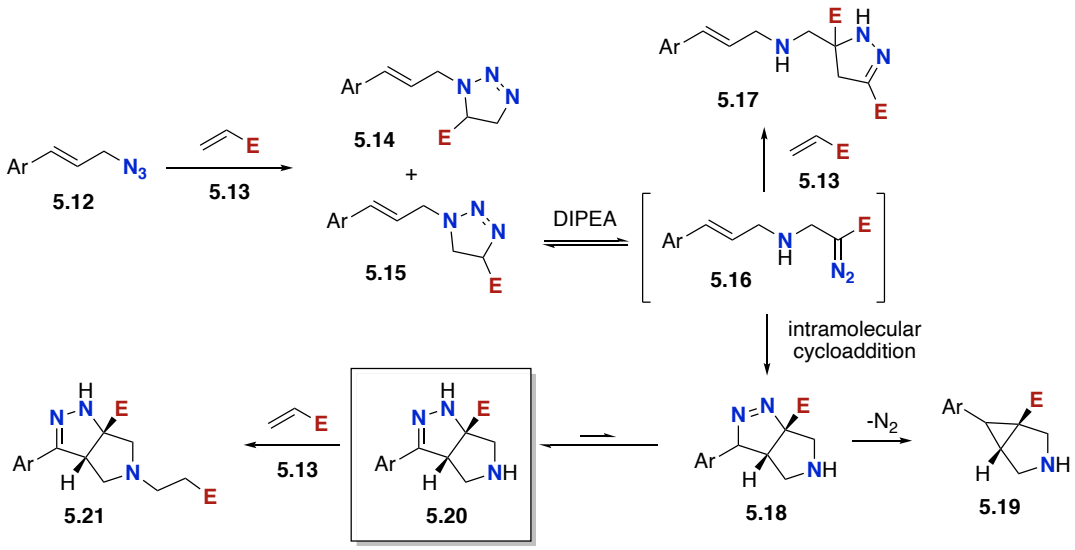

However, the biggest challenge of this cascade reaction is the side product formation. Diazo species **5.16** can undergo an intermolecular Huisgen cycloaddition with the excess alkene **5.13** to form a pyrazole species, which generates side product **5.17** upon isomerization. Instead of isomerizing to the conjugated product **5.20**, compound **5.18** can produce cyclopropane **5.19** via the extrusion of nitrogen. Lastly, compound **5.18** and the desired tetrahydro-pyrrolo-pyrazole **5.20** are sufficiently nucleophilic to engage excess acrylate in conjugate addition, affording compound **5.21**.[129,130] The formation of these side products significantly increases the challenge in the selectively obtaining compound **5.20**. It has been reported that simple alkenes do not react with azides or react very slowly.[139] The reaction time of several days or even months is not uncommon.[140] To address this issue, an excess amount of acrylate is utilized. However, excess acrylate substantially increases the formation of side products **5.17** and **5.21**. Alternatively, the formation of triazoline can be accelerated by increasing the reaction temperature. An elevated temperature increases

the risk of extrusion of nitrogen and facilitates cyclopropane **5.19** formation. Therefore, the reaction conditions, including the equivalence of acrylate and the reaction temperature, must be carefully examined.

5.2 Experimental Results

5.2.1 Reaction Screen

The investigation started with revisiting the thermally promoted cascade sequence between cinnamyl azide (**5.6**) and methyl acrylate (**5.7**) using the conditions originally reported by Yang (Table 5.1).[129,130] Yang's experimental procedure states that "cinnamyl azide (**5.6**, 5 M in THF) was mixed with alkene **5.7** (1 or 2 equiv) at ambient temperature for a time ranging between several hours to a few days."[129] In our hands, the room-temperature reaction with 1 equiv of alkene **5.7** did not fully consume azide **5.6** after 3 days (entry 1). Several intermediates and byproducts could be identified and quantified, including triazoline **5.22**, isomeric product **5.23**, and Michael adduct **5.24**. Even if both observable tautomers of the desired product (**5.8** and **5.23**), a yield below 25% was observed. The reaction with cinnamyl azide (**5.6**) was extensively screened, and in no case did we observe a yield exceeding 70%.[‡] These observations prompted a reoptimization of this cascade reaction.

[‡] For the full screen of other variables, see the Supporting Information of this manuscript: *J. Org. Chem.* **2020**, *85*, 6044–6059.

Table 5.1 Replicating Yang's Reported Conditions[a]

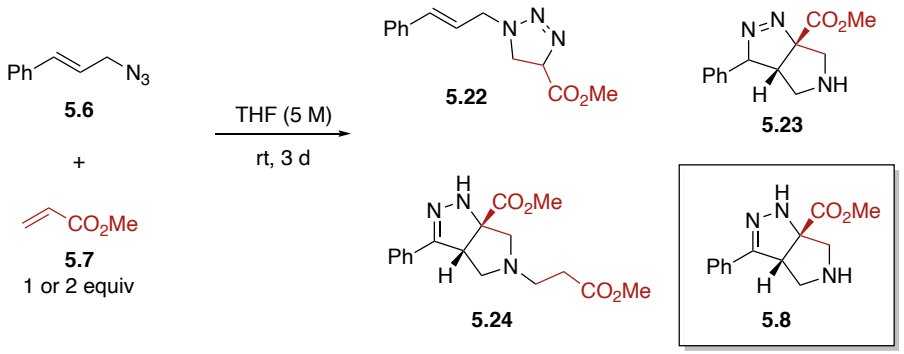

Entry	Equiv of **5.7**	% **5.6**	% **5.24**	% **5.22**	% **5.23**	% **5.8**
1	1	31	13	8	6	13
2	2	4	24	13	9	9

[a]Reactions were conducted with cinnamyl azide (**5.6**, 90 μmol) and methyl acrylate (**5.7**, 90 or 180 μmol) in THF (5 M) at rt. Conversion and yield were determined by ^{1}H NMR using naphthalene as an internal standard. Reactions were run in duplicate, and the average value is reported.

Qualitatively, the cascade reaction proceeded more effectively with a polarizing substituent on the phenyl of cinnamyl azide, including an electron rich group (*e.g.* OMe) or an electron deficient group (e.g. NO_2). The substrate 2-nitrocinnamyl azide (**5.25**) was selected for the optimization because of the commercial availability of 2-nitrocinnamyl aldehyde. Based on the proposed mechanism, several crucial variables were explored (Table 5.2). Solvents with a range of polarities were examined (entries 1−5). Polar solvents promoted the conjugate addition that formed Michael adduct **5.26** (entries 1 and 2), while less polar solvents suppressed the conjugate addition (entries 4 and 5). This observation is consistent with the need to form ionic intermediates during conjugate addition (Scheme 5.2). When hexane was used, a significant amount of the conjugate addition was observed because the desired product **5.27** was insoluble in hexanes, resulting in a reaction that was pseudoneat in methyl acrylate (entry 3). Having identified THF and benzene as the optimal

solvents, several additives were examined. The addition of acetic acid or HFIP promoted the conjugate addition (entries 6 and 7). Prior work from L'abbé indicated that the triazoline to diazo-ester equilibrium could be facilitated by the addition of an amine base (Scheme 5.2). Thus, the addition of an amine base proved most effective at converting triazoline to the desired product (entries 8−14). Given the complications associated with conjugate addition (e.g., polymerization of acrylate and over addition), it is perhaps unsurprising that DMAP and pyridine provided poor results and that less nucleophilic amine bases were preferred. Ultimately, conditions utilizing DIPEA in benzene (entry 11) were chosen as the optimal conditions. Toluene and THF were suitable alternative solvents (entries 12−14). It is worth noting that, at the end of the reaction, the desired product typically existed as a mixture of the two tautomers (**5.8** and **5.23** in Table 5.1). TFA was added during the workup to convert the mixture into the more stable conjugated tautomer **5.27**. In some instances, silica gel and DBU were also able to promote tautomerization.[‡] When compared to Yang's original conditions, this reoptimization reflects a change in the (i) solvent, (ii) concentration, (iii) temperature, (iv) equivalents of acrylate, (v) time, and (vi) addition of DIPEA.

[‡] For the investigation of additives facilitating the isomerization, see the Supporting Information of this manuscript: *J. Org. Chem.* **2020**, *85*, 6044−6059.

Table 5.2 Cascade Optimization with Methyl Acrylate[a]

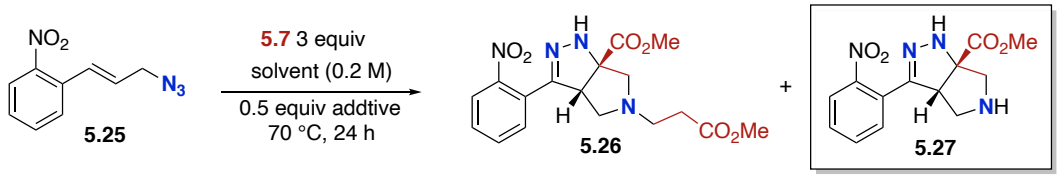

Entry	Solvent	Additive	% **5.25**	% **5.26**	% **5.27**
1	DMSO	-	nd	14	77
2	MeOH	-	nd	95	nd
3	hexanes	-	nd	54	35
4	THF	-	34	nd	46
5	C_6H_6	-	37	nd	11
6	C_6H_6	AcOH	nd	67	nd
7	C_6H_6	HFIP	nd	55	17
8	C_6H_6	DMAP	nd	8	80
9	C_6H_6	pyridine	5	nd	41
10	C_6H_6	TEA	nd	nd	85
11	**C_6H_6**	**DIPEA**	**nd**	**nd**	**91**
12	PhMe	DIPEA	nd	nd	83
13	THF	TEA	nd	nd	72
14	THF	DIPEA	nd	nd	78

[a]Reactions were conducted with azide **5.25** (70 µmol), **5.7** (210 µmol), and an additive (35 µmol) in solvent (0.2 M) at 70 °C. Conversion and yield were determined by calibrated GC-FID analysis. Reactions were run in duplicate, and the average value is reported. Not detected = nd.

5.2.2 Substrate Scope

With the reoptimized conditions in hand (entry 11, Table 5.2), a variety of cinnamyl azides were investigated (Table 5.3). Compound **5.27** was isolated in 94% yield under the reoptimized conditions. The product from cinnamyl azide (**5.6**) was crystalline, and diffraction analysis confirmed the structure. While the 64% yield of product **5.8** observed was a significant improvement over the data shown in Table 5.1, it was still lower than the yield originally reported by Yang.[129,130] Other cinnamyl azides containing electron-donating groups (**5.28**, **5.29**, and **5.33**) and electron-withdrawing groups (**5.31**, **5.32**, and

5.34) were tolerated. Substrates with *ortho* substitution were tolerated (**5.27**, **5.33**, and **5.34**). Lastly, it is worth noting that products with an electron-rich heteroarene (**5.35** and **5.36**) or an electron-deficient heteroarene (**5.37**–**5.39**) were isolated in good yields. As previously noted, substrates with polarizing groups on the arene appeared to be better suited for this cascade, with some of the highest yields observed for products **5.27** and **5.33** as well as **5.36** and **5.37**. Recent attention has been focused on developing reactions that are effective with heterocycles,[141,142] and the ability of this cascade to generate products **5.35**–**5.39** under identical conditions should be considered an attribute.

Table 5.3 Scope of the Cascade Reaction with Cinnamyl Azides[a]

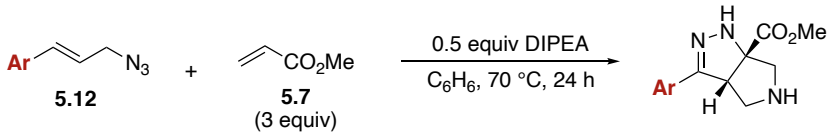

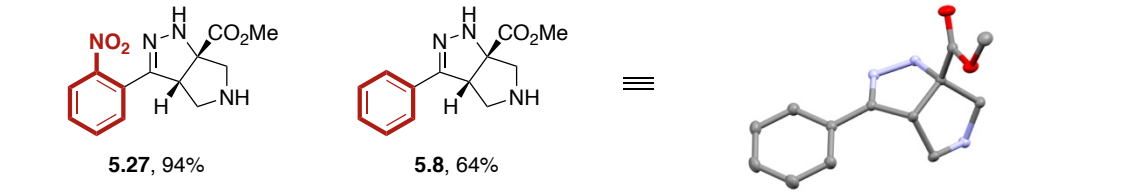

5.27, 94%

5.8, 64%

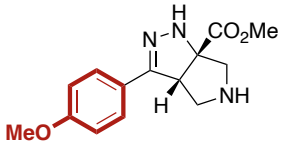

5.28, 82%

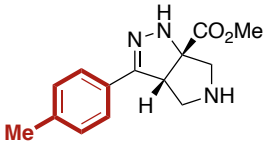

5.29, 73%

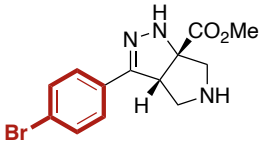

5.30, 69%

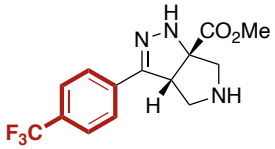

5.31, 79%

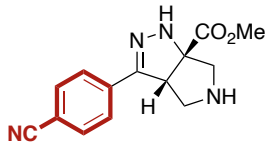

5.32, 77%

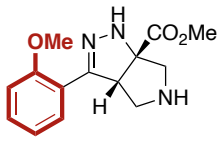

5.33, 84%

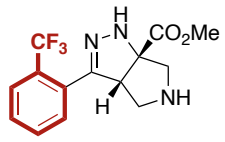

5.34, 63%

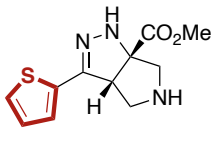

5.35, 74%

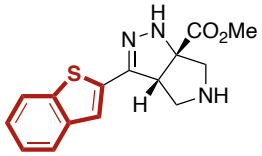

5.36, 80%

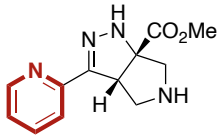

5.37, 89%

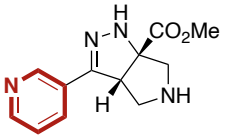

5.38, 68%

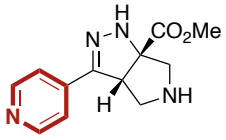

5.39, 60%

[a]Yields are reported for isolated and purified products. Yield values reflect the average of duplicated trials.

The substrate scope was further expanded (Table 5.4). A methyl or a phenyl group could be incorporated adjacent to the azide (**5.43** and **5.45**). For product **5.43**, a minor diastereomer was observed that could arise from the *Z*-alkene isomer of azide **5.42**. An *E*/*Z* alkene isomerization could be occurring under the reaction conditions via the Winstein rearrangement.[28,29,109] The relative configuration of product **5.45** was assigned based on a crystal structure,[‡] and that of product **5.44** was assigned by analogy to product **5.45**. Interestingly, a minor diastereomer was not detected for compound **5.45**. Tertiary azide **5.46** afforded product **5.47**, albeit the reaction time was prolonged to 72 h. A methyl group could be incorporated at the α or β position relative to the arene, affording compounds **5.49** and **5.51**. In both cases, a minor diastereomer was not detected. The relative configuration of compound **5.51** was assigned by 2D NMR and is consistent with the alkene geometry of the starting material as would be expected for a cycloaddition.[‡] The *trans* relationship between the methyl and hydrogen on starting azide **5.50** should be translated to product **5.51** if the reaction proceeds through a concerted cycloaddition. A branched allylic azide **5.52** was suitable and afforded product **5.53**, which demonstrated that a cinnamyl azide was not required. It is noteworthy that significant eclipsing interactions likely exist between the bridgehead substituents in product **5.53**. Furthermore, a cyclic azide afforded tricyclic products (**5.55**, **5.57**, and **5.59**). A proximal arene was not required for the reaction to proceed, and product **5.59** was derived from unsaturated ester **5.58**.

[‡] For the crystal structures and 2D-NMR analysis, see the Supporting Information of this manuscript: *J. Org. Chem.* **2020**, *85*, 6044−6059.

Table 5.4 Reaction Scope with Substituted Allylic Azides[a]

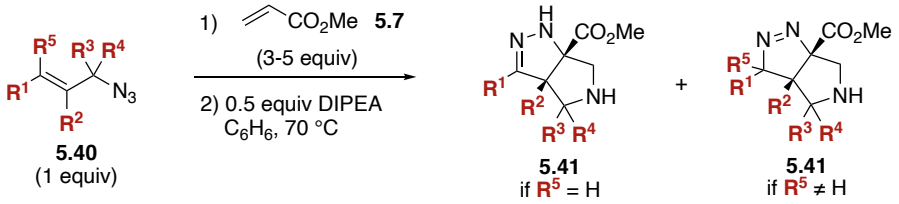

Starting Azide	Product	Starting Azide	Product
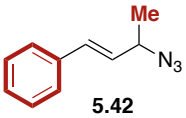 **5.42**	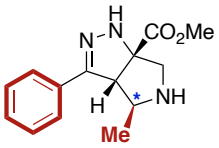 **5.43** 55%,[b] 8.8:1 dr[c]	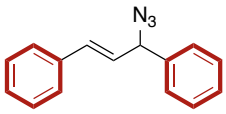 **5.44**	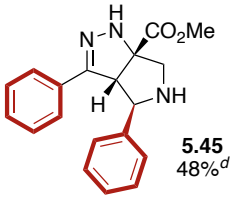 **5.45** 48%[d]
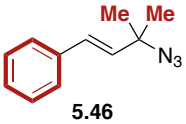 **5.46**	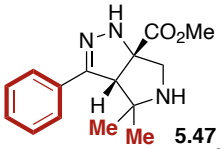 **5.47** 76%[e]	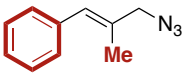 **5.48**	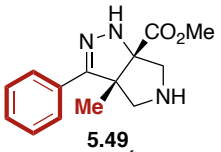 **5.49** 64%[f]
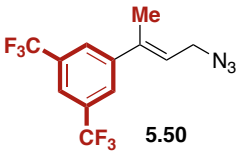 **5.50**	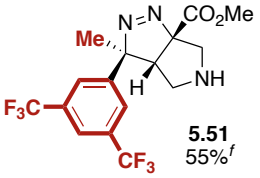 **5.51** 55%[f]	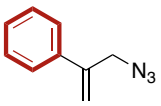 **5.52**	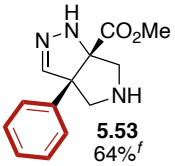 **5.53** 64%[f]
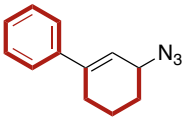 **5.54**	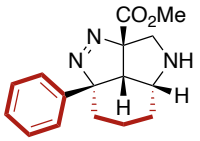 **5.55** 68%[f]	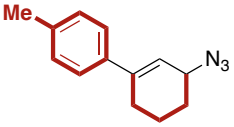 **5.56**	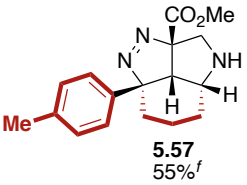 **5.57** 55%[f]
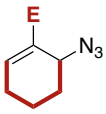 **5.58** E = CO_2Et	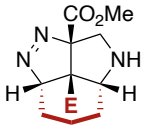 **5.59** 42%[d]		

[a]Yields are reported for isolated and purified products. Yield values reflect the average of duplicate trials. [b]Initial 72 h incubation at rt with an additional 24 h at 70 °C. [c]Diastereomeric ratio determined by crude ^{1}H NMR spectroscopy. [d]Reaction for 48 h at 70 °C. [e]Reaction for 72 h at 70 °C. [f]Initial 48 h incubation at rt with an additional 24 h at 70 °C.

It is noteworthy that most substrates in Table 5.4, except products **5.45**, **5.47**, and **5.59**, need extra incubation time at ambient temperature. Significantly decreased yields were obtained when the reaction was conducted using a one-pot fashion. It is because the intramolecular cycloaddition of diazo and alkene proceeds relatively slow (Scheme 5.2). The cycloaddition rate is decreased when branched substituents are present in the starting azides. In the presence of excess methyl acrylate (**5.7**), intermolecular cycloaddition is likely to proceed faster, causing the decreased yields. To address this issue, a two-pot fashion of synthesis was adapted. The triazoline **5.14** (Scheme 5.2) could be accessed at ambient temperature after 24-72 h. Before subjected to DIPEA, the excess methyl acrylate was removed under vacuum using the Schlenk technique. When the reaction was heated to an elevated temperature, the intermolecular cycloaddition was unlikely to happen in the absence of methyl acrylate. Although the triazoline formation is reversible and releases methyl acrylate and starting azides, the reaction yield can be increased using this two-staged synthesis.

An enantioenriched azide **5.56** was accessed via semi-prep HPLC technique using a known separation condition.[64] The azide enantiomer was subjected to the cascade reaction (Scheme 5.3). Product **5.57** was isolated as a single diastereomer with no loss in enantiomeric purity (>99:1 er). A crystal structure of (±)-**5.57·HCl** was obtained to confirm its identity and stereochemistry.[‡] This represents a tremendous amplification of stereochemical complexity. Azide **5.56** contains only a single stereocenter. Product **5.57** contains four contiguous stereocenters, three of which are generated from this cascade

[‡] For the crystal structures see the Supporting Information of this manuscript: *J*. *Org*. *Chem*. **2020**, *85*, 6044–6059.

reaction. Two stereocenters are formed at tetrasubstituted carbon atoms that bear a nitrogen substituent, which is known to be particularly challenging stereocenters to establish.[143]

Scheme 5.3 Stereospecific Cascade Reaction

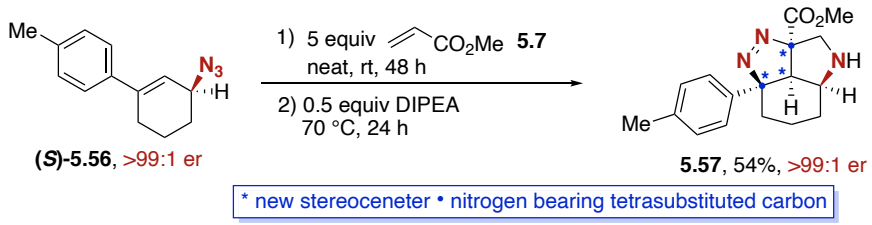

In addition to methyl acrylates, a series of Michael acceptors were investigated (Table 5.5). Similar alkyl acrylates could be applied. Ethyl (**5.60**), *tert*-butyl (**5.61**), and benzyl (**5.62**) esters were isolated in high yields. The selective formation of cinnamate **5.63** is interesting because the putative α-diazoester intermediate selectively engaged one of the two pendant alkenes. Both alkenes give [3.3.0] bicyclic products. The selective cycloaddition of the α-diazoester is probably due to the more polarized double bond caused by the nitro group on the phenyl. Alkyl crotonates afforded the corresponding methyl substituted products in high yields and modest dr's (**5.64** and **5.65**). The relative configuration of product **5.64** was determined by X-ray diffraction analysis, and the relative configuration of product **5.65** was assigned by analogy to product **5.64**. The methyl on compound **5.64** is *anti*- to the methyl ester, which reflects the concerted cycloaddition of the diazo intermediate to the (*E*)-configuration of the methyl crotonate. The use of methyl vinyl ketone afforded exclusively the product of conjugate addition (**5.17** in Scheme 5.2). The conjugated addition takes place at ambient temperature because of the high

reactivity of methyl vinyl ketone. To prevent this, TsCl and DMAP were added to trap the initial adduct prior to conjugate addition, which allowed the isolation of product **5.66**. Other Michael acceptors including acrylamide (**5.67**) and acrylonitrile (**5.68**) were also effective as partners in this cascade reaction. The lower yield of product **5.69** was obtained because a significant amount of regiomeric triazoline (**5.15** in Scheme 5.2, ca. 1:1) was formed. Despite lower yields of some products, this cascade cyclization provides a diverse array of functional groups.

Table 5.5 Reaction Scope with Michael Acceptors[a]

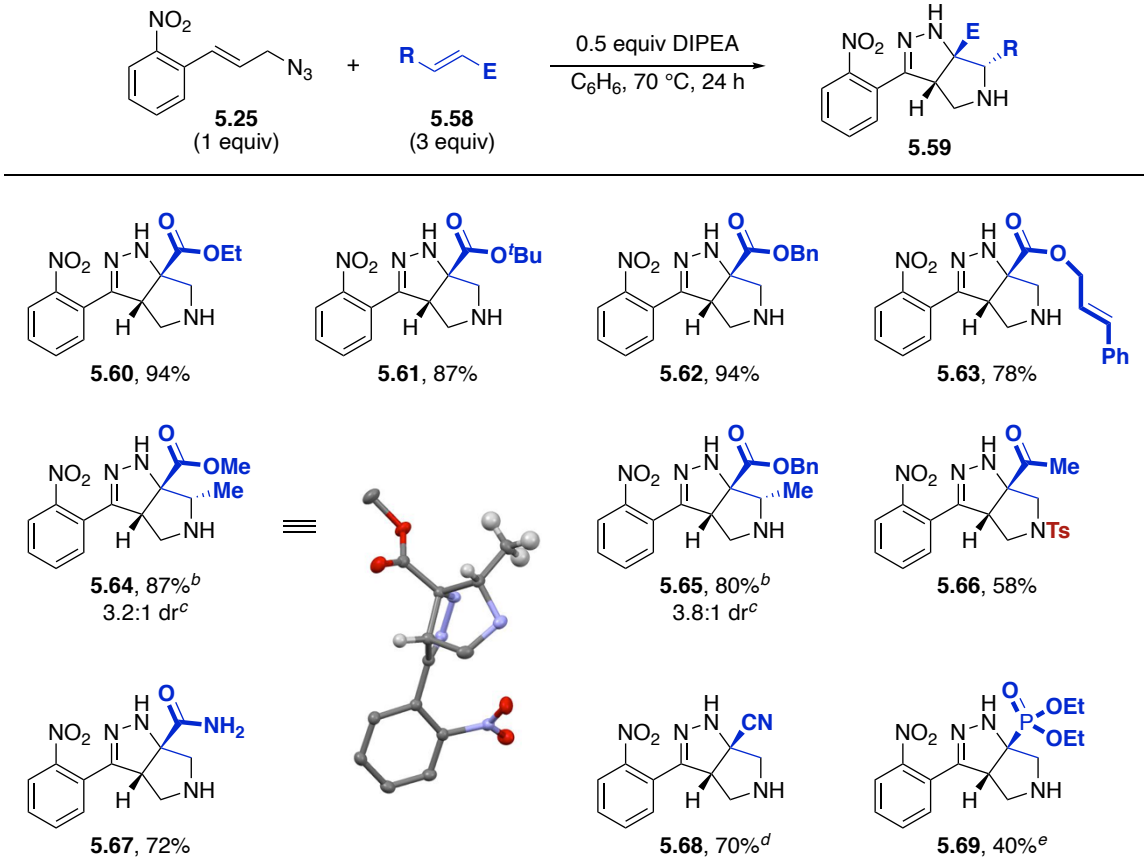

[a]Yields are reported for isolated and purified products. Yield values reflect the average of duplicate trials. [b]Reaction for 5 days at 70 °C. [c]Diastereomeric ratio determined by crude ^{1}H NMR spectroscopy.

[d]Initial 24 h incubation neat at 40 °C. Then C_6H_6 and DIPEA were added for an additional 24 h at 40 °C. [e]The reaction was heated to 90 °C.

Conducting the cascade reaction in the presence of various electrophiles was a productive means to extend the cascade process (Table 5.6). The addition of Boc_2O resulted in product **5.70**. Tosyl protected pyrrole **5.71** could be obtained when TsCl was utilized. When TrCl was used, the product was initially isolated as a mixture of tautomers. Tautomerization of this mixture was slower than for other substrates, and it was promoted by exposure to 0.5 equiv of DBU, after which only the conjugated isomer **5.72** was observed by ^{1}H NMR. Benzyl protected product **5.73** was generated when benzyl chloroformate (CbzCl) was added.

Table 5.6 Product Functionalization in Situ to Expand Cascade[a]

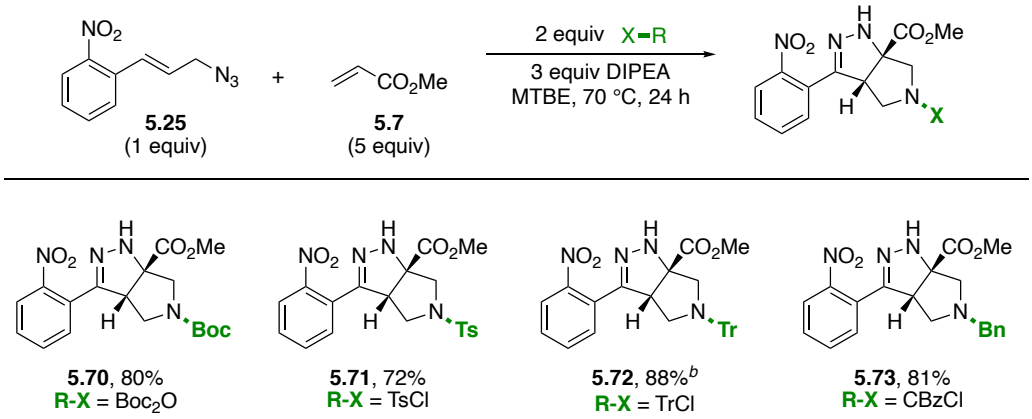

[a]Yields are reported for isolated and purified products. [b]Yield reflects the sum of both tautomers.

5.2.3 Product Derivatization

The cascade cyclization could be conducted on a gram scale without any decrease in efficiency (Scheme 5.4). Each of the functional groups present in product **5.27** could be selectively derivatized. The nitro group could be selectively reduced to afford aniline **5.74** in quantitative yield. The ester present in product **5.27** could be reduced to afford alcohol **5.75** or hydrolyzed to carboxylic acid **5.76**. The pyrrolidine nitrogen could be alkylated, arylated, or acylated to afford products **5.73**, **5.77**, and **5.78**, respectively. Lastly, the hydrazone motif could be acylated, yielding the allyl ester **5.79** in the presence of potassium carbonate. These results clearly highlight how the dense functionality present on the tetrahydro-pyrrolo-pyrazole core can be selectively elaborated and diversified.

Scheme 5.4 Gram-Scale Reaction and Product Derivatization

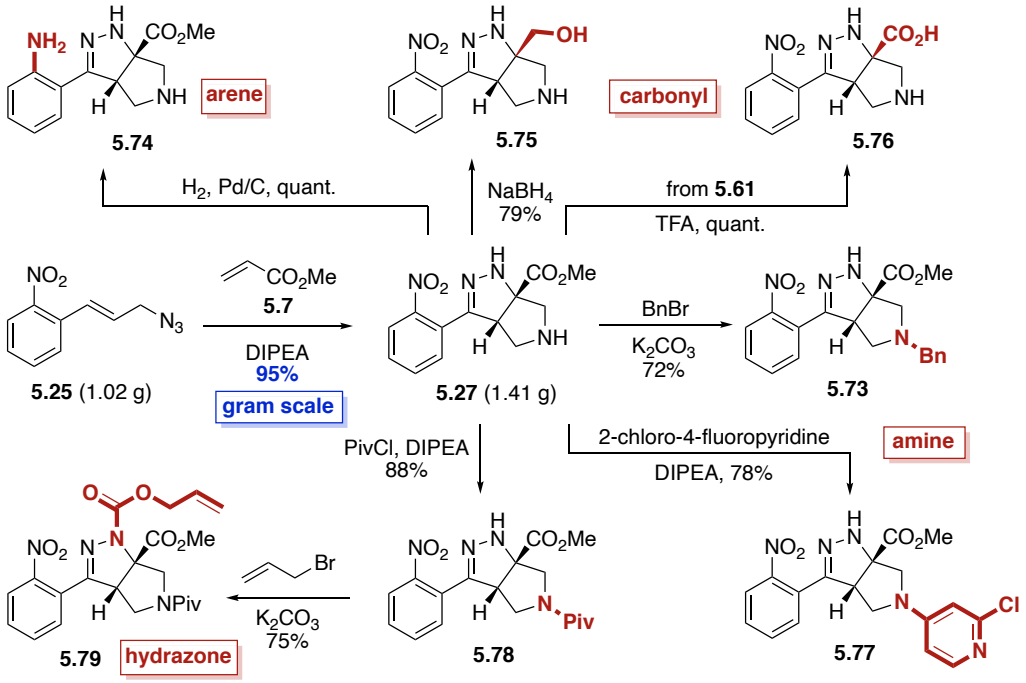

5.3 Conclusion

In conclusion, cinnamyl azides and Michael acceptors can engage in a modular cascade cyclization to directly generate fused tetrahydro-pyrrolo-pyrazole heterocycles. This cascade has expanded the reactivity of allylic azides beyond azide-alkyne cycloaddition. The reaction proceeds on an array of coupling partners. Furthermore, the products can be derivatized in situ. This reaction rapidly amplifies the complexity of two trivial starting materials and directly affords functionally dense bicyclic amine building blocks. This cascade is modular and amenable to diversification.

5.4 Global Summary

This graduate work has described the versatility of allylic azides to access heterocycles. Allylic azides were regarded as problematic substrates in organic synthesis because of the Winstein rearrangement. However, this graduate work takes the advantage of the rearrangement as a racemization pathway. This method provided efficient access to enantioenriched triazoles (chapter 2). The enantioselective copper-catalyzed alkyne-azide cycloaddition (E-CuAAC) via dynamic kinetic resolution provided α-*N*-chiral triazoles in excellent yield and selectivity. A series of the mechanistic investigation was conducted. The non-linear effect revealed that the active catalyst is a dimeric [copper(I)-PYBOX]$_2$ species. The matched/mismatched experiments indicated that the enantioselectivity was driven by the ligand. The newly developed PYBOX-ligand could be utilized in a kinetic resolution of secondary benzylic azides (chapter 3). Enantioenriched triazoles can be synthesized from racemic benzylic azides. The residual scalemic azides can be racemized and recycled by exposure to a Lewis acid catalyst. This outcome is the same as a dynamic

kinetic resolution. Furthermore, this graduate work also investigated the first enantioselective nickel-catalyzed alkyne-azide cycloaddition (E-NiAAC) to enantioenriched triazoles (chapter 4). The utilization of the nickel catalyst resulted in complementary access to 1,4,5-trisubstituted triazoles, which were not able to be achieved via a copper catalyst. The mechanistic investigation revealed that the catalytic cycle of E-NiAAC is very distinctive from that of E-CuAAC. The non-linear effect experiments showed that the active catalyst is a monomeric nickel species, and the initial rate studies indicated that the reaction is first ordered in the catalyst. Eventually, this graduate work also described that the cinnamyl azides, as a subclass of allylic azides, can be utilized to prepare densely functionalized heterocycles via a cascade reaction (chapter 5). The reoptimization of a precedent reaction enables a broader substrates scope with higher reaction yields. This highly diastereoselective reaction can give heterocyclic products with multiple newly formed stereogenic centers. These reactions turned allylic azides from a problematic precursor into versatile building blocks.

Reference

(1) Moss, G. P.; Smith, P. A. S.; Tavernier, D. *Pure Appl. Chem.* **1995**, *67*, 1307–1375.

(2) Kerru, N.; Gummidi, L.; Maddila, S.; Gangu, K. K.; Jonnalagadda, S. B. *Molecules* **2020**, *25*.

(3) Chen, D.; Su, S. J.; Cao, Y. *J. Mater. Chem. C* **2014**, *2*, 9565–9578.

(4) Lamberth, C. *Pest Manag. Sci.* **2013**, *69*, 1106–1114.

(5) Joule, J. A. *Natural Products Containing Nitrogen Heterocycles-Some Highlights 1990-2015*; Elsevier Ltd, 2016; Vol. 119.

(6) Vitaku, E.; Smith, D. T.; Njardarson, J. T. *J. Med. Chem.* **2014**, *57*, 10257–10274.

(7) Schmitz, R. *Pharm. Hist.* **1985**, *27*, 61–74.

(8) Tchounwou, P. B.; Yedjou, C. G.; Patlolla, A. K.; Sutton, D. J. *Volume 3: Environmental Toxicology*; 2012; Vol. 101.

(9) Parker, K. A.; Fokas, D. *J. Am. Chem. Soc.* **1992**, *114*, 9688–9689.

(10) Mulzer, J.; Dürner, G.; Trauner, D. *Angew. Chemie Int. Ed. English* **1996**, *35*, 2830–2832.

(11) White, J. D.; Hrnciar, P.; Stappenbeck, F. *J. Org. Chem.* **1999**, *64*, 7871–7884.

(12) Nagata, H.; Miyazawa, N.; Ogasawara, K. *Chem. Commun.* **2001**, *2*, 1094–1095.

(13) Taber, D. F.; Neubert, T. D.; Rheingold, A. L. *J. Am. Chem. Soc.* **2002**, *124*, 12416–12417.

(14) Varin, M.; Barré, E.; Iorga, B.; Guillou, C. *Chem. - A Eur. J.* **2008**, *14*, 6606–6608.

(15) Stork, G.; Yamashita, A.; Adams, J.; Schulte, G. R.; Chesworth, R.; Miyazaki, Y.; Farmer, J. J. *J. Am. Chem. Soc.* **2009**, *131*, 11402–11406.

(16) Hong, C. Y.; Kado, N.; Overman, L. E. *J. Am. Chem. Soc.* **1993**, *115*, 11028–11029.

(17) Gates, M.; Tschudi, G. *J. Am. Chem. Soc.* **1956**, *78*, 1380–1393.

(18) Trost, B. M.; Tang, W. *J. Am. Chem. Soc.* **2002**, *124*, 14542–14543.

(19) Jiang, J.; Ji, Y. *Synth. Commun.* **2013**, *43*, 72–79.

(20) Liu, N.; Hoogendoorn, S.; Van De Kar, B.; Kaptein, A.; Barf, T.; Driessen, C.; Filippov, D. V.; Van Der Marel, G. A.; Van Der Stelt, M.; Overkleeft, H. S. *Org. Biomol. Chem.* **2015**, *13*, 5147–5157.

(21) Abrecht, S.; Harrington, P.; Iding, H.; Karpf, M.; Trussardi, R.; Wirz, B.; Zutter, U. *Chimia (Aarau).* **2004**, *58*, 621–629.

(22) Ju, X.; Tang, Y.; Liang, X.; Hou, M.; Wan, Z.; Tao, J. *Org. Process Res. Dev.* **2014**, *18*, 827–830.

(23) Zheng, G.; Liu, Y. Y.; Chen, Q.; Huang, L.; Yu, H. L.; Lou, W. Y.; Li, C. X.; Bai, Y. P.; Li, A. T.; Xu, J. H. *ACS Catal.* **2017**, *7*, 7174–7181.

(24) Bräse, S.; Gil, C.; Knepper, K.; Zimmermann, V. *Angew. Chemie - Int. Ed.* **2005**, *44*, 5188–5240.

(25) Editor, S. *Synthesis of Heterocycles via Cycloadditions II*; 2008.

(26) Lee, H. L.; Aubé, J. *Tetrahedron* **2007**, *63*, 9007–9015.

(27) Rohloff, J. C.; Kent, K. M.; Postich, M. J.; Becker, M. W.; Chapman, H. H.; Kelly, D. E.; Lew, W.; Louie, M. S.; McGee, L. R.; Prisbe, E. J.; et al. *J. Org. Chem.* **1998**, *63*, 4545–4547.

(28) Gagneux, A.; Winstein, S.; Young, W. G. *J. Am. Chem. Soc.* **1960**, *82*, 5956–5957.

(29) Carlson, A. S.; Topczewski, J. J. *Org. Biomol. Chem.* **2019**, *17*, 4406–4429.

(30) Feldman, A. K.; Colasson, B.; Sharpless, K. B.; Fokin, V. V. *J. Am. Chem. Soc.* **2005**, *127*, 13444–13445.

(31) Liu, R.; Gutierrez, O.; Tantillo, D. J.; Aubé, J. *J. Am. Chem. Soc.* **2012**, *134*, 6528–6531.

(32) Zhan, G.; Du, W.; Chen, Y. C. *Chem. Soc. Rev.* **2017**, *46*, 1675–1692.

(33) Farina, V.; Reeves, J. T.; Senanayake, C. H.; Song, J. J. *Chem. Rev.* **2006**, *106*, 2734–2793.

(34) Diaz-Muñoz, G.; Miranda, I. L.; Sartori, S. K.; de Rezende, D. C.; Alves Nogueira Diaz, M. *Chirality* **2019**, *31*, 776–812.

(35) Wang, G. Z.; Bäckvall, J. E. *J. Chem. Soc. Chem. Commun.* **1992**, No. 4, 337–339.

(36) Almeida, M. L. S.; Beller, M.; Wang, G. Z.; Bäckvall, J. E. *Chem. - A Eur. J.* **1996**, *2*, 1533–1536.

(37) Larsson, A. L. E.; Persson, B. A.; Bäckvall, J. E. *Angew. Chemie (International Ed. English)* **1997**, *36*, 1211–1212.

(38) Kubo, A.; Kubota, H.; Takahashi, M.; Nunami, K. I. *J. Org. Chem.* **1997**, *62*, 5830–5837.

(39) O'Meara, J. A.; Gardee, N.; Jung, M.; Ben, R. N.; Durst, T. *J. Org. Chem.* **1998**, *63*, 3117–3119.

(40) Meldal, M.; Tomøe, C. W. *Chem. Rev.* **2008**, *108*, 2952–3015.

(41) Brittain, W. D. G.; Buckley, B. R.; Fossey, J. S. *ACS Catal.* **2016**, *6*, 3629–3636.

(42) Berrisford, D. J.; Bolm, C.; Sharpless, K. B. .

(43) Rodionov, V. O.; Presolski, S. I.; Díaz, D. D.; Fokin, V. V.; Finn, M. G. *J. Am. Chem. Soc.* **2007**, *129*, 12705–12712.

(44) Zhu, Z.; Chen, H.; Li, S.; Yang, X.; Bittner, E.; Cai, C. *Catal. Sci. Technol.* **2017**, *7*, 2474–2485.

(45) Meng, J. C.; Fokin, V. V.; Finn, M. G. *Tetrahedron Lett.* **2005**, *46*, 4543–4546.

(46) Song, T.; Li, L.; Zhou, W.; Zheng, Z. J.; Deng, Y.; Xu, Z.; Xu, L. W. *Chem. - A Eur. J.* **2015**, *21*, 554–558.

(47) Stephenson, G. R.; Buttress, J. P.; Deschamps, D.; Lancelot, M.; Martin, J. P.; Sheldon, A. I. G.; Alayrac, C.; Gaumont, A. C.; Page, P. C. B. *Synlett* **2013**, *24*, 2723–2729.

(48) Brittain, W. D. G.; Buckley, B. R.; Fossey, J. S. *Chem. Commun.* **2015**, *51*, 17217–17220.

(49) Osako, T.; Uozumi, Y. *Org. Lett.* **2014**, *16*, 5866–5869.

(50) Zhu, R. Y.; Chen, L.; Hu, X. S.; Zhou, F.; Zhou, J. *Chem. Sci.* **2020**, *11*, 97–106.

(51) Eno, M. S.; Lu, A.; Morken, J. P. *J. Am. Chem. Soc.* **2016**, *138*, 7824–7827.

(52) Osako, T.; Uozumi, Y. *Synlett* **2015**, *26*, 1475–1479.

(53) Chen, M. Y.; Xu, Z.; Chen, L.; Song, T.; Zheng, Z. J.; Cao, J.; Cui, Y. M.; Xu, L. W. *ChemCatChem* **2018**, *10*, 280–286.

(54) Zhou, F.; Tan, C.; Tang, J.; Zhang, Y. Y.; Gao, W. M.; Wu, H. H.; Yu, Y. H.; Zhou, J. *J. Am. Chem. Soc.* **2013**, *135*, 10994–10997.

(55) Nakajima, K.; Shibata, M.; Nishibayashi, Y. *J. Am. Chem. Soc.* **2015**, *137*, 2472–2475.

(56) Díez, J.; Gamasa, M. P.; Panera, M. *Inorg. Chem.* **2006**, *45*, 10043–10045.

(57) Worrell, B. T.; Malik, J. A.; Fokin, V. V. **2010**, *340*, 457–461.

(58) Misale, A.; Niyomchon, S.; Luparia, M.; Maulide, N. *Angew. Chemie - Int. Ed.* **2014**, *53*, 7068–7073.

(59) Ott, A. A.; Goshey, C. S.; Topczewski, J. J. *J. Am. Chem. Soc.* **2017**, *139*, 7737–7740.

(60) Wang, P. S.; Zhou, X. Le; Gong, L. Z. *Org. Lett.* **2014**, *16*, 976–979.

(61) Gandeepan, P.; Rajamalli, P.; Cheng, C. H. *ACS Catal.* **2014**, *4*, 4485–4489.

(62) Chuang, T. H.; Chang, W. Y.; Li, C. F.; Wen, Y. C.; Tsai, C. C. *J. Org. Chem.* **2011**, *76*, 9678–9686.

(63) Hari Babu, M.; Ranjith Kumar, G.; Kant, R.; Sridhar Reddy, M. *Chem. Commun.* **2017**, *53*, 3894–3897.

(64) Ott, A. A.; Topczewski, J. J. *Org. Lett.* **2018**, *20*, 7253–7256.

(65) Brittain, W. D. G.; Chapin, B. M.; Zhai, W.; Lynch, V. M.; Buckley, B. R.; Anslyn, E. V.; Fossey, J. S. *Org. Biomol. Chem.* **2016**, *14*, 10778–10782.

(66) Brittain, W. D. G.; Dalling, A. G.; Sun, Z.; Duff, C. S. L.; Male, L.; Buckley, B. R.; Fossey, J. S. *Sci. Rep.* **2019**, *9*, 2–10.

(67) Dutartre, M.; Bayardon, J.; Jugé, S. *Chem. Soc. Rev.* **2016**, *45*, 5771–5794.

(68) Zhou, J.; Tang, Y. *J. Am. Chem. Soc.* **2002**, *124*, 9030–9031.

(69) Zhou, J.; Ye, M. C.; Huang, Z. Z.; Tang, Y. *J. Org. Chem.* **2004**, *69*, 1309–1320.

(70) Zhou, J.; Ye, M. C.; Tang, Y. *J. Comb. Chem.* **2004**, *6*, 301–304.

(71) Ye, M. C.; Li, B.; Zhou, J.; Sun, X. L.; Tang, Y. *J. Org. Chem.* **2005**, *70*, 6108–6110.

(72) Cao, C. L.; Zhou, Y. Y.; Sun, X. L.; Tang, Y. *Tetrahedron* **2008**, *64*, 10676–10680.

(73) Zhou, Y. Y.; Sun, X. L.; Zhu, B. H.; Zheng, J. C.; Zhou, J. L.; Tang, Y. *Synlett* **2011**, No. 7, 935–938.

(74) Huang, Z. Z.; Kang, Y. B.; Zhou, J.; Ye, M. C.; Tang, Y. *Org. Lett.* **2004**, *6*, 1677–1679.

(75) Zhou, J.; Tang, Y. **2004**, 429–433.

(76) Chen, J. H.; Liao, S. H.; Sun, X. L.; Shen, Q.; Tang, Y. *Tetrahedron* **2012**, *68*, 5042–

5045.

(77) Zhou, Y. Y.; Li, J.; Ling, L.; Liao, S. H.; Sun, X. L.; Li, Y. X.; Wang, L. J.; Tang, Y. *Angew. Chemie - Int. Ed.* **2013**, *52*, 1452–1456.

(78) Xu, Z. H.; Zhu, S. N.; Sun, X. L.; Tang, Y.; Dai, L. X. *Chem. Commun.* **2007**, No. 19, 1960–1962.

(79) Ye, M. C.; Zhou, J.; Huang, Z. Z.; Tang, Y. *Chem. Commun.* **2003**, *9*, 2554–2555.

(80) Zhou, J.; Tang, Y. *Chem. Soc. Rev.* **2005**, *34*, 664–676.

(81) Jana, N.; Driver, T. G. *Org. Biomol. Chem.* **2015**, *13*, 9720–9741.

(82) Cao, P.; Deng, C.; Zhou, Y. Y.; Sun, X. L.; Zheng, J. C.; Xie, Z.; Tang, Y. *Angew. Chemie - Int. Ed.* **2010**, *49*, 4463–4466.

(83) Liu, S.; Edgar, K. J. *Biomacromolecules* **2015**, *16*, 2556–2571.

(84) Tanimoto, H.; Kakiuchi, K. *Nat. Prod. Commun.* **2013**, *8*, 1021–1034.

(85) Keith, J. M.; Larrow, J. F.; Jacobsen, E. N. *Adv. Synth. Catal.* **2001**, *343*, 5–26.

(86) Rostovtsev, V. V.; Green, L. G.; Fokin, V. V.; Sharpless, K. B. *Angew. Chemie Int. Ed.* **2002**, *41*, 2596–2599.

(87) Tornøe, C. W.; Christensen, C.; Meldal, M. *J. Org. Chem.* **2002**, *67*, 3057–3064.

(88) Kolb, H. C.; Finn, M. G.; Sharpless, K. B. *Angew. Chemie - Int. Ed.* **2001**, *40*, 2004–2021.

(89) Topczewski, J. J.; Liu, E.-C. *Nature* **2019**, *574*, 42–43.

(90) Hein, J. E.; Tripp, J. C.; Krasnova, L. B.; Sharpless, K. B.; Fokin, V. V. *Angew. Chemie - Int. Ed.* **2009**, *48*, 8018–8021.

(91) Yamada, M.; Matsumura, M.; Kawahata, M.; Murata, Y.; Kakusawa, N.; Yamaguchi, K.; Yasuike, S. *J. Organomet. Chem.* **2017**, *834*, 83–87.

(92) Krasiński, A.; Fokin, V. V.; Sharpless, K. B. *Org. Lett.* **2004**, *6*, 1237–1240.

(93) Hein, J. E.; Fokin, V. V. *Chem. Soc. Rev.* **2010**, *39*, 1302–1315.

(94) Meng, X.; Xu, X.; Gao, T.; Chen, B. *European J. Org. Chem.* **2010**, No. 28, 5409–5414.

(95) Liao, Y.; Lu, Q.; Chen, G.; Yu, Y.; Li, C.; Huang, X. *ACS Catal.* **2017**, *7*, 7529–7534.

(96) Song, W.; Zheng, N.; Li, M.; Ullah, K.; Zheng, Y. *Adv. Synth. Catal.* **2018**, *360*, 2429–2434.

(97) Banerji, B.; Chandrasekhar, K.; Killi, S. K.; Pramanik, S. K.; Uttam, P.; Sen, S.; Maiti, N. C. *R. Soc. Open Sci.* **2016**, *3*, 1–9.

(98) Song, W.; Zheng, N. *Org. Lett.* **2017**, *19*, 6200–6203.

(99) Chen, R.; Zeng, L.; Lai, Z.; Cui, S. *Adv. Synth. Catal.* **2019**, *361*, 989–994.

(100) Wu, Z. G.; Liao, X. J.; Yuan, L.; Wang, Y.; Zheng, Y. X.; Zuo, J. L.; Pan, Y. *Chem. - A Eur. J.* **2020**, *26*, 5694–5700.

(101) Kim, W. G.; Kang, M. E.; Lee, J. Bin; Jeon, M. H.; Lee, S.; Lee, J.; Choi, B.; Cal, P. M. S. D.; Kang, S.; Kee, J. M.; et al. *J. Am. Chem. Soc.* **2017**, *139*, 12121–12124.

(102) Kim, W. G.; Baek, S. Y.; Jeong, S. Y.; Nam, D.; Jeon, J. H.; Choe, W.; Baik, M. H.; Hong, S. Y. *Org. Biomol. Chem.* **2020**, *18*, 3374–3381.

(103) Boominathan, M.; Pugazhenthiran, N.; Nagaraj, M.; Muthusubramanian, S.; Murugesan, S.; Bhuvanesh, N. *ACS Sustain. Chem. Eng.* **2013**, *1*, 1405–1411.

(104) Zhang, L.; Chen, X.; Xue, P.; Sun, H. H. Y.; Williams, I. D.; Sharpless, K. B.; Fokin, V. V.; Jia, G. *J. Am. Chem. Soc.* **2005**, *127*, 15998–15999.

(105) Johansson, J. R.; Beke-Somfai, T.; Said Stålsmeden, A.; Kann, N. *Chem. Rev.* **2016**, *116*, 14726–14768.

(106) Gololobov, Y. G.; Kasukhin, L. F. *Tetrahedron* **1992**, *48*, 1353–1406.

(107) Rodrigo, S. K.; Powell, I. V.; Coleman, M. G.; Krause, J. A.; Guan, H. *Org. Biomol. Chem.* **2013**, *11*, 7653–7657.

(108) Ott, A. A.; Topczewski, J. J. *Arkivoc* **2019**, *2019*, 1–17.

(109) Ott, A. A.; Packard, M. H.; Ortuno, M. A.; Johnson, A.; Suding, V. P.; Cramer, C. J.; Topczewski, J. J. *J. Org. Chem.* **2018**, *83*, 8214–8224.

(110) Pellissier, H. *Tetrahedron* **2003**, *59*, 8291–8327.

(111) Pellissier, H. *Tetrahedron* **2008**, *64*, 1563–1601.

(112) Bhat, V.; Welin, E. R.; Guo, X.; Stoltz, B. M. *Chem. Rev.* **2017**, *117*, 4528–4561.

(113) Huerta, F. F.; Minidis, A. B. E.; Bäckvall, J. E. *Chem. Soc. Rev.* **2001**, *30*, 321–331.

(114) Girard, C.; Kagan, H. B. *Angew. Chemie - Int. Ed.* **1998**, *37*, 2922–2959.

(115) Liu, E.-C.; Topczewski, J. J. *J. Am. Chem. Soc.* **2019**, *141*, 5135–5138.

(116) Worrell, B. T.; Malik, J. A.; Fokin, V. V. *Science (80-.).* **2013**, *340*, 457–460.

(117) Zhai, M.; Wang, L.; Liu, S.; Wang, L.; Yan, P.; Wang, J.; Zhang, J.; Guo, H.; Guan, Q.; Bao, K.; et al. *Eur. J. Med. Chem.* **2018**, *156*, 137–147.

(118) Levin, J. I.; Venkatesan, A. M.; Chan, P. S.; Bailey, T. K.; Vice, G.; Coupet, J. *Bioorganic Med. Chem. Lett.* **1994**, *4*, 1819–1824.

(119) Liu, G. N.; Luo, R. H.; Zhou, Y.; Zhang, X. J.; Li, J.; Yang, L. M.; Zheng, Y. T.; Liu, H. *Molecules* **2016**, *21*, 1–12.

(120) Møllerud, S.; Pinto, A.; Marconi, L.; Frydenvang, K.; Thorsen, T. S.; Laulumaa, S.; Venskutonyte, R.; Winther, S.; Moral, A. M. C.; Tamborini, L.; et al. *ACS Chem. Neurosci.* **2017**, *8*, 2056–2064.

(121) Chen, P.; Feng, D.; Qian, X.; Apgar, J.; Wilkening, R.; Kuethe, J. T.; Gao, Y. D.; Scapin, G.; Cox, J.; Doss, G.; et al. *Bioorganic Med. Chem. Lett.* **2015**, *25*, 5767–5771.

(122) Deaton, D. N.; Haffner, C. D.; Henke, B. R.; Jeune, M. R.; Shearer, B. G.; Stewart, E. L.; Stuart, J. D.; Ulrich, J. C. *Bioorganic Med. Chem.* **2018**, *26*, 2107–2150.

(123) Quiclet-Sire, B.; Zard, S. Z. *Chem. Commun.* **2006**, No. 17, 1831–1832.

(124) Just, D.; Hernandez-Guerra, D.; Kritsch, S.; Pohl, R.; Císařová, I.; Jones, P. G.; Mackman, R.; Bahador, G.; Jahn, U. *European J. Org. Chem.* **2018**, *2018*, 5213–5221.

(125) Kapras, V.; Pohl, R.; Císařová, I.; Jahn, U. *Org. Lett.* **2014**, *16*, 1088–1091.

(126) Carlson, A. S.; Calcanas, C.; Brunner, R. M.; Topczewski, J. J. *Org. Lett.* **2018**, *20*, 1604–1607.

(127) Porter, M. R.; Shaker, R. M.; Calcanas, C.; Topczewski, J. J. *J. Am. Chem. Soc.* **2018**, *140*, 1211–1214.

(128) Hassner, A.; Fibiger, R.; Andisik, D. *J. Org. Chem.* **1984**, *49*, 4237–4244.

(129) Yang, C. H.; Shen, H. J. *Tetrahedron Lett.* **1993**, *34*, 4051–4054.

(130) Yang, C.; Sherf, H.-J.; Wang, R.; Wang, J.-C. *J. Chinese Chem. Soc.* **2002**, *49*, 95–102.

(131) L'abbé, G. *Chem. Rev.* **1969**, *69*, 345–363.

(132) Huisgen, R. *Proc. Chem. Soc.* **1961**, No. October, 357.

(133) Huisgen, R.; Szeimies, G.; Möbius, L. *Chem. Ber.* **1967**, *100*, 2494–2507.

(134) Liddon, J. T. R.; Lindsay-Scott, P. J.; Robertson, J. *J. Org. Chem.* **2019**, *84*, 13780–13793.

(135) Xie, S.; Lopez, S. A.; Ramström, O.; Yan, M.; Houk, K. N. *J. Am. Chem. Soc.* **2015**, *137*, 2958–2966.

(136) Krivopalov, V. P.; Shkurko, O. P. *Usp. Khim.* **2005**, *74*, 369–410.

(137) Broeckx, W.; Overbergh, N.; Samyn, C.; Smets, G.; L'abbé, G. *Tetrahedron* **1971**, *27*, 3527–3534.

(138) Herdeis, C.; Schiffer, T. *Tetrahedron* **1999**, *55*, 1043–1056.

(139) Scheiner, P. *Tetrahedron* **1968**, *24*, 349–356.

(140) Sebest, F.; Casarrubios, L.; Rzepa, H. S.; White, A. J. P.; Díez-González, S. *Green Chem.* **2018**, *20*, 4023–4035.

(141) Nadin, A.; Hattotuwagama, C.; Churcher, I. *Angew. Chemie - Int. Ed.* **2012**, *51*, 1114–1122.

(142) Kutchukian, P. S.; Dropinski, J. F.; Dykstra, K. D.; Li, B.; Dirocco, D. A.; Streckfuss, E. C.; Campeau, L. C.; Cernak, T.; Vachal, P.; Davies, I. W.; et al. *Chem. Sci.* **2016**, *7*, 2604–2613.

(143) Campos, K. R.; Coleman, P. J.; Alvarez, J. C.; Dreher, S. D.; Garbaccio, R. M.; Terrett, N. K.; Tillyer, R. D.; Truppo, M. D.; Parmee, E. R. *Science (80-.).* **2019**, *363*, 244–251.